

**Evaluation of finite dose skin absorption  
experiments with respect to experimental  
setup and mathematical modelling**



**Dissertation  
zur Erlangung des Grades  
des Doktors der Naturwissenschaften  
der Naturwissenschaftlich-Technischen Fakultät III  
Chemie, Pharmazie, Bio- und Werkstoffwissenschaften  
der Universität des Saarlandes**

von

Tsambika Hahn

Saarbrücken

2011

Tag des Kolloquiums:	19.12.2011
Dekan:	Prof. Dr. W. F. Maier
Berichterstatter:	Prof. Dr. U. F. Schäfer Prof. Dr. C.-M. Lehr Prof. Dr. T. Vogt
Vorsitz:	Prof. Dr. R. W. Hartmann
Akad. Mitarbeiter:	Dr. B. Diesel

Der Beginn ist der wichtigste Teil der Arbeit.

Platon



# Content

<b>Short summary</b> .....	<b>9</b>
<b>Kurzzusammenfassung</b> .....	<b>10</b>
<b>Introduction</b> .....	<b>11</b>
<b>1.1 Absorption pathways of the skin</b> .....	<b>12</b>
1.1.1 Structure of the skin.....	12
1.1.2 Application to the skin .....	13
1.1.3 Pathways across the SC.....	14
<b>1.2 In vitro skin absorption experiments</b> .....	<b>17</b>
1.2.1 Tissues used for <i>in vitro</i> skin absorption experiments.....	18
1.2.2 <i>In vitro</i> skin permeation models .....	19
1.2.3 <i>In vitro</i> skin penetration model.....	22
<b>1.3 Finite dose</b> .....	<b>23</b>
1.3.1 Comparison finite and infinite dosing.....	23
1.3.2 Challenges associated with experimental finite dose setup.....	23
1.3.3 Principles of finite dose kinetics.....	26
<b>1.4 Modelling of skin absorption</b> .....	<b>31</b>
1.4.1 Quantitative structure activity relationship (QSAR) models.....	34
1.4.2 Pharmacokinetic models.....	35
1.4.3 Diffusion models .....	37
<b>2 Aim of the thesis</b> .....	<b>41</b>
<b>3 Infrared densitometry: a fast and non-destructive method for exact stratum corneum depth calculation for in vitro tape-stripping</b> .....	<b>45</b>
<b>3.1 Abstract</b> .....	<b>46</b>
<b>3.2 Introduction</b> .....	<b>47</b>
<b>3.3 Materials and methods</b> .....	<b>50</b>
3.3.1 Chemicals .....	50
3.3.2 Skin .....	50
3.3.3 <i>In vivo</i> tape-stripping.....	51
3.3.4 <i>In vitro</i> tape-stripping.....	52
3.3.5 Infrared densitometry (IR-D).....	52
3.3.6 BCA protein assay.....	53
3.3.7 Influence of disinfectants on BCA assay.....	54
3.3.8 Determination of SC thickness .....	54
3.3.9 Determination of SC remaining on the skin after tape-stripping .....	55
3.3.10 Determination of cumulative depth inside the SC.....	55
3.3.11 Statistics .....	55
<b>3.4 Results</b> .....	<b>56</b>

3.4.1	BCA protein assay.....	56
3.4.2	Infrared densitometry.....	58
3.4.3	Tape-stripping <i>in vivo</i> – influence of tape-strip brand and anatomical site....	58
3.4.4	Determination of SC thickness <i>in vitro</i> .....	59
3.4.5	Determination of SC remaining on the skin after tape-stripping <i>in vitro</i> .....	60
3.4.6	Tape-stripping <i>in vitro</i> – influence of storage time.....	61
<b>3.5</b>	<b>Discussion</b> .....	<b>63</b>
3.5.1	Protein substitution for BCA calibration standards .....	63
3.5.2	IR-D <i>in vivo</i> versus <i>in vitro</i> .....	63
3.5.3	Determination of SC depth.....	64
3.5.4	Determination of endpoint of complete SC removal.....	64
<b>3.6</b>	<b>Conclusions</b> .....	<b>65</b>
<b>4</b>	<b><i>Influence of the application area on finite dose permeation in relation to drug type applied</i></b> .....	<b>67</b>
<b>4.1</b>	<b>Abstract</b> .....	<b>68</b>
<b>4.2</b>	<b>Introduction</b> .....	<b>69</b>
<b>4.3</b>	<b>Methods</b> .....	<b>71</b>
4.3.1	Materials and instruments.....	71
4.3.2	Skin .....	71
4.3.3	Permeation experiments.....	71
4.3.4	Application of the donor .....	72
4.3.5	Mass recovery .....	72
4.3.6	Drug quantification .....	73
4.3.7	Analysis of the application area .....	73
4.3.8	Lateral drug distribution.....	75
4.3.9	Statistics .....	75
<b>4.4</b>	<b>Results</b> .....	<b>76</b>
4.4.1	Permeation profiles, uncorrected surface distribution .....	76
4.4.2	Donor surface distribution .....	76
4.4.3	Permeation data combined with calculated application area/coverage.....	78
4.4.4	Lateral drug distribution.....	78
<b>4.5</b>	<b>Discussion</b> .....	<b>80</b>
4.5.1	Dye as a marker for skin contact with the donor formulation .....	80
4.5.2	Suitability of the automated computer-assisted approach for determination of coverage .....	80
4.5.3	Permeation profiles and lateral drug distribution .....	81
4.5.4	Clinical relevance.....	82
<b>4.6</b>	<b>Conclusion</b> .....	<b>83</b>
<b>5</b>	<b><i>Finite dose skin absorption – Comparison between simulation, pharmacokinetic modelling, and experiment</i></b> .....	<b>85</b>
<b>5.1</b>	<b>Abstract</b> .....	<b>86</b>
<b>5.2</b>	<b>Introduction</b> .....	<b>87</b>

<b>5.3</b>	<b>Materials and methods</b> .....	<b>89</b>
5.3.1	Materials and instruments .....	89
5.3.2	Skin .....	89
5.3.3	Skin absorption experiments .....	89
5.3.4	Isolation of the different skin compartments .....	90
5.3.5	Determination of the stretching factor for data correction .....	90
5.3.6	Validation of the stretching factor .....	92
5.3.7	Mass balance .....	92
5.3.8	Quantification.....	92
5.3.9	Pharmacokinetic modelling.....	93
5.3.10	Detailed diffusion model.....	94
5.3.11	Statistics .....	95
<b>5.4</b>	<b>Results</b> .....	<b>96</b>
5.4.1	Validation of the stretching factor .....	96
5.4.2	FFA mass profiles.....	97
5.4.3	Caffeine mass profiles .....	100
<b>5.5</b>	<b>Discussion</b> .....	<b>104</b>
5.5.1	Experimental data .....	104
5.5.2	Pharmacokinetic model .....	104
5.5.3	Detailed diffusion model.....	105
5.5.4	Comparison of the models .....	105
5.5.5	Lateral skin parts .....	105
<b>5.6</b>	<b>Conclusion and outlook</b> .....	<b>107</b>
<b>6</b>	<b><i>Finite dose skin penetration: Concentration depth profiles – Comparison between experiment and simulation</i></b> .....	<b>109</b>
<b>6.1</b>	<b>Abstract</b> .....	<b>110</b>
<b>6.2</b>	<b>Introduction</b> .....	<b>111</b>
<b>6.3</b>	<b>Materials and Methods</b> .....	<b>112</b>
6.3.1	Penetration experiments .....	112
6.3.2	Tape-stripping procedure.....	112
6.3.3	Cryo-sectioning of the deeper skin layers.....	112
6.3.4	Mass balance .....	112
6.3.5	Quantification by HPLC.....	112
6.3.6	Concentration depth profiles .....	113
6.3.7	Detailed diffusion model.....	113
<b>6.4</b>	<b>Results</b> .....	<b>114</b>
6.4.1	FFA.....	114
6.4.2	Caffeine .....	117
<b>6.5</b>	<b>Discussion</b> .....	<b>121</b>
6.5.1	Experimental data .....	121
6.5.2	Correlation between experiment and simulation.....	122
<b>6.6</b>	<b>Conclusion</b> .....	<b>123</b>
<b>7</b>	<b>Summary</b> .....	<b>125</b>

<b>8</b>	<b><i>Zusammenfassung</i></b> .....	<b>127</b>
<b>9</b>	<b><i>Appendix: A detailed description of skin segmentation</i></b> .....	<b>149</b>
9.1	<b><i>Abstract</i></b> .....	<b>150</b>
9.2	<b><i>Tape-stripping</i></b> .....	<b>151</b>
9.3	<b><i>Cryo-sectioning of the deeper skin layers</i></b> .....	<b>153</b>
9.4	<b><i>Extraction of drug from tape-strips and deeper skin layers</i></b> .....	<b>155</b>
9.5	<b><i>Measurement of the skin thickness</i></b> .....	<b>155</b>
9.6	<b><i>Data treatment and plotting</i></b> .....	<b>157</b>
<b>10</b>	<b><i>Abbreviations</i></b> .....	<b>167</b>
<b>11</b>	<b><i>Curriculum vitae</i></b> .....	<b>169</b>
<b>12</b>	<b><i>List of publications</i></b> .....	<b>171</b>
<b>13</b>	<b><i>Acknowledgement</i></b> .....	<b>175</b>



## Short summary

In this thesis finite dose skin absorption experiments were evaluated with respect to experimental setup and mathematical modelling. To increase the comparability between experiment and modelling, the experiments need to be carefully assessed. Thus, the use of infrared densitometry was judged suitable to quantify *SC* on tape-strips *in vitro* to increase the accuracy of the obtained concentration depth profiles in the *SC*.

*In vivo*, usually a small dose of the formulation is applied to the skin, a so-called finite dose. Finite dose skin absorption experiments were performed, which are closer to the *in vivo* reality. The influence of non-homogeneous donor surface distribution was investigated with respect to the permeated drug amount as this had not been done before. A dependence on the physicochemical parameters of the drug was found.

With the knowledge obtained before, finite dose skin penetration experiments were performed. The experimental data was analyzed with different mathematical models. A pharmacokinetic model developed for this study could describe the mass profiles in all compartments well, even in the lateral skin part. A 2D diffusion model previously developed for infinite dose and adapted to finite dose could predict the mass profiles and concentration depth profiles of finite dose experiments for the model drugs caffeine and flufenamic acid reasonably.

## Kurzzusammenfassung

In dieser Arbeit wurden finite dose Hautabsorptionsversuche evaluiert im Hinblick auf experimentellen Aufbau und mathematische Modellierung. Um die Vergleichbarkeit zwischen Experiment und Mathematik zu verbessern, müssen die Versuche sorgfältig überprüft werden. Deshalb wurde Infrarot Densitometrie untersucht und als geeignet befunden, SC auf Tape-strips *in vitro* zu quantifizieren, um die Präzision von Konzentrationsschichttiefenprofilen im SC zu erhöhen.

*In vivo* wird üblicherweise eine kleine Donormenge auf die Haut aufgetragen, eine sogenannte finite dose. Finite dose Hautabsorptionsversuche wurden durchgeführt, ähnlich der *in vivo* Situation. Der Einfluss von inhomogener Donorverteilung auf der Hautoberfläche wurde in Abhängigkeit der permeierten Arzneistoffmenge analysiert, was bisher noch nicht getan wurde. Es wurde eine Abhängigkeit von den physikochemischen Eigenschaften des Arzneistoffes gefunden.

Mit dem zuvor erhaltenen Wissen wurden Hautpenetrationsversuche mit finiter Dosierung durchgeführt. Die experimentellen Daten wurden mit verschiedenen mathematischen Modellen analysiert. Ein für diese Studie entwickeltes pharmakokinetisches Modell konnte die Massenprofile in allen Kompartimenten gut beschreiben, sogar im lateralen Hautteil. Ein zuvor für infinite dose entwickeltes und nun für finite dose adaptiertes 2D Diffusionsmodell konnte die Massenprofile und Konzentrationsschichttiefenprofile für die Modellarzneistoffe Coffein und Flufenaminsäure plausibel vorhersagen.

## Introduction

Parts of this chapter have been published in:

Measuring skin absorption in vitro

Hahn T, Schaefer UF, Lehr CM

SOFW-Journal | 136 | 1/2-2010

Das geht unter die Haut – Aufbau der humanen Haut und mögliche Invasionswege

Hahn T, Selzer D, Neumann D, Schaefer U F

PZ Prisma, 1; 35-43, 2011

## 1.1 *Absorption pathways of the skin*

Even though the skin is a strong barrier for exogenous substances into the body, it has become an interesting target for drug absorption. Mainly, this is due to the large surface area of the skin, and of the possibility of easy and pain free application of the drug.

### 1.1.1 Structure of the skin

The skin is the biggest organ of the human body with a surface area of 1.7 to 2 m<sup>2</sup> and a weight of more than 10% of the body mass. It is the outer barrier between the body and the environment and protects the body from external influences.

The skin is made up of three cellular layers, of which each has its own structure and function. The outermost cellular layer of the skin is the epidermis, which itself can be divided into the viable epidermis consisting of living cells, and the non-viable stratum corneum (SC). The latter is the strongest barrier of the skin. The dermis lies directly underneath the epidermis and consists of compact connective tissue nerved with blood and lymph vessels. These supply the epidermis with nutrients and remove absorbed exogenous substances, acting as sink. The subcutaneous fatty tissue consists of loose connective tissue, and its dimensions vary greatly on different regions and individuals.

For further information about the anatomical structure of the skin, the reader is referred to [1-3].

#### *Stratum corneum (SC)*

The SC as the outermost layer of the epidermis is normally between 10 and 25 µm thick and consists of 15 to 25 layers of corneocytes [4,5]. These are completely cornified squamous epithelial cells, which are around 1 µm thick. They consist mainly of keratin, a structure protein with high mechanical and chemical stability. Each corneocyte is surrounded by a cornified envelope, which allows for covalent linkage with the intercellular lipids. The corneocytes are embedded in a lipid matrix, which is arranged in lipid bilayers and consists of ceramides, free fatty acids, and cholesterol.

This characteristic structure of the SC is represented in the so called brick-and-mortar model [6] (**fig. 1-1**). In this model, the bricks represent the corneocytes embedded in the mortar as the lipid phase.

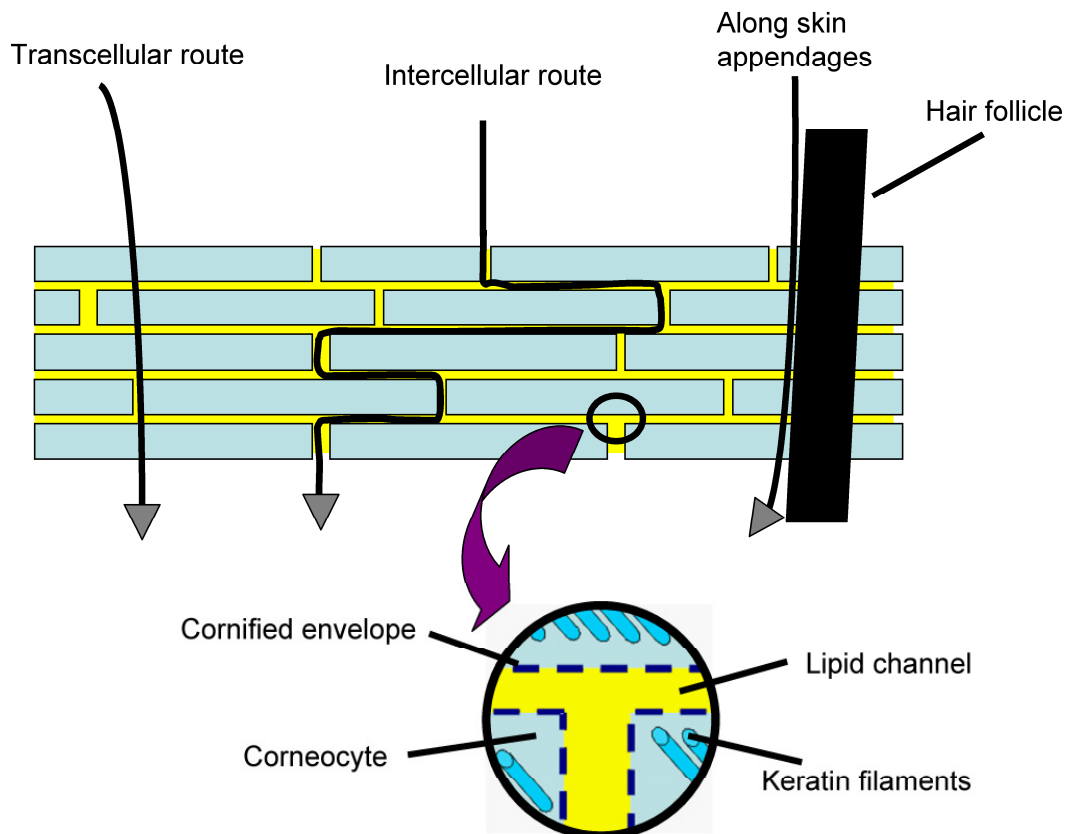


**Figure 1-1** Brick and mortar model of the SC and possible penetration pathways through the SC. Modified from [2] and [7].

### 1.1.2 Application to the skin

When describing the application of a formulation to the skin, different cases can be distinguished: formulation **remaining on the skin**, or **absorption to the skin**, which can be further divided into **penetration** and **permeation** (fig. 1-2).

The formulation **remaining on the skin** surface is the part of the formulation that does not enter the skin and is not absorbed into the skin. For certain formulations, this is the target site and the whole formulation should remain on the surface to protect the skin, e.g. sunscreens.

**Penetration** refers to the absorption of a substance into the different skin layers, which is important e.g. for locally acting drugs and most cosmetic products. Therefore, penetration experiments are mostly performed on full-thickness skin to account for the different skin layers available for the drug, e.g. the SC and the deeper skin layers. To determine the penetrated amount in the different layers, skin segmentation is required (for details see *chapter 10 Appendix*).

When a substance during incubation penetrates only into the upper SC layers, it is not completely lost for further absorption. Instead, it was shown that the SC may act as a reservoir for certain substances [8,9]. For glucocorticoids, a skin blanching effect after re-occlusion of pre-incubated skin could be shown [10]. In another study, the antifungal drug miconazole remained in the SC for 24 h after removal of the drug formulation [11].

**Permeation** on the other hand is defined as the transport of a substance across a membrane into an acceptor. In the case of skin, the permeated drug amount becomes systemically bioavailable after reaching the blood vessels. This aspect is most relevant in the context of transdermal therapeutic systems, but also to assess systemic toxicity of compounds applied to the skin. Permeation experiments are often carried out with thinner skin layers, e.g. heat-separated epidermis. As blood vessels can be found below the viable epidermis, the permeation through heat-separated epidermis represents the absorption of a substance into the systemic circulation.

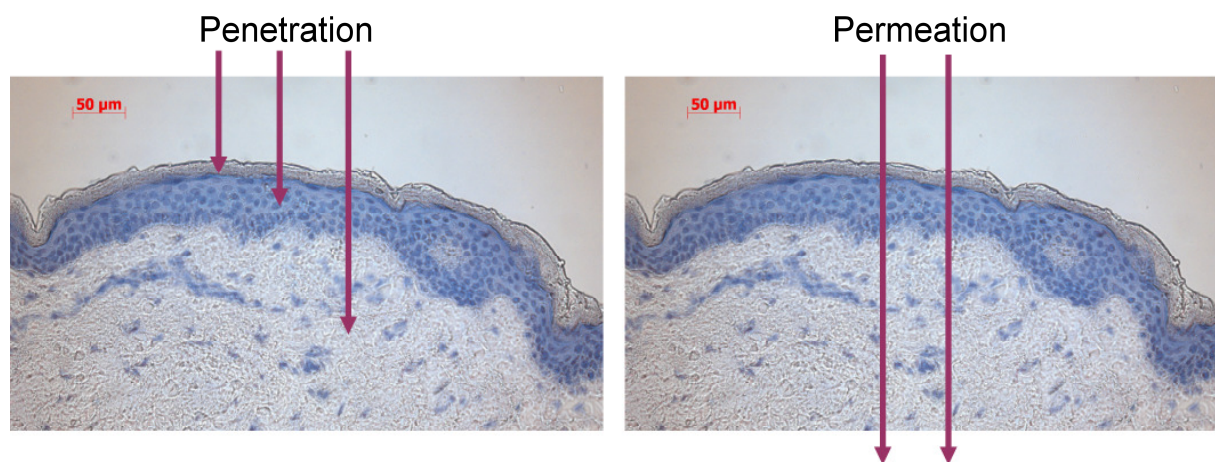


**Figure 1-2** Absorption to the skin: Penetration vs. permeation illustrated on histological cross-sections of full-thickness skin stained with haematoxylin at 200 x magnification.

### 1.1.3 Pathways across the SC

Based on its anatomical structure the skin acts as a strong barrier both for exogenous substances into the body and for endogenous substances out of the body, e.g. water evaporation from the skin. The SC with its unique brick and mortar structure is the most important layer for the barrier function of the skin. When a substance is applied to intact skin different absorption pathways across the SC are possible (**fig. 1-1**).

- *Along the skin appendages (macroscopic ways)*

The appendages route is composed of both glandular and follicular pathways, of which the latter one seems to be predominant. Recent studies report that the follicular route may be of particular relevance to liposomes and nanoparticles [12,13], even though they only contribute to around 0.1% to 1% of the skin surface area [4,14,15].

A pump effect is discussed, which could transport the particles deep into the hair follicle by movement of the hair [13].

- *Across the intact stratum corneum (microscopic ways)*

In general, the transport through the SC is regarded as a passive diffusion process. Two pathways are possible:

#### *Intercellular route*

The intercellular route is considered as the predominant one for most compounds. In this case, substance transport occurs within the continuous, bilayer-structured intercellular lipid domain of the SC. Although this pathway is very tortuous due to corneocyte overlapping [16,17] and, hence much longer than the total thickness of the SC, it is considered to result in much faster absorption due to a higher diffusion coefficient of most substances within the lipid phase compared to the corneocytes [18,19]. As in the intercellular route diffusion occurs in the identical medium, partition effects are not relevant.

#### *Transcellular route*

Normally, the transcellular route is considered as of minor importance for dermal absorption due to low permeability of most substances in the corneocytes. In this transport route, substances have to partition from the hydrophilic corneocytes to the intercellular lipid layers of the SC and vice versa several times. However, the transcellular pathway may become more important after application of a penetration enhancer, e.g. urea. Thus, the permeability of the corneocytes increases due to alteration of the keratin structure.

Recently, the transcellular pathway has been investigated and may be more relevant than expected before [18-20].

The barrier function of the skin can easily be determined by measuring the TEWL (transepidermal water loss) *in vivo*. In this method, the amount of water evaporating

through the skin per time and area is measured. As this method is non-invasive, it is often used for cosmetic studies, e.g. to show that the barrier function of the skin is restored after application of a certain formulation.

In normal skin, there is always a certain amount of water leaving the skin to the environment. On most anatomical sites values of less than  $10 \text{ g/m}^2\cdot\text{h}$  can be found [21,22]. If the barrier function of the skin is disturbed, e.g. by tape-stripping or contact with detergents, the TEWL might reach values of  $40 \text{ g/m}^2\cdot\text{h}$  or higher [23,24]. Similar values are obtained on intact skin on certain anatomical sites, e.g. the palms of the hands [22].



## 1.2 *In vitro* skin absorption experiments

Quantitative data on the bioavailability of compounds applied to the skin are of increasing interest, not only for the pharmaceutical, but also for the cosmetic industry. Apart from studying the efficacy of a substance, information on the rate and extent of dermal and transdermal absorption is most relevant also for the safety assessment for all kinds of xenobiotics, such as e.g. sun blockers or pesticides. In fact, such information is explicitly requested by the EU initiative REACH - Registration, Evaluation, Authorisation and Restriction of Chemicals [25].

Clinical studies, i.e. *in vivo* experiments on humans, will always remain the gold standard to proof the safety and efficacy of drugs in dermal therapy. However, considering ethic aspects as well as high costs of clinical studies, pre-clinical *in vitro* skin absorption models are still very valuable as development tools and frequently used for such purposes. Also, detailed knowledge of the skin absorption process, such as e.g. drug distribution into the deeper skin layers or accumulation in a distinct skin layer is not readily available from *in vivo* experiments.

Besides, since 2009 *in vivo* animal testing of cosmetic products is banned by EU regulation 76/768/EEC throughout the European Union [26]. Therefore, other techniques must be used to obtain the desired information. One possibility is the use of *in vitro* penetration and permeation models. General instructions concerning skin absorption studies are provided by the OECD Guideline 428 [27] in combination with Guidance document 28 [28], Scientific Committee on Consumer Products [29], by the European Commission [4], and the Food and Drug Administration (FDA) of the United States [30]. However, all of these documents lack detailed information on practically suitable methods.

Experiments have shown that *in vitro* experiments are predictive for *in vivo* skin absorption [31-36]. *In vitro* permeation and penetration experiments with excised human skin are therefore useful tools to obtain knowledge of drug transport across or into the skin, respectively.

### 1.2.1 Tissues used for *in vitro* skin absorption experiments

Due to its good accessibility, the volar forearm is commonly used for human *in vivo* studies, whereas for *in vitro* studies, mostly abdominal or breast skin is used. Dependent on the anatomical region, the absorption rate through the skin might be up to 40 fold different [37]. Human skin is usually obtained from cadavers, plastic surgery or amputations. The skin can be used either directly after excision or after proper storage in a freezer. Storage for several months without impairment of the barrier function is possible, provided that repeated thawing and freezing of the skin is avoided [38-41]. The advantage of fresh skin is that a certain metabolic activity may be maintained during the experiments, which is essential when skin absorption is influenced by active metabolic processes. However, it is generally assumed for most substances that the skin absorption is a passive diffusion process and that the main absorption barrier is the SC. Furthermore, the absence of dermal blood flow *in vitro* may build up a significant hindrance to diffusion [42]. Moreover, reducing the membrane thickness will generally reduce the run time of an experiment and thus minimize the risk of microbial contamination.

*Full-thickness skin* is often used for penetration experiments since information about all skin layers can be gained. For permeation experiments full-thickness skin is often not appropriate, because the permeated amount is quite low and the diffusion resistance of the dermis is over predicted [43].

In that case, *full-thickness skin* can be treated with a dermatome, which cuts a surface-parallel skin layer with a defined thickness. *Dermatomed skin* or *split skin* comprises epidermis including SC and parts of the dermis. Dermatomed skin is often used in a thickness between 200 to 400  $\mu\text{m}$  for human skin [28,44].

*Heat-separated epidermis* can be prepared by complete removal of the dermis by mechanical, thermal or chemical techniques. Usually, the epidermis is split from the dermis by placing the skin in water of 60°C for 30-120 seconds [45]. It has been shown that the barrier function was not impaired by this treatment [43,46].

Finally, the *stratum corneum* may be isolated by enzymatic digestion of the connective epidermal tissue. This may be achieved by complete immersion of full-thickness skin in a trypsin solution buffered at pH 7.4 or by placing heat-separated epidermis on a filter paper soaked with the enzyme preparation for 24 h at 37°C [32,45].

Human skin is preferred for all *in vitro* skin experiments, as animal skin often leads to different absorption behaviour [47,48]. However, sources of human skin are limited and therefore alternatives may be required. Due to its high similarity to human skin, both in morphology and permeability, pig skin is a convenient alternative [49]. Skin of other animal species should only be used, if the method is fully validated. For comparison of relative permeability of different formulations only, animal skin, preferably from hairless strains, might be useful. Nonetheless, the results need to be confirmed by relevant additional experiments.

Due to the limited availability of human skin, there has been an increasing demand for bioengineered human skin equivalents, of which several have become commercially available and been evaluated for their use as *in vitro* dermal absorption models. However, a first validation study has revealed that bioengineered human skin equivalents have a significantly lower barrier function than natural human skin and thus a much higher permeability for the tested compounds [50]. Nevertheless, bioengineered skin epidermis equivalents have been shown to be suitable for corrosivity and phototoxicity testing [51]. Recently, reconstructed skin equivalents have been validated for corrosion testing and approved by the OECD [26,52].

Even when using human skin, care has to be taken to choose the appropriate set-up and preparation of the tissue, depending on the objectives of the study. However, if these critical points are correctly addressed, skin absorption studies *in vitro* may provide valuable information.

### **1.2.2 *In vitro* skin permeation models**

Over the last decades, many methods have been designed to study drug transport through the skin (permeation) and drug distribution within the different skin layers (penetration). This information is essential for pharmaceutical and medical applications with respect to drug invasion, drug bioavailability and safety aspects as well as for risk assessment of chemicals [25].

For years, researchers have used variations of two-compartment *in vitro* test systems to measure the diffusion of a compound from one side of a membrane to the other. Different setups have been compared previously [53]. Both static and dynamic diffusion cells are available and approved by the authorities [28,44].

In general, a donor compartment is separated from an acceptor compartment by a membrane of native skin, specific skin layers, or some artificial skin equivalents. Samples from the acceptor compartment, usually a physiological buffer solution of pH 7.4, can either be taken continuously or at pre-determined time points.

Experiments should be carried out in a way that surface temperature is 32°C mimicking the *in vivo* situation. The temperature may be controlled by a water bath, a water jacket around each cell, or by placing the diffusion cell in a drying oven.

To simplify data analysis, experiments are generally run under sink conditions. These are generally maintained as long as no more than 10% of the compound has been transported out of the donor compartment [44]. Moreover, to maintain sink conditions, no more than 10% of the saturation concentration of the drug in the acceptor should be reached [28]. If not, the absorption might be reduced by low solubility of the drug in the acceptor fluid.

### *Franz Diffusion Cell*

The most commonly used permeation test system is the static Franz diffusion cell [31]. The Franz diffusion cell consists of a donor compartment and an acceptor compartment (**fig. 1-3**) with the appropriate membrane sandwiched between these two compartments. The donor compartment contains the drug preparation, which might be an ointment, a solution or even a patch. The chamber beneath the membrane holds an acceptor fluid, which is continuously mixed with a magnetic stir bar.

The Franz diffusion cell combines many advantages: It is an inert, robust instrument, which is easy to handle. It is maintainable at a constant temperature and has precisely calibrated volumes and diffusion areas, and it facilitates easy sampling and replenishment of the acceptor medium.

The permeation behaviour of a substance through the membrane can be determined by sampling at predefined time points. Aliquots of the acceptor fluid are removed through the sampling arm for analysis to determine the rate and extent of transdermal absorption. After removing a probe from the sampling arm, the volume is replaced by fresh medium. Care needs to be taken to avoid any air bubbles below the membrane.

The donor chamber may either be left open or be occluded. Non-occluded conditions permit an exchange with the environment, such as evaporation of volatile substances and drying of the skin surface. This setup is usually desired for liposome examination for they are

supposed to be better absorbed due to the water gradient across the skin [54]. In contrast, a tight occlusion of the skin surface may lead to excessive skin hydration. This effect is sometimes desired to achieve a higher drug absorption, e.g. in Transdermal Therapeutic Systems (TTS).

One problem often encountered with this setup is the realization of sink conditions for low soluble substances in aqueous media. For such purposes organic solvents, non-ionic surfactants, proteins (BSA) or cyclodextrines are sometimes added as solubility enhancers [28]. However, it is important to keep in mind that these additives may have a severe impact on skin integrity and barrier function, and therefore interpretation of such data has to be done very cautiously.

Franz diffusion cell experiments can also be adapted to penetration experiments as the skin can be segmented after incubation in the Franz diffusion cell [32].

All skin absorption experiments presented in this thesis were performed with Franz diffusion cells.

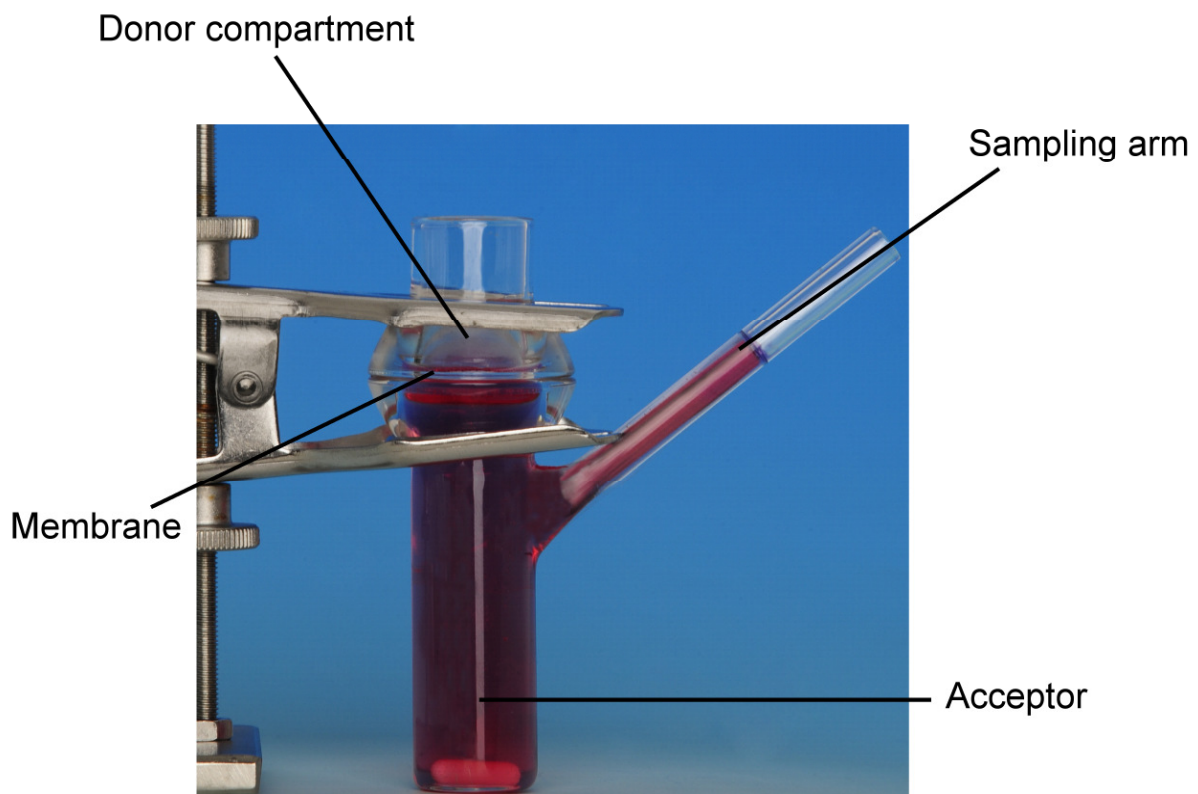


**Figure 1-3** Franz Diffusion Cell. Images courtesy of Mr. Puetz, Saarland University.

### *Flow-through diffusion cell*

In the flow-through diffusion cell the fresh buffer is continuously pumped through the acceptor chamber [55]. Thus, sink conditions can be maintained more easily throughout the whole experimental period. This is important if the absorption rate of the substance is high and/or the solubility in the acceptor phase is low. A minimum flow-rate is necessary to ensure thorough mixing, to remove the absorbed material rapidly, and to minimize unstirred layers [56]. For the majority of substances a higher flow-rate does not change the absorption characteristics, with the exception of very low soluble substances, such as e.g. testosterone. Furthermore, the skin viability is prolonged [55,57,58] due to constant replacement of the physiological acceptor solution. Therefore, possible metabolism in the skin can be investigated.

Contrastingly, the constant flow of fresh donor below the skin leads to an increased partitioning of hydrophobic compounds from the skin to the acceptor solution. This may change skin properties and therefore influence the permeation process.

### **1.2.3 *In vitro* skin penetration model**

#### *Saarbruecken penetration model*

The Saarbruecken penetration model was developed to study the rate and extent of drug penetration into the different skin layers [32,59]. Here, in contrast to the Franz diffusion cell and the flow-through cell, the skin for itself acts as the acceptor for the penetrating drug. The major advantage of this set-up is that excessive hydration of the skin can be avoided. In addition, possible changes of the skin's quality and barrier function caused by the acceptor medium are prevented. Depending on the drug, the incubation time should be limited to the time until the drug reaches the lowermost layer of the skin. After this point, sink conditions are not further maintained, resulting in complicated kinetics which are difficult to interpret.

## 1.3 *Finite dose*

### 1.3.1 Comparison finite and infinite dosing

In contrast to infinite dose experiments with an infinitely large donor and therefore negligible changes in the donor concentration over the whole incubation time (less than 10%), in the finite dose regime only a limited amount of the donor formulation is applied to the skin surface. The application of a finite dose best resembles the *in vivo* patient exposure situation when applying e.g. an ointment. Due to the small applied formulation volume the donor concentration will significantly decrease during the time course of the experiment (donor depletion). The nature of finite dose experiments allows for observation of special effects, like the influence of evaporation of excipients [60]. These effects are not visible in infinite dose experiments.

Per definition in OECD guideline 428 [27] and guidance document 28 [28], finite dose skin absorption experiments are characterized by the application of  $\leq 10 \mu\text{l}/\text{cm}^2$  of a liquid formulation to the skin. For semisolid and solid substances, values range between 1 and  $10 \text{ mg}/\text{cm}^2$  [27-29]. Although most publications dealing with finite dose follow this definition [61-71], other values are also reported [72-79].

This thesis follows the definition of the OECD guidelines [27,28].

### 1.3.2 Challenges associated with experimental finite dose setup

In normal *in vivo* patient regime, the semisolid formulation is applied to the skin and distributed by a finger or hand. However, for *in vitro* finite dose experiments, an adaptation of this method is required to ensure the application of a defined drug amount to the skin and a homogeneous drug distribution. Therefore, this chapter gives a short overview about experimental challenges.

#### *Experimental incubation time*

As shown above, the definition of finite dose experiments varies in different papers. To harmonize the results, a generally accepted definition would be the aim. However, a general definition for all substances is difficult since finite dose characteristic kinetics, e.g. donor depletion, may be obtained only after long exposure times for some chemicals and may not

be reached during the course of the experiment. Thus, the incubation time needs to be adapted to the experimental setup, e.g. the drug and the vehicle.

### *Application and distribution of the drug*

The application of a clearly defined amount of drug to the skin is essential for the correct evaluation of the experiments, e.g. for calculation of the mass balance.

Furthermore, a homogeneous drug distribution over the entire incubation area is important. If a homogeneous distribution can not be ensured, the variation between the experiments may increase [72]. It is quite difficult to spread the donor formulation evenly over the incubation area since only a very small volume of the donor formulation is applied to the skin.

To ensure both requirements are fulfilled, semisolid formulations are mostly applied and distributed manually, employing metal [80], glass [65,81] or plastic [82] spatulas [83], or a glass rod [64,70,84-87].

As it is crucial to know the exact applied dose in finite dose experiments, the amount of drug remaining on the mechanical distribution device, unapplied to the skin, is essential. Thus, the application device needs to be analyzed for the exact amount of applied formulation, which can be determined by weight [65,70,81,84,85] or extraction of the remaining formulation from the application device [64].

For liquid formulations the weight determination is delicate, as evaporation might affect the measurement. Thus, a defined volume of the liquid formulation is usually applied with a positive displacement pipette [62,63,88] or a micro syringe [84]. For standardization, for each experiment a reference volume can be pipetted, and the drug amount analyzed.

Liquid formulations are often distributed over the skin surface by the positive displacement pipette used for application [62,88]. Other methods are placing a teflon disc onto the formulation to increase spreading [50] or using an appliance, e.g. a micro centrifuge tube [11] or the rubber tip of a 1 ml syringe plunger [63] or an inoculating loop [71] for distribution.

Further methods, such as massage of the skin lead to uniform distribution of the formulation, but the mechanical stress might have an influence on the absorption behaviour. In some cases, e.g. for nanoparticles, this might even be desired, leading to higher concentrations in hair follicles after massage of the skin due to a pumping mechanism [13].



As the SC is a lipophilic layer, the distribution of lipophilic formulations over the surface may be more homogeneous than for hydrophilic formulations. Also, the distribution can be increased by adding an emulsifier to the formulation. However, both methods may change the absorption characteristics of the substance under investigation.

Ideally, the application method should result in a homogeneous layer of the drug formulation over the whole incubation area. The influence of inhomogeneous donor distribution over the skin surface on permeation is investigated further in *chapter 4*.

#### *Mass balance*

Due to the limited amount of drug applied to the skin, a mass balance is required for each experiment to ensure the recovery of the entire drug. A reproducible and quantitative recovery is indispensable for correct evaluation of the data. In the OECD guidelines [27,28], it is stated that  $100\pm 10\%$  of the drug should be recovered after the experiment. In another guideline the range was broadened to  $100\pm 15\%$  [29]. To achieve these limits, not only the skin and the surface of the skin need to be analyzed, but also all instruments/devices in contact with the drug, e.g. the diffusion cell. Furthermore, a low limit of quantification for the substance under investigation is required.

### 1.3.3 Principles of finite dose kinetics

The absorption process of a substance into or through the skin is usually assumed to be a passive process, controlled by diffusion. Thus, both infinite dose and finite dose experiments can be described by Fick's laws.

Diffusion across a homogeneous membrane between donor and acceptor compartment can be described by Fick's first law [89], treating the skin layer as a pseudo-homogeneous membrane

$$J = -D \frac{\partial C}{\partial x} \quad (\text{Equation 1-1})$$

with the flux  $J$  [ $\mu\text{g}/\text{cm}^2 \cdot \text{h}$ ] as the transport rate per time of a compound, the concentration gradient  $\partial C/\partial x$ , and the diffusion coefficient  $D$ . Assuming that sink conditions apply, the concentration inside the membrane is zero at the beginning of incubation. Furthermore, at  $x=0$  the concentration is in local equilibrium with the vehicle.

To simulate the varying concentration of a drug within the membrane, Fick's second law [89] can be employed.

$$\frac{\partial C}{\partial t} = D \frac{\partial^2 C}{\partial x^2} \quad (\text{Equation 1-2})$$

This equation is derived from the combination of a differential mass balance with Fick's first law. This equation assumes that the compound neither binds, nor is metabolized, and that the barrier properties remain constant over time and position.

The maximum absorption rate to the skin may be reached for some time during finite dose experiments, but is not maintained [28], which is due to the depletion of drug in the donor compartment. Under finite dose conditions the donor decrease is more than 10% of the initial concentration [4]. An effect of this donor depletion can only be seen after some time in the absorption profile when the flux decreases over time. Thus, a 'quasi-steady-state' at the beginning of the incubation might be reached for a short time.

In general, the absorption process can be divided into three main phases as described in [90]: In the lag-phase the drug diffuses into the skin and slowly fills up the different skin layers. In the following rising phase some drug enters the acceptor compartment and rises with time. Afterwards, in the falling phase the strongly decreased drug amount in the donor compartment (donor depletion) leads to a decreasing flux across the skin.

- *Permeation*

Permeation experiments often employ a thinner skin membrane than penetration experiments, e.g. heat-separated epidermis. Thus, the drug enters the acceptor faster. The accumulation in the acceptor is measured at different sampling intervals.

When comparing the permeation profile of a finite dose experiment to an infinite dose experiment, at the early stage, the finite dose permeation profile resembles the infinite dose profile (**fig. 1-4 A**). However, after a certain time, the infinite dose experiments reach a steady-state, characterized by a constant flux  $J_{ss}$  of the drug through the membrane (**fig. 1-4 B**). This is not the case in finite dose experiments, where after reaching donor depletion the absorption rate (flux) decreases and the cumulative drug amount in the acceptor approaches a maximum.

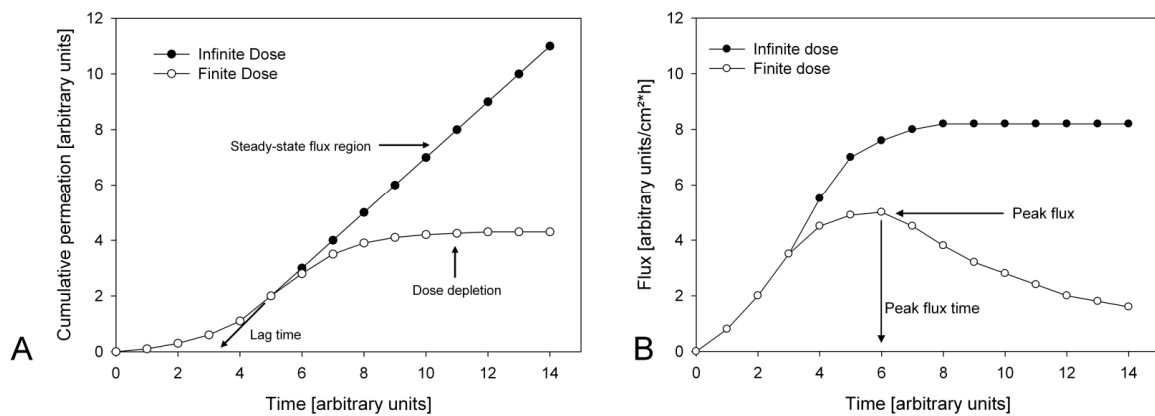


**Figure 1-4** Permeation kinetics of infinite and finite dose. A: Cumulative permeated amount over time. B: Flux over time. Modified from [4].

- *Penetration*

In penetration experiments, usually full-thickness skin is employed and the absorption of the drug into the different skin layers is investigated. For analysis of the drug distribution within the different layers, the skin is segmented and the drug concentration in the different skin sections is calculated. The segmentation of the skin is usually performed by first tape-stripping the SC and then horizontal cutting of the deeper skin layers (*DSL*). Following quantification of the drug amount in each sample, the drug concentration normalized to the respective skin volume can be determined for a certain skin depth. From analysis of samples from different skin depths, concentration depth profiles can be established (**fig. 1-5**). For more information see *chapter 10 Appendix*.

Infinite dose concentration depth profiles at all times have a higher concentration at the outer SC layers compared to the innermost SC layers. The concentration of the drug in the SC slowly increases with increasing incubation time, thus changing the shape of the profile from an exponential decay to a linear regression over depth at steady-state (**fig. 1-5 A**).

For finite dose experiments, the concentration depth profile at the first time point is similar to the infinite dose scheme. Then, the drug concentration in the deeper SC layers increases over time, still similar to infinite dose, however with the concentration at the outermost SC part not increasing. Afterwards, the concentration in the outer SC layers decreases as the donor depletes, the shape of the curve slowly turning from exponential decay to linear but flat profiles at the longest incubation times (**fig. 1-5 B**).

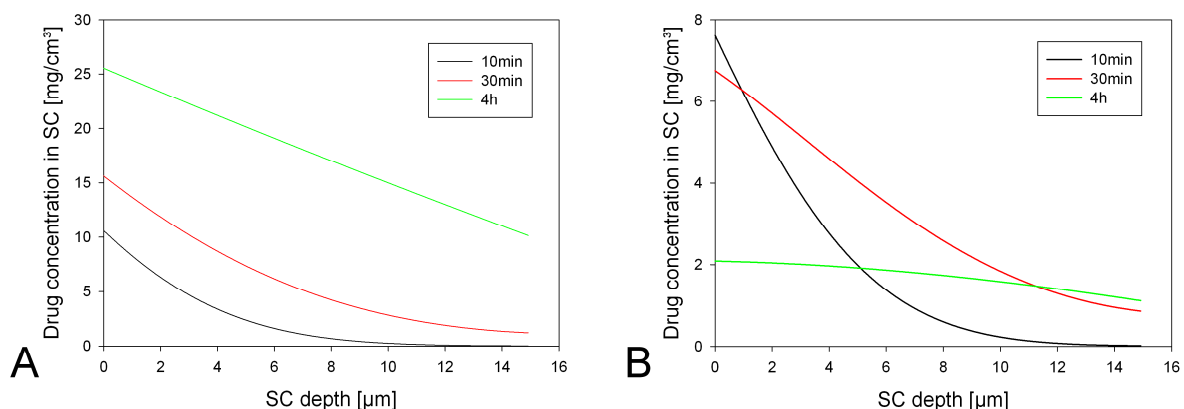


**Figure 1-5** Concentration depth profiles in the SC for different incubation times. A: Infinite dose. B: Finite dose. Example data calculated with DSkin (developed by Dominik Selzer, Master Thesis).

Another information that can be obtained from penetration studies is the cumulative drug amount in each skin layer, e.g. in the *SC* or the *DSL*. This data can be plotted against the time resulting in mass profiles of the drug in the different compartments. From these results, information about certain kinetic characteristics can be analyzed, e.g. the formation of a drug reservoir in a skin layer.

For infinite dose experiments, the drug amount in the *SC* approaches a maximum representing the steady-state and thus saturation of the drug in the respective layer (**fig. 1-6**, dashed line). The data can be fitted to Michaelis-Menten-kinetics [32], which is applicable to saturable processes. With this method the drug amount during steady-state in the *SC* can be determined for infinite dose, as well as the time until half of the maximum drug amount is reached.

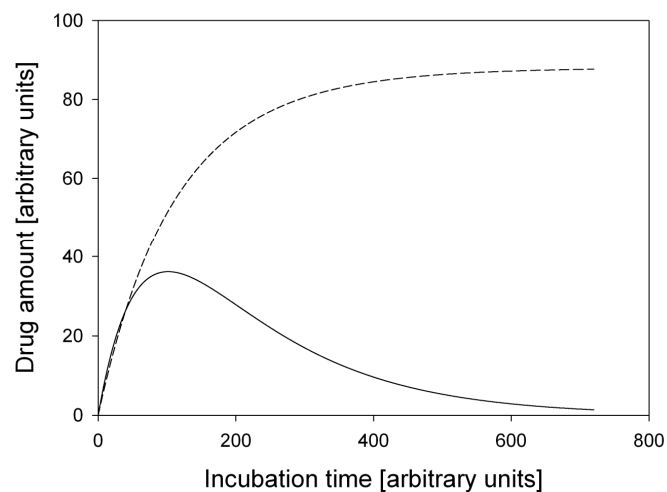


**Figure 1-6** Schematic accumulation of a model drug in the *SC* for finite dose (solid line) and infinite dose (dashed line) scenario. Not drawn to scale.

In contrast to infinite dose experiments, the donor depletes over time in the finite dose scenario (**fig. 1-7 Donor**). The drug amount in the *SC* increases at the beginning, but after donor depletion the rate of absorption of drug to the *SC* is decreased and the drug amount in the *SC* decreases over time (**fig. 1-7 SC**). Thus, the amount of drug in the *SC* will continue to diffuse into the *DSL*, whereas this layer is not filled up as strongly as at the beginning from the donor side (**fig. 1-7 DSL**). The *DSL* is then still constantly filled up with drug, and drug enters the acceptor. At long incubation times the drug amount in the *DSL* will decrease, too. The acceptor is constantly filled up over time, reaching a maximum (**fig. 1-7 Acceptor**).

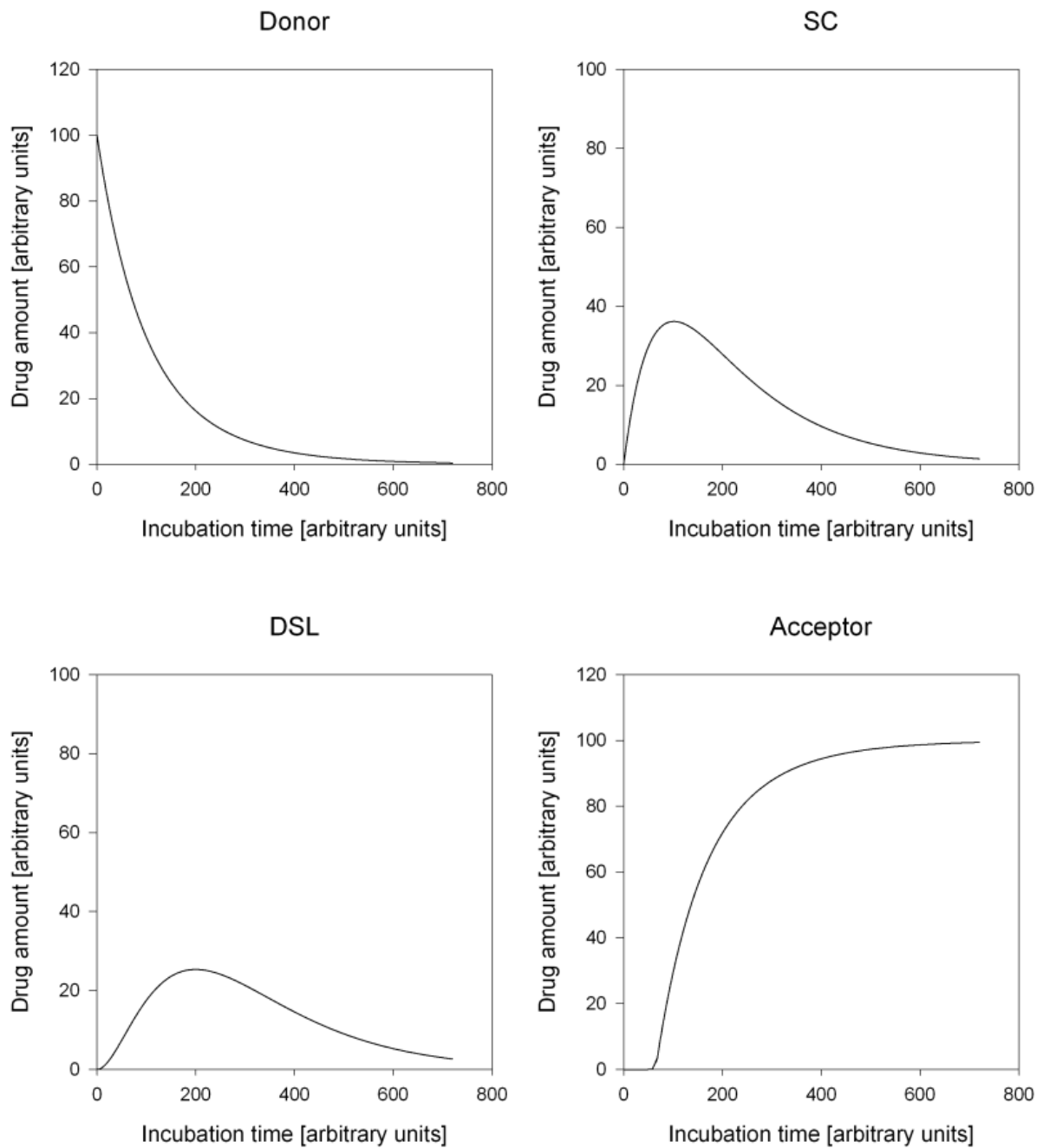


**Figure 1-7** Schematic accumulation of a model drug after finite dose application in the different skin compartments. Not drawn to scale. Establishing of the profiles with the help of Dominik Selzer.

## 1.4 Modelling of skin absorption

Since skin absorption experiments are time consuming and expensive, easier and faster ways of predicting the absorption kinetics of a drug to the skin are of great interest. With the help of mathematical calculations, valuable information can be gained about the absorption of the substance under investigation.

Most mathematical predictions require physicochemical parameters of the substance, e.g. the molecular weight  $MW$  and partition coefficient  $\log K_{o/w}$  [91]. In general, smaller substances penetrate the  $SC$  faster than larger substances and the absorption of compounds above 500 Da rapidly decreases with increasing size [92].

The partition coefficient has a major influence on skin absorption due to the lipophilic character of the  $SC$ , leading to low partitioning of hydrophilic compounds into this layer. Thus, lower concentrations are available for further partitioning into the hydrophilic viable skin layers. On the other hand, highly lipophilic compounds partition easily into the  $SC$ , but only reluctantly to the viable skin layers. Thus, systemic absorption is also hindered. A value of 1 to 3 for  $\log K_{o/w}$  has been proposed to indicate good skin absorption [93].

A factor, which has recently been investigated, is the binding property of a drug to proteins in the corneocytes [20,94], which would decrease the speed and amount of drug absorption [95]. Furthermore, dependent on the drug the ionization state may change the absorption of the compound [96]. Due to the lipophilic nature of the  $SC$ , most compounds are better absorbed in the non-ionized form, e.g. flufenamic acid. The  $K_{o/w}$  for ionisable compounds can be corrected with respect to the pH of the buffer applied, resulting in the  $\log D$  value [94].

In addition to the substance characteristics, the vehicle also has a great influence on the absorption rate to the skin [97,98]. Lipophilic ointments for example have an occlusive effect on the skin and might increase the absorption of certain substances. This is due to the prevention of water evaporation from the  $SC$ , thus swelling the tissue [99]. The same effect can be found in a diffusion cell with an aqueous acceptor and donor formulation. In fully hydrated  $SC$ , for most substances the water diffusivity in the corneocytes is increased [100].

For predicting skin absorption of a substance, the  $DSL$  is usually regarded as an unstirred aqueous layer for simplification and the acceptor as perfect sink to simplify analysis.

One problem associated with mathematical predictions of substance permeability is the determination of the input factors. Even a small change in the parameters might lead to

significant changes in the results. Thus, experimental protocols need to be carefully evaluated and validated.

### *Analysis of experimental data*

- *Permeation experiments*

The data of the cumulative amount from permeation experiments is usually plotted versus the time and certain parameters can be determined from this graph. From permeation experiments, the cumulative permeated drug amount  $Q_t$  through the membrane can be determined by the following equation:

$$Q_t = \frac{D \cdot A \cdot \Delta c \cdot t}{l} \quad (\text{Equation 1-3})$$

with the incubation area  $A$ , the concentration gradient across the membrane  $\Delta c = c_1 - c_2$ , a time period  $t$ , and the membrane thickness  $l$ . For the infinite dose case, the concentration difference across the membrane  $\Delta c$  is constant.

For infinite dose experiments,  $J_{ss}$  can be determined by simple linear regression from the graph, or can be calculated using Fick's first law. The steady-state flux can be estimated by:

$$J_{ss} = \frac{D \cdot c}{l} \quad (\text{Equation 1-4})$$

Here,  $c$  is the concentration in the membrane, which is related to the easily obtainable concentration in the donor  $c_{don}$  and the partition coefficient between donor and membrane  $K_m$ :  $c = K_m \cdot c_{don}$ . When  $K_m$  is not available and the vehicle consists of an aqueous donor phase, often estimates using  $K_{o/w}$  are employed. The boundary conditions for an infinite donor and perfect sink are:  $c=\infty$  at  $x=0$  and  $c=0$  at  $x=l$ .

$$J_{ss} = \frac{D \cdot K_m \cdot c_{don}}{l} \quad (\text{Equation 1-5})$$

Furthermore, the lag time  $t_{lag}$  can be determined by extrapolation of the linear part of the graph to the x-axis. Mathematically, the lag time can be determined as follows according to [89]:

$$t_{lag} = \frac{l^2}{6D} \quad (\text{Equation 1-6})$$



The permeability coefficient  $k_p$  allows for normalizing the steady-state flux to the applied donor concentration in the vehicle  $c_v$ . Thus, formulations with different drug concentrations can be compared:

$$k_p = \frac{D \cdot K_m}{l} = \frac{J_{ss}}{c_v} \quad (\text{Equation 1-7})$$

For finite dose, steady-state is not established, thus steady-state parameters like  $J_{ss}$  and  $k_p$  can not be calculated. Instead, the momentary flux can be estimated by fitting to a non-steady-state solution of Fick's law, and the peak flux value and the time to reach peak flux can be determined (**fig. 1-4 B**) [101].

A transfer coefficient  $k_t$  as the ratio of the instantaneous flux  $J_i$  normalized to the specific dose can be determined according to [102]:

$$k_t = \frac{J_i \cdot 100}{\text{specific dose}} \quad (\text{Equation 1-8})$$

- *Penetration experiments*

From penetration experiments concentration depth profiles can be obtained, which give information about the distribution of the drugs within the different skin layers (**fig. 1-5**). To be able to calculate concentration depth profiles, the drug concentration in each skin pool is required, as well as the volume of the skin layer removed, and the depth inside the skin. For better understanding, the calculation of concentration depth profiles with the help of infrared densitometry is thoroughly explained in *chapter 10 Appendix*. In short, the normalized drug concentration within the different skin layers is determined over depth.

Furthermore, the cumulative drug amount in the skin layers, e.g. the SC can be calculated for the different incubation times (**fig. 1-6, fig. 1-7**). Thus, comparison between different formulations and anatomical sites is possible. Also, saturation effects in the skin layers can be investigated, e.g. with Michaelis-Menten kinetics according to [32]:

$$m_{act} = \frac{m_{max} \cdot t_{inc}}{t_{max/2} + t_{inc}} \quad (\text{Equation 1-9})$$

With  $m_{max}$  as the maximum drug amount present in the skin layer after establishment of the steady-state,  $t_{max/2}$  as the time until half of the maximum drug amount in the skin layer is reached,  $t_{inc}$  as the incubation time, and  $m_{act}$  as the actual drug amount at  $t_{inc}$ .

Several approaches of calculating the skin absorption or permeability of different substances are available. The three most common types of mathematical models are presented in the following chapters.

#### 1.4.1 Quantitative structure activity relationship (QSAR) models

Quantitative structure activity relationship (QSAR) models employ the substance's physicochemical properties to estimate the permeability of a substance to the skin. The input parameters can be calculated from the molecular structure or derived from experiments. QSARs are based on the assumption that the permeability of a substance can be calculated by its physicochemical properties only and completely neglect the structure of the skin.

The most important (and most often applied) properties employed are the molecular weight  $MW$  and the octanol/water partition coefficient  $\log K_{o/w}$ . As molecular weight and volume are related by a factor of  $\sim 0.9$  g/ml, both parameters can be used in the models [103].

The simplest models solely employ  $\log K_{o/w}$  and  $MW$  for prediction of the absorption of a substance. The most commonly used model was developed by Potts and Guy [91]:

$$\log k_p = \log\left(\frac{D^0}{\partial}\right) + f \cdot \log K_{o/w} - \beta'' \cdot MW \quad (\text{Equation 1-10})$$

with  $D^0$  as the diffusivity of a hypothetical molecule with a  $MW$  of zero,  $\partial$  as diffusion path length,  $f$  a coefficient to correct for  $SC$  partition coefficient, and  $\beta''$  as another coefficient to correct for  $MW$ . Assuming  $\log D^0/\partial$  as constant and including a database of permeability of more than 90 chemicals [104] a more detailed equation was developed, being able to explain around 70% of the variability of the experimental data.

$$\log k_p = -6.3 + 0.71 \cdot \log K_{o/w} - 0.0061 \cdot MW \quad (\text{Equation 1-11})$$

Since then, many adaptations have been made to this model, like applying the models to different data sets [105]. Further physicochemical characteristics of the chemicals were included, like hydrogen bonding [106,107], and in other models,  $MW$  was replaced by  $MW^x$ , where an exponent  $x$  was introduced [105].

With QSAR models, information about the permeability of a substance can easily be estimated without extensive computational effort. It needs to be taken into account, however, that not for all substances the permeability can be correctly estimated and that they do not allow for the prediction of the absorption with time. Thus, they are limited to

the steady-state and therefore only suitable for infinite dose conditions. Furthermore, they do not consider the influence of the vehicle or other physicochemical parameters, limiting the informative value of the QSAR results.

#### 1.4.2 Pharmacokinetic models

Pharmacokinetic (PK) models describe the skin layers as well-stirred compartments with a uniform drug concentration in each compartment. The transport between the different compartments is modelled with first order rate constants. Due to these simplifications, the computing time is strongly reduced compared to more complex models, e.g. diffusion models.

The simplest compartmental model for skin absorption consists of solely one skin compartment, sandwiched between a donor compartment and an acceptor compartment [78,108]. The latter one may represent the blood and thus systemic distribution and elimination. The number of compartments can also be increased, dividing the skin into the *SC* and the *DSL* [78,108,109]. The two compartment model is advanced because the actual conditions can be better fitted/simulated than in a homogeneous skin compartment with identical properties. **Fig. 1-8** shows the schematic structure of a two compartment PK model with the *SC* and the *DSL* as the two skin compartments.

Also, three compartmental PK models have been developed, further segmenting the viable skin layers [78]. Even more compartments are possible, dividing the different skin layers into a certain number of compartments, thus being able to fit the different concentrations within one skin layer [78]. Besides, the advantage over diffusion models has not yet been evaluated.

In general, two compartment models are assumed to be best suited to make the compromise of accuracy and complexity [78].

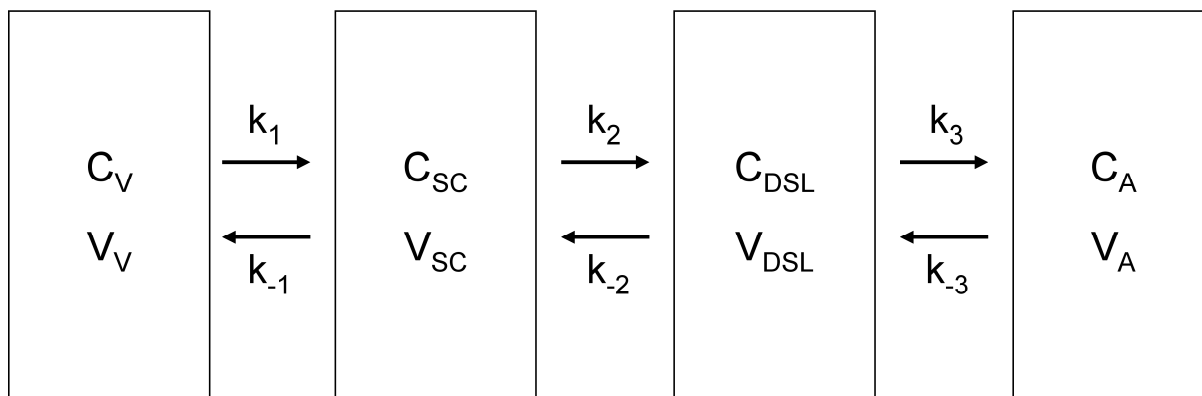


**Figure 1-8** Schematic diagram of a two-compartment PK model with the different compartments (V: vehicle, SC: stratum corneum, DSL: deeper skin layers (viable epidermis + dermis), A: acceptor/blood) and the rate constants

For a one compartmental PK model the differential mass balance of chemical can be determined as:

$$V_{skin} \frac{d\langle C_{skin} \rangle}{dt} = k_1 C_V - k_{-1} \langle C_{skin} \rangle - k_2 \langle C_{skin} \rangle + k_{-2} C_b \quad (\text{Equation 1-12})$$

according to [103,108] with  $\langle C_{skin} \rangle$  as the position averaged concentration in the skin compartment. For a two-compartment model the position averaged concentration in the viable skin layers  $\langle C_{ve} \rangle$  is included:

$$V_{sc} \frac{d\langle C_{SC} \rangle}{dt} = k_1 C_V - k_{-1} \langle C_{SC} \rangle - k_2 \langle C_{SC} \rangle + k_{-2} \langle C_{ve} \rangle \quad (\text{Equation 1-13})$$

$$V_{ve} \frac{d\langle C_{ve} \rangle}{dt} = k_2 \langle C_{SC} \rangle - k_{-2} \langle C_{ve} \rangle - k_3 \langle C_{ve} \rangle + k_{-3} C_b \quad (\text{Equation 1-14})$$

In general, pharmacokinetic models without rate constants as input parameters only fit experimental mass profiles. The rate constants describing drug transport may however be related to physicochemical parameters of the drug or to anatomical characteristics [109,110]. However, a correlation between rate constants and physicochemical or anatomical parameters is difficult.

PK models are well suited to describe the finite dose scenario as mass profiles.

### 1.4.3 Diffusion models

In contrast to QSAR and pharmacokinetic models, diffusion models not only employ physicochemical parameters of the substance for their calculations, but they also take into account the anatomical structure of the skin. Thus, the models usually reproduce the geometry of the skin and the diffusion characteristics in the different skin layers, introducing more realistic parameters to the calculations. For example, the SC is generally regarded as a more lipophilic layer with other diffusion properties than the viable skin layers.

Diffusion models are based on the principle that transport mainly occurs via passive diffusion. Thus, the degree of diffusion is determined by the concentration gradient and diffusion laws can be applied. Applying Fick's first law, diffusion models are able to simulate the steady-state characteristics of a substance, e.g. the lag-time, the flux, or the permeability. Fick's second law is solved in time and space dimensions to simulate the diffusion process in temporal and local resolution.

In contrast to steady-state models, non-steady-state models also allow for predicting transient processes like the changes of drug concentration in the different skin layers or the acceptor at certain time points of interest. Also, non-steady-state models are best capable of obtaining information about the mechanisms of skin absorption.

Diffusion of the substance under investigation can be simulated in varying degrees of complexity. One dimensional (1D) diffusion models assume the drug transport solely in one direction, strongly simplifying the absorption process. In these models, the SC is modelled as a homogeneous membrane, assuming that the transport is constant throughout the membrane. Some models only include the lipid phase as diffusion pathway through the SC, due to higher diffusion rates in this phase. 1D models have short computing times, but are not able to account for the heterogeneous structure of the SC with the different possible diffusion pathways through corneocytes or lipids [60,111,112].

Two-dimensional (2D) diffusion models include the drug transport in a second spatial dimension. Here, the brick and mortar structure of the SC is simulated, with corneocytes embedded in the lipid matrix [16,19]. Other approaches assume not only two distinct compartments in the SC, but also include a detailed resolution of the lipid channel [113,114].

Homogenized models simulate the *SC* as a homogeneous membrane, but include the different diffusion parameters of the corneocytes and lipids in the three different spatial directions [115,116].

The diffusion and partition parameters for diffusion models can be calculated or determined experimentally. In the past, corneocytes have often been regarded as impermeable [17]. Thus, diffusion was solely simulated in the lipid phase with the diffusion coefficient  $D_{lip}$ . As determined with fluorescence recovery after photo bleaching (FRAP) measurements,  $D_{lip}$  is generally inversely related to molecular weight [117].

For heterogeneous models, the diffusion was modelled along the long, tortuous pathways around the corneocytes [16]. The length of the pathways around the corneocytes has been evaluated previously [17,118,119], and calculated as multiple times the thickness of the *SC*. Due to the tortuosity of the *SC*, lateral diffusion is usually regarded faster than transversal diffusion [113,120].

However, recent investigations showed that there is indeed absorption of the drugs into the corneocytes, first of all water [20]. This is especially important for hydrophilic compounds, which can be dissolved in the water inside the corneocytes and diffuse through the cells. If corneocytes are modelled as permeable cells, diffusion parameters in the corneocytes  $D_{cor}$  and partitioning between corneocyte and lipid phase  $K_{cor/lip}$  need to be included. Lipophilic phase and corneocytes do not, however, contribute to drug absorption to the same degree. Therefore, different ratios of  $D_{cor}/D_{lip}$  and the partitioning between the structures defined as corneocyte/lipid partition coefficient  $K_{cor/lip}$  were investigated towards the permeability of the drug [16,121].

Only, if the drug enters the corneocytes and is dissolved, binding to the intercellular keratin is possible [122]. Keratin binding has recently been investigated for different drugs, e.g. for flufenamic acid (FFA) [18,20], testosterone [20], and other drugs [94].

Another complicating factor is the varying diffusivity over depth in the *SC*, which has been explained by changing lipid conformational ordering over depth inside the *SC* [123,124]. Also, the water content in the *SC* changes over depth [125]. The influence of varying partitioning and diffusion characteristics over depth has been investigated previously, and the partition coefficient was found to have a stronger effect on the predicted flux [126].

Furthermore, degradation of the desmosomes between the corneocytes leads to a loosening between the corneocytes and changed diffusion characteristics. The effect of desquamation

on drug absorption with the help of a mathematical model has been investigated precedently [127].

In the case of a heterogeneous *SC*, the partitioning of the donor to the *SC* ( $K_{sc/don}$ ) of the different *SC* parts has to be included as  $K_{lip/don}$  and  $K_{cor/don}$ , too. The first can be estimated from  $a \cdot K_{o/w}^b$ , where  $b$  can range from 0.7 to 0.86 [128-130].

In most diffusion models the viable skin layers are modelled and the partitioning into this layer  $K_{lip/DSL}$  and the diffusion in this layer  $D_{DSL}$  are included. The viable skin layers are mostly regarded as a homogenous, well-stirred layer with constant diffusion parameters. The diffusion coefficient in the donor  $D_{don}$  varies with the vehicle applied.

With the inclusion of many input parameters, different target results can be obtained. In most publications, the permeation is modelled and from this the permeability, the lag-time or the steady-state flux can be determined. Only few studies however attempt to simulate concentration depth profiles of a drug in the skin.

A 2D diffusion model based on experimentally determined input parameters was previously developed in this working group together with the Wittum group in Frankfurt [18,19]. The input parameters employed for this model are schematically visualized in **fig. 1-9**. The geometry of the model was adapted from [16], increasing the number of corneocyte layers to 16 and adding a *DSL* compartment. Fickian type diffusion behaviour was assumed.

This model was able to correctly predict experimentally determined infinite dose concentration depth profiles in the *SC* and the *DSL* for FFA and caffeine. The big advantage of this model was the use of experimentally determined diffusion and partition parameters, allowing for more realistic simulations. Up to now, most simulations have not been validated by experimental data, which is a big deficit.

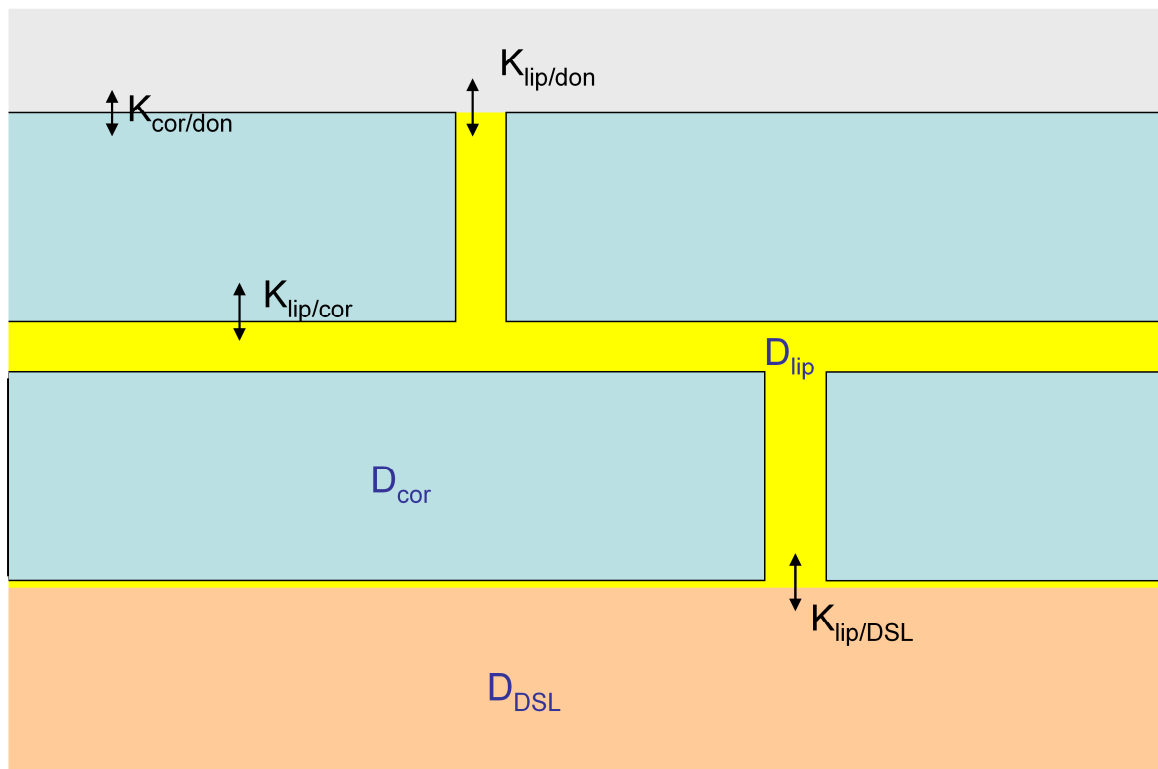


**Figure 1-9** Schematic visualization of the diffusion and partition parameters employed in the 2D diffusion model of [19]. Here, the SC is plotted with the corneocytes (cor) and lipid phase (lip). The DSL is shown as homogeneous, well-stirred layer. Not drawn to scale and not all corneocyte layers are plotted. Adapted from [18].

Finite dose skin absorption experiments are much more complex than infinite dose experiments. As finite dose experiments do not reach a steady-state, the diffusion parameters change over incubation time. Due to this reason and because of the high variability between the experiments, derivation of input parameters from finite dose experiments is quite difficult [128]. Therefore, input parameters for predicting the finite dose permeation profiles are often derived from infinite dose experiments, which has been shown to give reasonable results [128].



## 2 Aim of the thesis

Skin absorption experiments are of interest for toxicological and therapeutic drug evaluation. In this respect, finite dose experiments are even more interesting for skin researchers since the application of a finite dose to the skin is much closer to the *in vivo* situation than the application of an infinitely large amount of formulation. However, finite dose experiments are difficult to perform and to analyze. Therefore, many studies still only regard the infinite dose case when investigating the absorption behaviour of substances to the skin. Thus, still plenty of work needs to be done to fully understand finite dose skin absorption behaviour.

Over the past decades, non-experimental methods are gaining importance for predicting the experimental results while also reducing lab time and costs, e.g. the use of mathematical modelling. This method is very promising due to easy accessible information about the absorption behaviour of a substance to the skin. Due to the high sensitivity of the mathematical methods to input parameters, it is essential to employ these parameters as accurate as possible. Input parameters may be calculated by models based on physicochemical properties of the substances or determined experimentally. Especially, if experimental data is addressed, a full validation is needed to minimize data error.

Therefore, this thesis focuses on the evaluation of skin absorption experiments and the improvement of experimental data for comparison with mathematical modelling. The following points are addressed:

- *Improvement of accuracy of concentration depth profiles obtained from tape-stripping (chapter 3)*

For the horizontal segmentation of the SC in skin penetration experiments usually tape-stripping is employed. The drug concentration in the different SC layers can be determined from the extracts of the different tape-strips. Tape-stripping is applied in many research groups with different methods for determination of the SC depth after each strip. As these methods are often not practicable or lack accuracy, a non-destructive method for SC quantification on tape-strips, infrared densitometry, is investigated for its use *in vitro*.

- *Evaluation of the influence of the application area of a finite dose on the permeation of the drug through heat-separated epidermis (chapter 4)*

For finite dose experiments, usually a uniform donor surface distribution is assumed. However, this is difficult to achieve due to the small applied dose and wrinkles in the skin. Thus, the influence of the donor surface distribution on the permeation of two model drugs is investigated: caffeine and flufenamic acid. For determining the application area the donor solutions are stained and a method to address surface distribution (coverage) is developed.

- *Analysis of finite dose mass profiles over time (chapter 5) and concentration depth profiles in SC and DSL (chapter 6) of skin penetration experiments, both experimentally and in comparison with mathematical models*

These chapters aim at combining both aspects mentioned above: to properly perform finite dose skin penetration experiments, and to compare the experimental data with mathematical models. After improvement of the SC quantification on tapes and the evaluation of the finite dose setup, these adaptations are included in the experimental procedure of finite dose skin penetration experiments. Furthermore, the experimental setup is carefully investigated to ensure the thorough separation of the different skin compartments.

The experimental data of mass profiles in the different skin compartments over time (*chapter 5*) are then analyzed with two mathematical models: A pharmacokinetic model, and a two dimensional (2D) diffusion model with high geometric resolution.

The pharmacokinetic model is developed to describe the mass profiles over time in all compartments of skin penetration experiments performed in a Franz diffusion cell, including the lateral skin part. The latter comprises compressed skin, which during incubation has been tightly squeezed between the two parts of the diffusion cell. This skin part is usually neglected in skin absorption studies. The pharmacokinetic model in our study is a first attempt to also describe the lateral skin part and the drug transport to it during incubation (*chapter 5*).

Previously, the 2D detailed diffusion model has been developed for predicting concentration depth profiles of infinite dose penetration experiments [19]. This model was now adapted to finite dose to simulate both mass profiles (*chapter 5*) and

concentration depth profiles (*chapter 6*). In this context it was investigated, if input parameters from infinite dose experiments [18] can also be used for predicting finite dosing.



### **3 Infrared densitometry: a fast and non-destructive method for exact stratum corneum depth calculation for *in vitro* tape-stripping**

Parts of this chapter have been published in:

Hahn T, Hansen S, Neumann D, Kostka K-H, Lehr C-M, Muys L, Schaefer U F

Infrared densitometry: a fast and non-destructive method for exact stratum corneum depth calculation for *in vitro* tape-stripping

Skin Pharmacol Physiol 2010;23:183–192

DOI: 10.1159/000288165

The author of the thesis made the following contributions to the publication: Performed and interpreted all experiments. Wrote the manuscript.

### 3.1 **Abstract**

The investigation of drug penetration into the *stratum corneum* (SC) by tape-stripping requires an accurate measure of the amount of SC on each tape-strip in order to determine the depth inside the SC. This study applies infrared densitometry (IR-D) to *in vitro* tape-stripping using the novel Squame Scan® 850A. The device had recently been shown to provide accurate measurements of the SC depth for tape-stripping *in vivo*. Furthermore, the suitability of IR-D for determining the endpoint of tape-stripping, i.e. complete SC removal was tested. The SC depth was computed from the IR-D data of sequential tape-strips and compared to the results of a protein assay as gold-standard. IR-D provided accurate depth results both for freshly excised skin and for skin stored frozen for up to three months. In addition, the lower limit of quantification (LLOQ) of IR-D indicates the complete removal of the SC (less than 5% of the total SC remaining) and can be used for adjusting the number of tapes applied *in situ*. Therefore, IR-D is an accurate, fast and non-destructive method for SC depth determination.

## 3.2 Introduction

Recently, studying skin absorption has gained a high interest not only for drug administration but also for toxicological substance evaluation, a result of the European REACH programme (Regulation (EC) No. 1907/2006) [25]. For most molecules, the SC is regarded as the rate-determining and hence the most important skin layer. Penetration experiments are performed to evaluate whether and to what extent a drug can invade the SC. This can be done by tape-stripping, where the SC is divided into sections parallel to the skin surface. By analyzing tapes from different depths inside the SC, information about the drug distribution within the SC can be gained. To generate correct concentration depth profiles, however, two parameters need to be exactly known. These are 1) the total thickness of the SC and 2) the exact depth inside the SC that is reached after a defined number of tape-strips. In addition, an experimental indicator for complete removal of the SC is necessary (i.e. when tape-stripping should be stopped). Different approaches have been developed to determine both parameters and the end point.

*In vivo*, the total SC thickness may be assessed non-invasively from the trans-epidermal water loss (TEWL) [24,131]. However, it was shown by Netzlaff et al. that this approach is not applicable *in vitro* [132]. Another more recent method for estimating the SC thickness *in vivo* is the application of confocal Raman microspectroscopy [133]. *In vitro*, the thickness of the complete SC can accurately be determined microscopically from cross-sections of skin biopsies.

The depth inside the SC may be estimated using either mathematical or experimental methods. For the mathematical approach, the thickness of SC on each tape-strip is determined by simply dividing the total thickness of SC by the number of tapes used in the stripping procedure [32]. However the amount of SC removed by tape-stripping is different on every tape-strip and for every volunteer [134,135]. An overview of the various experimental approaches is given in **table 3-1** alongside with their individual sources of error. Obviously there is no widely available method that is at the same time fast, non-destructive, and generally applicable.

To ascertain complete removal of the SC, several experimental methods may be employed [136-138], but their systematic error is unknown. Therefore, it is still common practice to apply a more or less arbitrary number of sequential tapes ranging from 20 to as high as 100

[18,32,137,139-143]. An instrumental method would need to provide a sufficiently fast read-out so that on this basis it can be decided in the course of the experiment when to stop tape-stripping.

Recently, infrared densitometry (IR-D) was introduced as a new method for SC quantification on tape-strips [142]. Here, a beam of light of 850 nm is directed through a tape-strip containing SC and the decrease in light intensity is measured (pseudo-absorption). For tape-stripping *in vivo*, the optical absorption on a tape was shown to be linearly proportional to the protein content. Furthermore, although the data distribution within different subject groups varied, the regression was always very similar and independent of gender, age, skin hydration, anatomical site (volar forearm, ventral forearm, and shoulder), and skin pH [142]. Based on these promising *in vivo* results, this method might also be suited to determine the SC amount on each tape-strip and the end point for tape-stripping *in vitro*.

To evaluate the potential of this new method the following topics will be addressed: At first, an abridged *in vivo* study was performed with D-Squame® tape (i.e. the identical tape as in the previous *in vivo* study on the volar forearm [142]). These experiments proved that this method could be reproduced in our lab. In addition, we used the same method with a different type of tape: tesa® Film kristall-klar was used *in vivo* on the volar forearm and abdominal skin.

The main focus of the present study was the evaluation of IR-D, first as a method for accurate SC quantification on tape-strips *in vitro*, and further to calculate the SC depth by means of these values. Here, in contrast to tape-stripping *in vivo*, freezing and storage of the skin may change the cohesiveness of the SC. Therefore, we investigated the amount of SC removed by stripping with tesa® Film kristall-klar for storage times of up to three months. The results of the IR-D measurements were compared to a standard method for quantification of the SC amount on tapes, a BCA-protein quantification assay (bicinchoninic acid).

The second focus of the study was whether IR-D can be used for objective and immediate determination of complete SC removal. For this purpose, biopsies were taken after *in vitro* tape-stripping as soon as the lower limit of quantification (LLOQ) of the IR-D instrument was reached. Cross-sections were inspected microscopically for remaining SC and the systematic error of the method was evaluated.



**Table 3-1** Overview of common methods used for the determination of SC amount on tape-strips. (Pseudo-absorption: decrease of transmitted light due to reflection, diffraction and scattering; BCA: bicinchoninic acid)

Method	Sources of Errors	Literature
<b>gravimetry</b>		
differential weighing	non-specific weight increase due to sweat, lipids, formulation excipients	[24,131,144,145]
<b>optical methods</b>		
protein absorption at 278 nm	non-specific absorption due to other substances at 278 nm	[146]
pseudo-absorption at 430 nm	non-specific pseudo-absorption due to sweat, lipids, formulation excipients, absorption due to coloured substances	[136,141,145,147]
Trypan blue staining, absorption at 652 nm	low sensitivity due to background colouring of tapes; low resolution of small differences in degree of coverage of the tape	[148]
<b>protein quantification</b>		
colorimetric quantification of NaOH-extractable protein by a Lowry-, Bradford-, or BCA assay	destructive, therefore determination of depth and concentration of penetrating drug on different skin sites; non-specific reaction with a wide range of substances, e.g. penetrating drugs	[142,144,149,150]

### 3.3 Materials and methods

#### 3.3.1 Chemicals

The following reagents were used: sodium hydroxide, potassium dihydrogen phosphate and potassium chloride (Merck, Darmstadt, Germany), hydrochloric acid (Grüssing, Filsum, Germany), sodium hydrogen phosphate dihydrate (Riedel-deHaën/Sigma-Aldrich Laborchemikalien, Seelze, Germany), sodium chloride (VWR Prolabo, Leuven, Belgium), Ringer solution (Fresenius Kabi, Bad Homburg, Germany), type I-Trypsin, from bovine pancreas, and bovine serum albumin (Sigma-Aldrich, Steinheim, Germany). Purified water was prepared by a Millipore Synthesis device (Millipore GmbH, Schwalbach, Germany).

The BCA protein assay kit (BCA Kit, Sigma-Aldrich, Steinheim, Germany) includes reagent A (bicinchoninic acid in 0.1 N NaOH with sodium carbonate, sodium tartrate, and sodium bicarbonate) and reagent B (4 % (w/v) copper(II) sulphate pentahydrate solution)), which were mixed together in a ratio of 50:1 (V:V) according to the manufacturer's instruction.

Tesa® Film kristall-klar, (t-tape, 33 m x 19 mm, #57330-00000-02, cut to pieces of 16 x 19 mm) was provided by the tesa AG, Hamburg, Germany. Standard D-Squame® (d-tape, 22 mm in diameter) was provided by Cuderm Corporation, Dallas, USA.

#### 3.3.2 Skin

The *in vivo* study included seven healthy female Caucasian volunteers (age range 24-50 years) with no active skin disease in the stripping area. These were tape-stripped on the volar forearm and/or the abdomen with two different tape-strip brands (v.i.). The volunteers were asked not to apply any cosmetics on the stripping area and to wash the skin with water only within the 24 hours prior to the experiment. All volunteers had previously signed informed consent forms.

Human skin for *in vitro* experiments was obtained from plastic surgery of Caucasian patients from the Department of Plastic and Hand Surgery, Caritaskrankenhaus, Lebach, Germany. The study included abdominal skin from four female Caucasian patients (age range 31-41 years) and breast skin from one male donor (30 years). After excision and cleaning the SC side with purified water, the subcutaneous fatty tissue was removed with a scalpel. The skin was cut into pieces of 10 x 10 cm, wrapped in aluminium foil and stored in impermeable

polyethylene bags at  $-26^{\circ}\text{C}$  until use. The study was approved by the Ethical Commission of Department of Plastic and Hand Surgery, Caritaskrankenhaus, Lebach, Germany.

Based on a protocol by Kligman et al. [45] SC was prepared as previously described [18]. Briefly, skin punches of 25 mm diameter were punched out from frozen skin and the skin was put on a filter paper soaked with Ringer solution and allowed to thaw. To accelerate the separation procedure of the SC, full thickness skin was first separated into epidermis and dermis by immersing the skin punch in purified water of  $60^{\circ}\text{C}$  for two minutes then peeling off the epidermis from the dermis by means of forceps. The epidermis was transferred into a petri dish, and incubated in a 0.15% trypsin solution in PBS (phosphate-buffered saline, composed of 0.2 g potassium chloride, 8.0 g sodium chloride, 1.44 g disodium hydrogen phosphate dihydrate, and 0.2 g potassium dihydrogen phosphate to a litre of purified water) at  $37^{\circ}\text{C}$  for at least 24 hours until the SC was completely separated from the underlying tissue. The SC was washed three times with purified water and after drying it was stored in a desiccator filled with silica gel until constant weight.

### 3.3.3 *In vivo* tape-stripping

*In vivo* experiments were performed with a small number of volunteers as the suitability of this method for *in vivo* had already been shown. Three female Caucasian volunteers (age range 24-50 years) were tape-stripped with d-tape in the middle of the volar forearm (minimum distance from wrist and elbow: 5 cm). Four female Caucasian volunteers (age range 24-30 years) were tape-stripped with t-tape both on the volar forearm and on the abdomen (minimum distance from the navel: 5 cm). Before tape-stripping, the skin was cleaned with purified water and allowed to dry for five minutes.

Tape-stripping with d-tape was performed using the entire adhesive area of the tape of 22 mm diameter. After placing the first tape on the skin, the contour of the tape was outlined on the skin with a permanent marker in order to ensure the use of the same stripping area for each following tape.

For tape-stripping with t-tape a teflon mask with an opening of 15 mm in diameter was tightly fixed to the skin with band-aid. Then a tape was placed centrally above the stripping area and pressed to the skin with the flat side of forceps to ensure homogeneous pressure. Then, the tape was removed with forceps in one swift move. Tape-stripping was performed with 20 sequential tapes.

### 3.3.4 *In vitro* tape-stripping

*In vitro* tape-stripping was performed under highly standardized conditions as published [32]. In short, a punch biopsy (25 mm diameter) was taken, cleaned with a cotton pad soaked with purified water and then blotted dry with a piece of cotton. The skin was stretched and fixed on cork disks with needles. A teflon mask with an opening of 15 mm in diameter was tightly fixed above the skin in order to restrict the stripping area. Then, a tape was placed centrally over the stripping area. After applying a weight of 2 kg for ten seconds, the tape was removed in one rapid move. Tape-stripping was performed with 20 sequential tapes.

The *in vitro* study included the excised abdominal skin of four female donors and breast skin of one male donor. Tape-stripping was performed directly after excision (“fresh skin”) and repeatedly after one week, one month and after three months (“frozen skin”). For experiments after storage of the skin, punch biopsies of the same size were taken from the frozen skin and put on a filter paper soaked with Ringer solution to thaw. Care was taken to strictly avoid repeated freezing and thawing of skin pieces when taking out skin punches. At each time point and for each donor, tape-stripping experiments were performed on two skin punches and the amount of adherent SC was determined by IR-D and BCA assay. The SC amount was translated into the SC depth as explained in section 3.3.10 and *chapter 10 Appendix*.

### 3.3.5 Infrared densitometry (IR-D)

IR-D is based on the determination of the pseudo-absorption of a sample, e.g. a tape-strip. For tape-strips, this can be due to the tape itself and additional items on the surface of the tape, e.g. SC. The IR-densitometer Squame Scan® 850A (Heiland electronic GmbH, Wetzlar, Germany) was designed to measure the optical absorption of tape-strips and thus to indirectly determine the SC amount on the tape [142].

The instrument produces a circular beam of light ( $\lambda = 850 \text{ nm}$ ) that is directed through the tape-strip containing SC and the decrease in light intensity (in % of the initial intensity) is measured over an area of 13 mm in diameter. The large measured area is a big advantage, as inhomogeneities in corneocyte distribution on the tape are balanced. In contrast to measurements at 430 nm (see **table 3-1**), at a measuring wavelength of 850 nm errors due to molecular absorption are practically irrelevant and thermal denaturation is prevented.

Upon placing the tape-strip under the measuring head, the absorption values are immediately displayed on the instrument without destruction of the sample, allowing for fast and non-destructive readout of the results.

Immediately prior to the experiment, the instrument was calibrated by setting the absorption of an empty sample holder to 0% absorption. The absorption of an ambient light filter provided for calibration by the manufacturer should then return 33.8%. According to the manufacturer, linearity of the instrument is given in the range of 0-40% absorption with a resolution of 0.1%. None of the analyzed tapes returned absorption values above the linear range of 40%. The absorption of an empty tape is subtracted from the signal to correct for background noise. The lower limit of quantification (LLOQ) was calculated from the five-fold background noise of the empty tape.

After stripping, all tapes were placed in a sample holder with the adhesive side facing up and measured with the IR-densitometer according to [142]. As a constant absorption value is reached only after three minutes after stripping, the tapes were always measured after this time.

### 3.3.6 BCA protein assay

Immediately after IR-D, the tapes were processed for protein quantification. The tapes were transferred into scintillation vials and the protein was extracted with 750  $\mu$ l 1 N sodium hydroxide solution for two hours at room temperature. After neutralization with 750  $\mu$ l neutralizing reagent (1 N hydrochloric acid containing 3.3 mM  $\text{Na}_2\text{HPO}_4$  and  $\text{KH}_2\text{PO}_4$ ), the extract was homogenized by shaking thoroughly. From each sample extract 100  $\mu$ l were transferred into a 96-well plate and 200  $\mu$ l of BCA reagent were added. The samples were incubated at 37°C for 30 min and the UV absorption was measured at  $\lambda = 550$  nm using a UV/Vis plate reader (Tecan, Crailsheim, Germany).

Standards used for calibration were BSA as model protein and SC extract. The SC extract was prepared as follows. An accurately weighed piece of dried SC was placed in a scintillation vial and 1 ml 1 N sodium hydroxide was added. The vial was exposed to ultrasound for 15 min and then proteins were extracted for 24 hours at room temperature on an orbital shaker. Afterwards, the extract was again sonicated for 15 min. After neutralization with the neutralizing agent, the extract was filtered (Chromafil® GF/PT – 45/25, Macherey-Nagel, Düren, Germany).

External standards from SC were prepared in the range of 0.5 µg to 50 µg per well. The SC extract was always prepared from the same donor as the tested skin to avoid inter-individual variations. This was not possible for fresh skin, because the preparation of SC extract takes at least four days. Therefore, BSA was used as a substitute. BSA standards were prepared in the range of 0.25 µg to 20 µg per well. A mixture of equal parts of 1 N sodium hydroxide and the neutralizing agent was used as a solvent. An identical mixture containing no BSA or SC extract served as negative control and for evaluation of background noise. The lower limit of quantification (LLOQ) was calculated from the five-fold background noise.

### **3.3.7 Influence of disinfectants on BCA assay**

To exclude an influence of the disinfectants on the BCA assay, typical disinfectants commonly used during surgery, Braunoderm® and Octenisept®, were tested as substrates in the assay. Different dilutions of the disinfectants were prepared in the concentration range 5 µg/ml to the undiluted disinfectant (1 g/ml). From each of the twelve dilutions 100 µl were transferred into a 96-well plate and 200 µl of the BCA reagent were added. Thus, the mass of the disinfectants ranged from 0.5 µg to 100 mg per well. As reference and for preparing the dilutions of the disinfectants, 1 N sodium hydroxide and neutralizing reagent in a ratio of 1:1 (V/V) was used. The samples were incubated at 37°C for 30 minutes. Afterwards, the UV absorption was measured at  $\lambda = 550$  nm using a UV/Vis plate reader.

### **3.3.8 Determination of SC thickness**

To determine the thickness of the total SC skin biopsies (4 mm diameter) were taken from intact frozen abdominal skin. Cross-sections with a thickness of 8 µm were cut with a cryomicrotome (Slee, Mainz, Germany) and transferred to microscopic slides. The cross-sections were dyed with haematoxylin (Carl Roth GmbH & Co KG, Karlsruhe, Germany) and inspected with a light microscope at 400 x magnification (Leica, Wetzlar, Germany). Microscopic pictures were taken with a camera (Jenoptik, Jena, Germany) and analyzed with a software (Carl Zeiss Axio Vision Rel. 4.7) using a graduated scale bar with a resolution of 0.13 µm/pixel. The mean total SC thickness was determined from measurements at ten different spots on the pictures.

### 3.3.9 Determination of SC remaining on the skin after tape-stripping

The degree of SC removal was determined with a skin biopsy from skin that had been tape-stripped until the LLOQ of the IR-D had been reached. Pictures of the cross-section were taken at 200 x magnification with a resolution of 0.25  $\mu\text{m}/\text{pixel}$  and the area of the remaining SC was determined over the entire length of the biopsy (i.e. 2.1 to 3.1 mm, note that this value is less than the diameter of the biopsy of 4 mm as it is difficult to organize the entire biopsy on the microscopic slide without damage). The same procedure was repeated for non-stripped SC and the ratio of both areas was calculated.

#### 3.3.10 Determination of cumulative depth inside the SC

The cumulative depth inside the SC was determined from the cumulative absorption values of IR-D or the SC amount determined by the BCA assay, as published previously [137,139,147].

$$d_i = d_{tot} \frac{\sum_{n=1}^i x_n}{\sum_{n=1}^{n_{max}} x_n} \quad (\text{Equation 4-1})$$

Here  $d_i$  is the depth reached inside the SC after  $i$  tape-strips and  $d_{tot}$  is the total SC thickness, which has been determined microscopically;  $x$  is the absorption measured by IR-D corrected for background noise (empty tape) or the protein amount determined by the BCA assay, and  $n_{max}$  is the total number of tapes (20).

#### 3.3.11 Statistics

Linear regression analysis and determination of confidence intervals were performed by Sigma Plot 8.0. Mean values and standard deviations were determined using Microsoft Office Excel 2003.

## 3.4 Results

### 3.4.1 BCA protein assay

#### a) Calibration

For the calibration of the BCA assay BSA dilutions as well as SC extracts were used as standards. Both types of standards provide a linear relationship between the absorption at 550 nm and the mass of protein, for BSA in the range of 0.25 µg to 20 µg and for SC extract in the range of 0.5 µg to 50 µg. A regression analysis was performed over all individual data points (for BSA standards these are 30 individually prepared samples for each concentration; SC standards were prepared for a total of four skin donors using two to four pieces of SC from each donor). **Figure 3-1** shows the results of the linear regression analysis and mean absorption values (BSA standards mean  $\pm$  SD for  $n = 30$ ; SC standards mean for 4 skin donors with  $n = 2-4$ , scattering of the data is shown via 95% confidence intervals). The SC standards prepared from different skins are narrowly distributed (**fig. 3-1**). The slope of the individual SC extracts is between 0.012 and 0.013 and the intercept between 0.021 and 0.025 with coefficients of determination between 0.992 and 0.996 (**table 3-2**). BSA calibration standards constantly give approximately a three-fold higher absorption value compared to the SC extract. The slope covers the range of 0.033 to 0.045 and the intercept -0.005 to 0.021 with coefficients of determination between 0.994 and 0.999 (**table 3-2**). For d-tape the LLOQ was 1.45 µg for SC extract and 0.48 µg for BSA. For t-tape the LLOQ was 1.05 µg for SC extract and 0.35 µg for BSA (**table 3-3**).

#### b) Influence of disinfectants

Only a very low absorption of 0.005 was found for very high amounts of the disinfectant (500 µg per well for Octenisept® and 10 mg per well for Braunoderm®, data not shown). As this amount of disinfectant is not reachable under the conditions of the tape-stripping and extraction protocol, the influence of the disinfectants on the BCA assay was neglected.



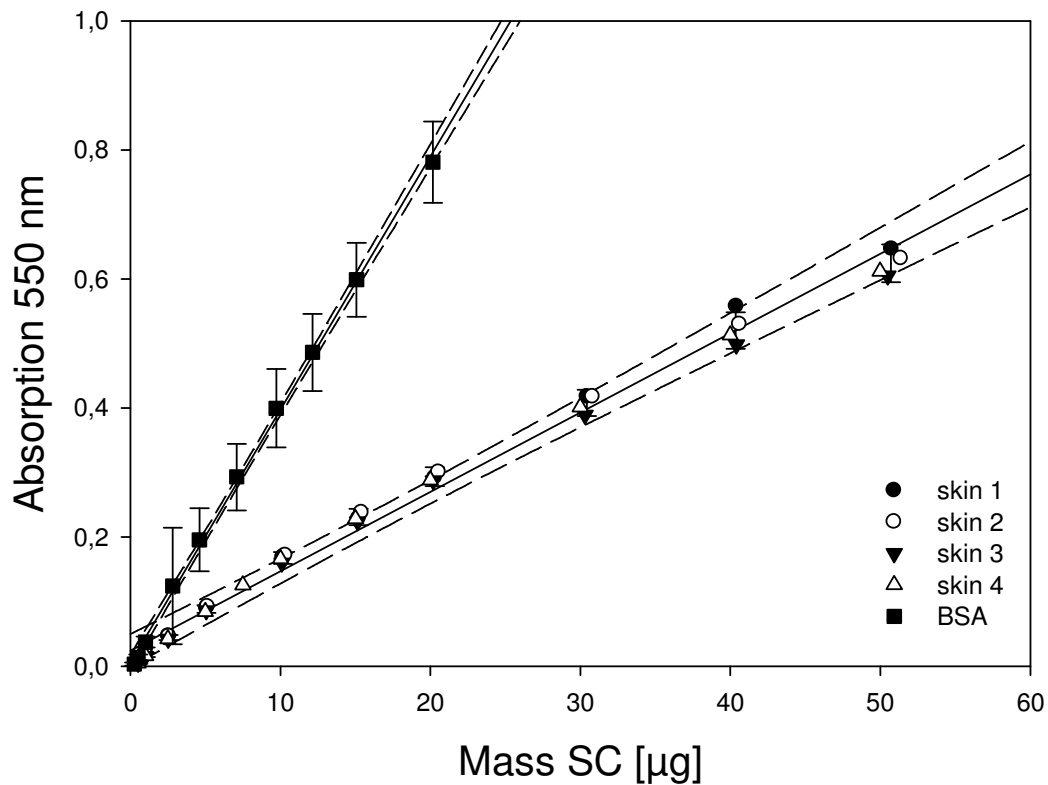


**Figure 3-1** Absorption of SC extracts of different donors compared to BSA solution at 550 nm in BCA assay. Number of calibration series: (skin 1) = 2, (skin 2) = 4, (skin 3) = 2, (skin 4) = 3; (BSA) = 30. BSA: mean  $\pm$  SD with 95 % confidence interval, SC extracts: mean with 95 % confidence interval.

**Table 3-2** Data range of linear regression lines for SC extracts of the different donors and of BSA in the BCA assay

Standard	Slope [1/ $\mu\text{g}$ ]	Intercept	$r^2$	n (Number of calibrations)
SC extract 1	0.012 – 0.013	0.024 – 0.030	0.996 – 0.997	2
SC extract 2	0.012 – 0.013	0.020 – 0.029	0.991 – 0.993	4
SC extract 3	0.011 – 0.012	0.019 – 0.024	0.991 – 0.995	2
SC extract 4	0.012 – 0.013	0.021 – 0.025	0.991 – 0.993	3
BSA	0.033 – 0.045	-0.005 – 0.021	0.994 – 0.999	30

**Table 3-3** Lower limit of quantification (LLOQ) of tapes for IR-D and BCA assay and the percentage of tape-strips that were found below these limits

	IR-D		BCA assay			
	d-tape	t-tape	d-tape		t-tape	
			SC extract	BSA	SC extract	BSA
LLOQ	8.2%	8.1%	1.45 µg	0.48 µg	1.05 µg	0.35 µg
Tapes below LLOQ <i>in vivo</i>	0% (60 tapes)	0% (80 tapes)	0% (60 tapes)	0% (60 tapes)	0% (40 tapes)	0% (160 tapes)
Tapes below LLOQ <i>in vitro</i>	n.a.	2.5% (720 tapes)	n.a.	n.a.	1.0% (210 tapes)	0% (720 tapes)

### 3.4.2 Infrared densitometry

The LLOQ for IR-D was calculated from the five-fold standard deviation added to the mean background signal of the empty tape. A total of 240 empty t-tapes and 85 empty d-tapes were measured. D-tape and t-tape returned a similar LLOQ of 8.2% and 8.1%, respectively (**table 3-3**).

### 3.4.3 Tape-stripping *in vivo* – influence of tape-strip brand and anatomical site

Our results confirm the findings published by Voegeli et al. [142]. We found a high linear correlation ( $r^2=0.632$ ) between the pseudo-absorption measured with IR-D and the mass of protein per area of tape-strip measured by a BCA assay for *in vivo* tape-stripping on the volar forearm with d-tape (**fig. 3-2 A**). A similar correlation between both methods was found for tape-stripping *in vivo* with t-tape both on the volar forearm and on the abdomen (**fig. 3-2 B**). Stripping with d-tape led to closely distributed data points, indicating that similar amounts of SC had been removed by each strip independent of the number of tape-strips that had already been taken on the respective site (IR-D: approx. 2.5-12.5%; BCA: approx. 2.5-15 µg/cm<sup>2</sup>). This was different with t-tapes. The amount of SC removed with consecutive tape-strips varied in a wider range (IR-D: approx. 5-25%; BCA: approx. 2.5-45 µg/cm<sup>2</sup>) (**fig. 3-2**). For both tape-strip brands no sample was below the LLOQ of either IR-D or the BCA assay (**table 3-3**).

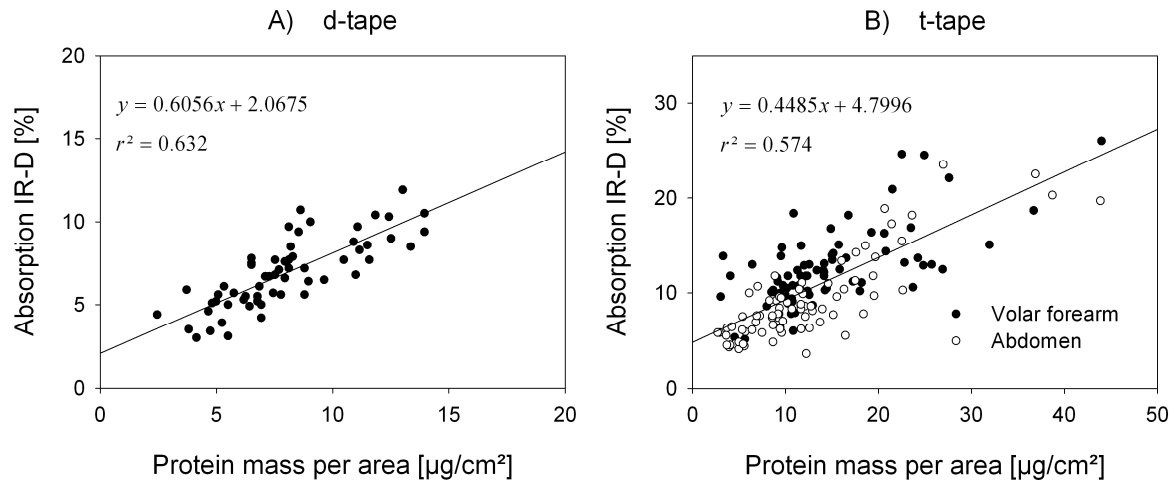


**Figure 3-2** *In vivo* tape-stripping on the volar forearm (A) with D-Squame® (n = 3) and (B) with tesa® Film kristall-klar on both the volar forearm and abdominal skin (n = 4). Each donor was tape-stripped with 20 sequential tapes on the according anatomical site. Linear regression is plotted for both graphs.

### 3.4.4 Determination of SC thickness *in vitro*

The total thickness of the SC ranged from 13.2  $\mu\text{m}$  to 19.2  $\mu\text{m}$  (table 3-4; fig. 3-3 A, C, E), which is in accordance with published data [138,151,152].

**Table 3-4** Mean SC thickness of the different donors. 1-4: female abdominal skin, 5\*: male breast skin. Cross-sections of the skin were analyzed under the light microscope and SC thickness was determined by Carl Zeiss Axio Vision Rel. 4.7. using a graduated scale bar.

Donor	Mean thickness of SC $\pm$ SD [ $\mu\text{m}$ ]
1	13.2 $\pm$ 2.65
2	15.3 $\pm$ 2.37
3	19.2 $\pm$ 1.55
4	17.0 $\pm$ 1.99
5*	18.1 $\pm$ 2.27

### 3.4.5 Determination of SC remaining on the skin after tape-stripping *in vitro*

Exemplarily the skin of three donors was stripped until the LLOQ of the IR-D was reached. The ratio of remaining to total SC area ranged between  $3.2 \pm 2.5\%$  to  $5.0 \pm 2.0\%$  for the different donors (**fig. 3-3 B, D, F**). This amount is negligible, therefore in this study it was concluded that the complete SC was removed when reaching the LLOQ of the IR-D.

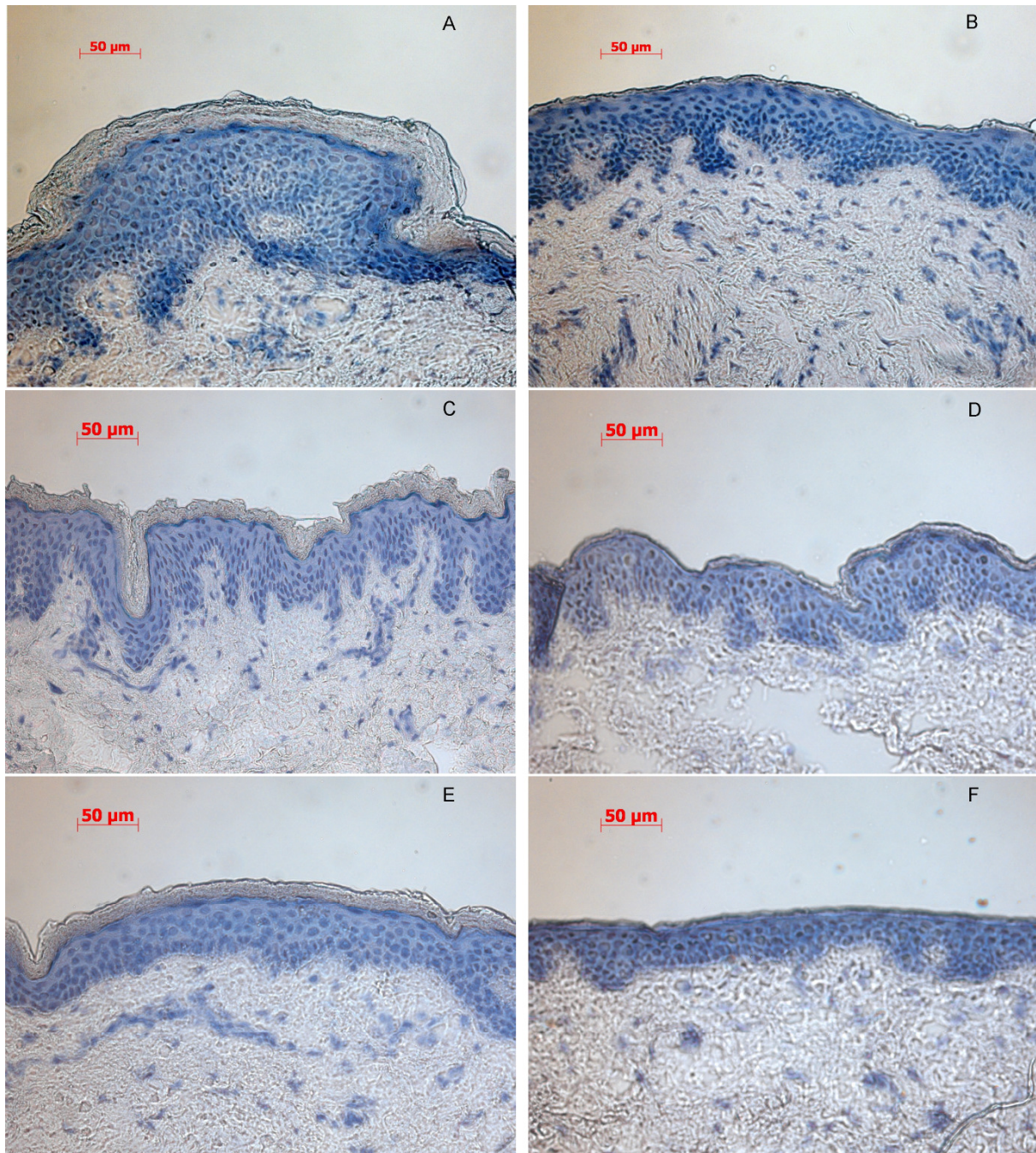


**Figure 3-3** Cross-sections of intact skin (A, C, E) and skin after tape-stripping with tesa® Film kristall-klar until the lower limit of quantification of IR-D was reached (B, D, F) for skin of three different donors.

### 3.4.6 Tape-stripping *in vitro* – influence of storage time

The influence of freezing and storing *in vitro* human abdominal skin on tape-stripping was tested for skin of four donors. Tape-stripping results of fresh, unfrozen skin were compared to skin stored frozen for one week, one month, and three months. **Figure 3-4** shows the results of two representative donors displaying two replicates (indicated as circle and triangle) of fresh skin and skin stored for three months. The cumulative depth was calculated as described in section 3.3.10 from the pseudo-absorption measured with IR-D (open symbols) and the protein amount per cm<sup>2</sup> measured with the BCA assay (filled symbols) and was plotted against the tape-strip number.

Usually the SC was removed in a relatively linear fashion (**fig. 3-4**, donor 1, 3 month storage; donor 2, fresh skin). In a number of cases a plateau was reached which indicates that less than 20 sequential tapes were sufficient to approach the SC-epidermal junction. This is evident for example in donor 1 with both “fresh”/ non-stored skin punches (18 strips); and donor 2 for skin punch A after a storage of three months (14 strips) (**fig. 3-4**).

A single time during the study our lab received male breast skin. Therefore this was treated separately (data not shown). At all time points except after one month with male breast skin less than 20 tapes were needed to remove the SC completely.

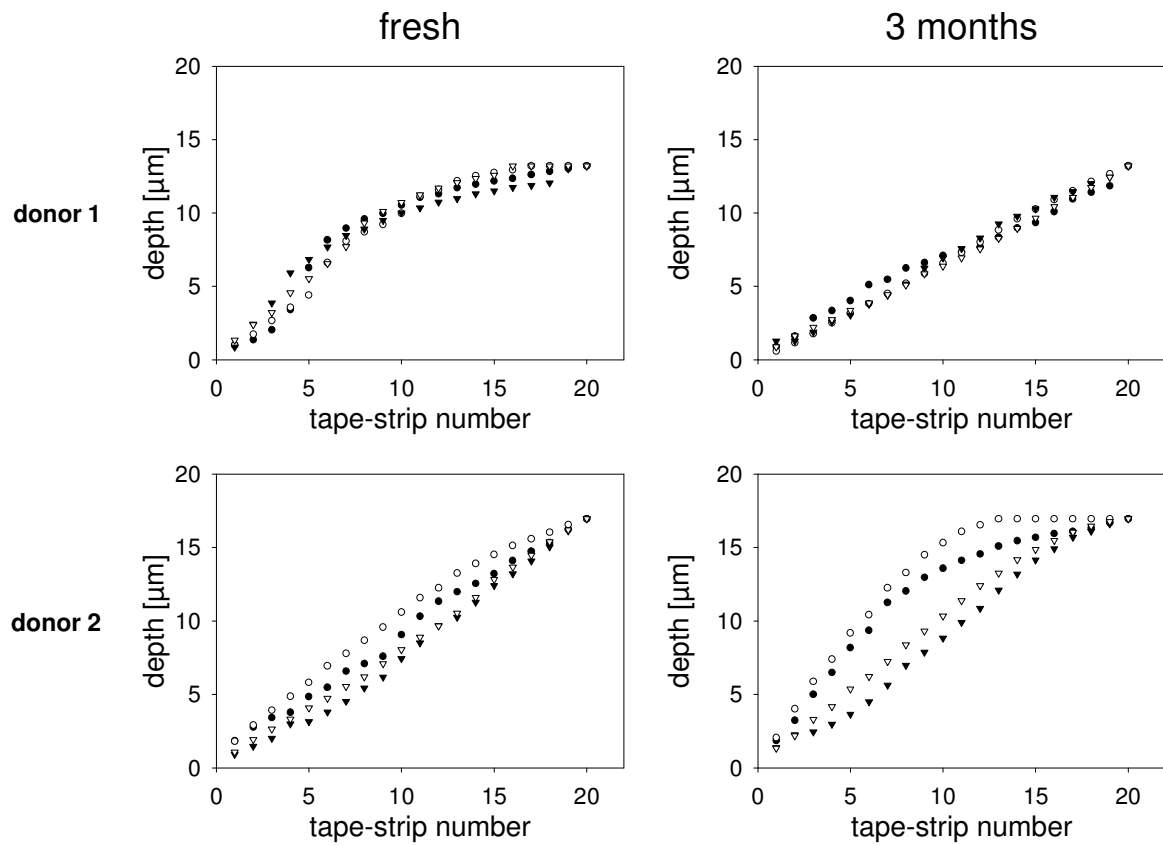


**Figure 3-4** Depth inside the SC reached after sequential tape-strips for abdominal skin of two different donors. Tape-stripping was performed in vitro with tesa® Film kristall-klar on fresh, unfrozen skin and after storage of the skin at  $-26^{\circ}\text{C}$  for three months. Open symbols represent the depth calculated with IR-D and filled symbols show the depth calculated with BCA assay.  $n = 2$  skin punches with 20 sequential tapes for each time point and for every donor. Skin punch A: circle, skin punch B: triangle.

## 3.5 Discussion

### 3.5.1 Protein substitution for BCA calibration standards

Different protein quantification assays have been used in the past successfully for the determination of the amount of protein removed by tape-stripping and the calculation of the SC depth from these values. Ideally, the assay is calibrated with a protein extract prepared from the SC of the same skin that is used in the tape-stripping study to avoid possible inter-individual differences. As this is not possible *in vivo*, Dreher et al. suggested substituting SC extracts with BSA or  $\gamma$ -globulin [144]. In addition, this avoids the time-consuming preparation of the SC extract and produces a steeper calibration curve. However, when using other proteins than SC extracts for calibration, a direct comparison of tape-stripping results of different individuals is only possible if differences in protein content, protein extraction efficiency, and assay reaction efficiency are negligible. This had not been investigated in detail before. Therefore, in the present study we prepared calibration curves from SC extracts of different donors and compared them to a calibration curve prepared with BSA. Both standards under the present conditions resulted in linear calibration curves with quantification limits that are reasonable for protein determination on tapes after tape-stripping (**table 3-3**). The slopes and offsets of the calibration curves prepared with SC extract from different donors were very similar (**table 3-2, fig. 3-1**). Therefore, BSA solution can be used as a calibration agent for protein quantification and the tape-stripping results of different individuals can directly be compared.

### 3.5.2 IR-D *in vivo* versus *in vitro*

Recently, IR-D has been introduced as a fast and non-destructive method for the quantification of the SC amount for tape-stripping *in vivo* [142]. The authors reported a linear correlation between the pseudo-absorption measured by IR-D and the protein amount per area measured by a BCA assay. We could not only reproduce these results in the present *in vivo* study also using D-Squame<sup>®</sup> (d-tape; **fig. 3-2 A**), but we could also carry over the method to a different tape-strip brand, i.e. tesa<sup>®</sup> Film kristall-klar (t-tape; **fig. 3-2 B**). *In vivo* only d-tape removed a similar amount of SC that was independent from the tape-strip number and thus would allow for easily estimating the SC depth mathematically. For t-tape, this was not always possible.

*In vitro*, in the majority of the profiles the SC was removed linearly, however in some cases the curve shape was sigmoidal or a plateau was reached indicating that the SC was completely removed already with less than 20 tapes (**fig. 3-4**). In contrast, this was not observed *in vivo* (data not shown). A potential reason for the discrepancy between *in vivo* and *in vitro* profiles is the different pressure applied to improve the contact between tape and skin surface [149].

Moreover, the depth that was reached *in vitro* with a defined number of tape-strips varied even for two different skin punches of the same donor at the same time point (**fig. 3-4**). These results once more emphasize the necessity for using an instrumental method for exact quantification of SC on each tape-strip.

### **3.5.3 Determination of SC depth**

Regarding the main question of this study, we proved that IR-D does give a similar depth inside the SC for all donors and all time points compared to the standard method (BCA assay), no matter whether the SC was removed in a linear fashion or not. This shows that using this instrumental method to quantify the SC amount on each tape, the SC depth can be determined correctly and thus meets the desired aim of being a non-destructive method for SC depth determination *in vitro*.

### **3.5.4 Determination of endpoint of complete SC removal**

Concerning the second focus of this study, our results show that IR-D is also well-suited for determining the endpoint for complete SC removal as it allows fast in-process monitoring of the results (**fig. 3-3**). Consequently, this method allows for adjusting the total number of tape-strips that are performed for a single skin site during the experiment. Thereby, the SC depth profiles can be determined more accurately.



### **3.6 Conclusions**

IR-D is a suitable method for the quantification of SC on D-Squame® and tesa® Film kristallklar. From the measured pseudo-absorption the cumulative depth inside the SC can be calculated with comparable accuracy as from the protein quantification with a BCA assay. IR-D has two main advantages compared to protein assays such as BCA: The measurement is non-destructive so that the depth inside the SC and the drug amount can be determined on the identical tape-strip. Furthermore, IR-D can be used for individual and in process determination of the total number of tapes that need to be performed for removing the SC quantitatively. This is important as this study demonstrated that it is not advisable to work with a fixed total number of tape-strips. Therefore, using IR-D for tape-stripping improves the quality of skin-concentration-depth-profiles both *in vivo* and *in vitro*.



## **4 Influence of the application area on finite dose permeation in relation to drug type applied**

Parts of this chapter are in press in Experimental Dermatology:

Hahn T, Selzer D, Neumann D, Kostka K-H, Lehr C-M, Schaefer U F

Influence of the application area on finite dose permeation in relation to drug type applied

DOI:10.1111/j.1600-0625.2011.01424.x

The author of the thesis made the following contributions to the publication: Performed and interpreted all major experiments. Wrote the manuscript.

Dominik Selzer developed the mathematical method of determining the coverage and z-score.

#### **4.1 Abstract**

For finite dose skin absorption experiments, a homogeneous donor distribution over the skin surface is usually assumed. However, the influence of the surface distribution on skin absorption is still unknown. The aim of this study was to evaluate the influence of the application area on the permeation of drugs during finite dose skin absorption experiments in static Franz diffusion cells. Permeation experiments with stained aqueous drug formulations were conducted and the application area was determined by a suitable, objective, automated computational approach. In contrast to the maximum incubation area possible in the diffusion cell setup, the application area was the area actually in contact with the donor at the start of incubation

The permeation of caffeine is strongly dependent on the application area: The variability between the single experiments decreased when including the application area. In addition, biopsies from the stained skin area contained significantly more caffeine than biopsies of non-stained skin. For the lipophilic flufenamic acid this was not the case. The variability highly increased after inclusion of the application area. In contrast to caffeine, flufenamic acid distributes fast in the stratum corneum covering the maximal possible diffusion area. Thus, a correction of the area is misleading. In summary, depending on the drug's physicochemical characteristics, the real application area may influence skin absorption.

## 4.2 Introduction

In skin absorption studies infinite dosing is usually employed to evaluate kinetic parameters like permeation coefficient [43,105]. However, this does not represent the *in vivo* situation, where usually a finite dose is applied to the skin, and additional effects may influence the drug absorption, e.g. evaporation of excipients [60].

In the OECD guideline 428 [27] and the guidance document 28 [28] finite dose experiments are defined as experiments with a maximum applied donor volume of 10  $\mu\text{l}/\text{cm}^2$  of liquid formulations. For semisolid and solid substances, values range from 1 to 10  $\text{mg}/\text{cm}^2$  [27-29]. The ideal application should result in a homogeneous layer of the drug formulation over the whole incubation area. Otherwise, the variation between the experiments will increase [72]. However, a homogeneous drug distribution over the whole incubation area is problematic due to wrinkles of the skin.

For creams and ointments even distribution may be confirmed visually, but for uncoloured aqueous solutions and gels the distribution can not easily be determined. To this day the distribution of a drug over the incubation area has only scarcely been analyzed: In two publications, the distribution of a fluorescent model drug in sunscreens over the skin was investigated *in vivo* [153,154] to correlate the results with the sun protection factor. Another publication investigated the distribution of the formulation containing a fluorescent dye with and without microparticles over the incubation area by *in vivo* laser scanning microscopy [155]. These publications, however, did not correlate the skin surface distribution to the absorption of the model drug into the skin.

To address this topic concerning the effect of inhomogeneous donor formulation distribution on *in vitro* permeation results, *in vitro* finite dose permeation experiments were performed applying a donor by two different methods, i) distribution with a punch, and ii) distribution with a disc. To distinguish between skin with and without contact to the donor formulation, aqueous drug solutions were stained with a dye. The drugs employed in this study were caffeine and flufenamic acid (FFA). After incubation, the application area was determined by a newly developed computer-based method to ensure objectivity and to handle high-throughput data processing.

The influence of the application area on the permeation was investigated with respect to its impact on the variability of the data.

Furthermore, lateral drug distribution was analyzed by quantification of skin biopsies with and without contact to the donor formulation.

## 4.3 Methods

### 4.3.1 Materials and instruments

All materials used were of highest analytical grade and were used as purchased.

Ringer's solution was provided by Fresenius Kabi, Bad Homburg, Germany. Purified water was prepared by a Millipore Synthesis device (Millipore GmbH, Schwalbach, Germany).

The following instruments were used: static Franz diffusion cells type 4G-01-00-20 (PermeGear, Riegelsville, PA, USA), incubation area 1.767 cm<sup>2</sup> and acceptor volume 12.1 ml, dialysis membranes with MW-cut-off of 12-14 kDa (Medicell International Ltd, London, Great Britain), 25 mm syringe filters 0.2 µm cellulose acetate membrane (VWR International, West Chester, PA, USA).

### 4.3.2 Skin

Human abdominal skin was obtained from female Caucasian donors undergoing plastic reduction surgery at the Department of Plastic and Hand surgery, Caritaskrankenhaus, Lebach, Germany. The skin was prepared according to [32] and stored in the freezer at -26°C for a maximum of six months. During this time the skin's absorption properties are not changed [38-40]. For this study, skin of three donors was used. The study was approved by the Ethical Committee of the Aerztekammer des Saarlandes no. 204/08.

Heat-separated epidermis (HSE) was prepared according to [45].

### 4.3.3 Permeation experiments

Permeation experiments were performed in a static Franz diffusion cell as described elsewhere [43]. Before incubation, the epidermis was equilibrated with the acceptor solution for one hour resulting in complete hydration. The acceptor solution consisted of PBS pH 7.4 for caffeine and Soerensen phosphate buffer pH 7.4 for flufenamic acid (FFA). To prevent microbial contamination the acceptor was stabilized with 0.05% (w/v) sodium azide. Caffeine was used in a concentration of 1mg/ml in PBS without NaCl and stained with 0.1% (w/v) methylene blue (sodium chloride was omitted due to salt formation with methylene blue). Previous studies have shown that the same permeation coefficients are obtained with and without NaCl.

FFA was used in a concentration of 1 mg/ml in Soerensen phosphate buffer stained with 0.1% (w/v) eosin Y.

All permeation experiments were performed with the donor chamber sealed by parafilm and aluminium foil to avoid crystallization due to solvent evaporation.

Samples were taken from 0 h to 41 h. For each set of experiments 6 to 8 single experiments were carried out. The removed acceptor solution (400  $\mu$ l) was replaced immediately by fresh buffer. The drug concentration in the acceptor never exceeded 10% of the solubility of the drugs in the respective receptor solution.

#### 4.3.4 Application of the donor

Different finite dose application schemes were applied:

- **Punch:** application of 17.6  $\mu$ l of the donor formulation, then distribution of the formulation by 360° rotation of a Teflon punch (in-house, 14 mm diameter), removal of the punch and covering with a Teflon disc with a diameter of 14 mm. The drug amount removed with the punch was later determined by extraction.
- **Disc:** application of 15.6  $\mu$ l of the donor formulation, then distribution and covering with a Teflon disc with a diameter of 14 mm according to [50].

In all finite dose experiments, a dose less than 10  $\mu$ l/cm<sup>2</sup> was incubated with the skin to meet finite dose conditions.

#### 4.3.5 Mass recovery

After incubation, all compartments were thoroughly examined for drug content: the remaining donor on the surface of the skin, drug on the parts of the Franz diffusion cell, and the skin. Caffeine was extracted from the skin with methanol 50% (v/v), sonication for 30 min and further shaking for one hour followed by filtration through a cellulose acetate filter. FFA was extracted with 0.05 N NaOH for two hours at room temperature and filtration through cotton.

In all experiments, a total mass recovery of 92.4 to 99.7% for caffeine and 94.0 to 114.5% for FFA were found.

The extraction power of the drug from HSE was determined with standard solutions being  $97.8 \pm 3.8\%$  for FFA [32] and  $87.4 \pm 5.1\%$  for caffeine [18].



#### 4.3.6 Drug quantification

Caffeine and FFA were quantified according to [18]. For calibration, both substances were dissolved in the respective extraction medium in concentrations of 0.03 – 20 µg/ml.

Stability tests were performed for both substances in all solvents used for at least 41 h at 32°C to ensure no degradation would take place during incubation. The dyes had no influence on the analytics and the permeation of the drugs.

#### 4.3.7 Analysis of the application area

For accurate determination of the application area, the donor formulation was stained with a dye. After incubation, the dye was still visible on the skin surface and the contact area of the donor formulation with the skin could be analyzed.

Following incubation, the skin was removed from the Franz diffusion cell and the donor distribution over the skin surface was visualized by means of a scanner with a resolution of 1200 dpi as .tif data. The scans were analyzed by a two-step approach to check for formulation coverage and homogeneity of distribution.

The application area of each experiment was calculated individually. First, the coverage was determined by using a hue-saturation-value (HSV) colour model [156] and by comparison to a non-stained skin sample. Second, the stained area was inspected for homogeneity by comparison to a perfectly stained skin sample from infinite dose experiments using a red-green-blue (RGB) colour model.

To obtain the fraction of formulation coverage  $\phi$  (Eq. 4-1) each image file was mapped to HSV colour space using appropriate thresholds in the hue channel to separate stained and non-stained pixels (**fig. 4-1 B, D**).

$$\phi = \frac{\text{stained pixels of the incubation area}}{\text{number of total pixels of the incubation area}}$$

(Equation 4-1)

To analyze the homogeneity of dye distribution the stained area of the sample skin after incubation (**fig. 4-1 A, C**) was compared to a reference image from infinite dose application with perfect staining (**fig. 4-1 E, F**).

To measure the difference to perfect staining the images were mapped to RGB colour space and the absolute robust z-score (z-score) of intensities of a dye-dependent colour channel of a reference staining (infinite dose case) and the stained parts of finite dose sample image,

previously identified by the HSV method, was calculated according to:

$$z = \frac{|x - ref|}{\sigma_{ref}} \quad (\text{Equation 4-2})$$

Here,  $x$  is the median of intensities in the separation channel of the sample image,  $ref$  is the median of intensities in the separation channel of the infinite dose reference image and  $\sigma_{ref}$  is the median absolute deviation of the intensities in the separation channel of the infinite dose reference image.

For methylene blue stained skin the red channel showed a Gaussian like distribution in intensities and allowed a clear separation (peak shift) between stained and unstained areas. For eosin Y stained skin the green channel showed the best separation potential.

All methods were implemented using MATLAB 7.8.0 (The MathWorks, Natick, Massachusetts, USA) with the Image Processing Toolbox.

Coverage, expressed as percentage of the whole incubation area and the homogeneity of distribution ( $z$ -score) were determined for each experiment and the mean of all experiments was calculated.

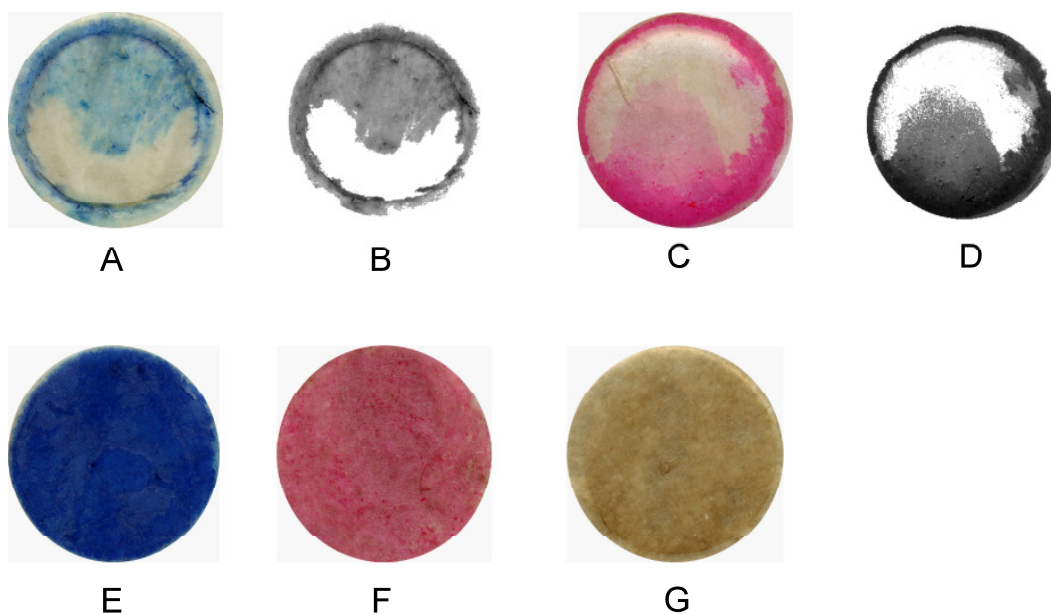


**Figure 4-1** Visualization of the application area from scans. A: caffeine stained with methylene blue, finite dose; B: caffeine stained with methylene blue, finite dose, coverage; C: FFA stained with eosin Y, finite dose; D: FFA stained with eosin Y, finite dose, coverage; E: caffeine stained with methylene blue, infinite dose (reference); F: FFA stained with eosin Y, infinite dose (reference); G: incubated with unstained drug solution (blank), identical for both drugs.

#### **4.3.8 Lateral drug distribution**

Drug distribution in stained and unstained skin parts was analyzed after incubation in the permeation setup. 15.6  $\mu\text{l}$  of the stained drug formulation were applied to the skin as a drop without further distribution. This setup led to inhomogeneous formulation distribution over the incubation area. Thus, not all skin available for diffusion was in contact with the donor formulation. After predetermined time intervals of incubation (after 41 h, and additionally for FFA after 2 h and 20 h), 5 mm biopsies were taken from both completely stained and from completely unstained skin parts of the skin inside the donor area of the Franz diffusion cell and analyzed for their drug content. This allowed for comparison of the biopsy with contact to the donor formulation to the one without contact.

#### **4.3.9 Statistics**

Statistical tests (student's t-test) were performed with Sigma Stat 3 (SYSTAT Software Inc., Point Richmond, CA, USA) to determine significant differences in results. A significant difference was detected at  $p < 0.05$ .

## 4.4 Results

### 4.4.1 Permeation profiles, uncorrected surface distribution

The permeation profiles of caffeine were only slightly in accordance with typical finite dose profiles including an approach of the curve to a maximum (**fig. 4-2**, black circles). A flattening of the curve can only be assumed. For the disc application the profile is similar to infinite dose behaviour (**fig. 4-2 B**, black circles).

In both application schemes, a similar cumulative drug amount permeated after 41 h incubation (punch:  $38.4 \pm 9.4$  %/cm<sup>2</sup>, disc:  $37.7 \pm 10.5$  %/cm<sup>2</sup>) and a high variability between the single experiments was found (**fig. 4-2**).

The permeation profiles of FFA resembled typical finite dose permeation graphs (**fig. 4-3**, black circles) approaching a maximum after longer incubation times. Both application methods led to this characteristic permeation profile. With the punch, however, the maximum was statistically lower than for the disc (**fig. 4-3 B**), i.e.  $40.5 \pm 2.6$  %/cm<sup>2</sup> versus  $48.2 \pm 3.4$  %/cm<sup>2</sup> after 41 h incubation. The variability between the individual experiments was low.

### 4.4.2 Donor surface distribution

Coverage was similar for both dyes with high variability for all experiments (**table 4-1**). Results of this identification method for methylene blue are shown in **fig. 4-1 B** (compared to **fig. 4-1 A**), and for eosin Y in **fig. 4-1 D** (compared to **fig. 4-1 C**).

Z-scores were dependent on the dye; however, within each group very similar (**table 4-1**).

**Table 4-1** Coverage and z-score of FFA and caffeine using different application methods. Mean  $\pm$  SD.

	FFA Disc	FFA Punch	Caffeine Disc	Caffeine Punch
Employed dye	Eosin Y	Eosin Y	Methylene blue	Methylene blue
Coverage [%]	$67.9 \pm 18.6$	$68.5 \pm 16.2$	$74.2 \pm 18.5$	$73.7 \pm 18.1$
z-score	$0.7 \pm 0.5$	$0.9 \pm 0.7$	$4.9 \pm 1.7$	$5.9 \pm 0.4$

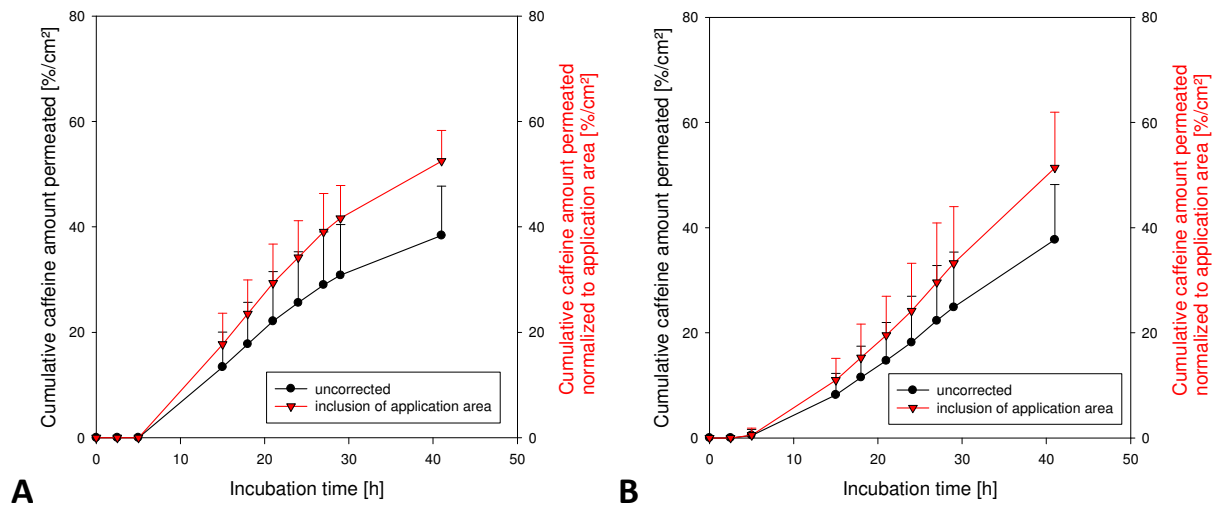


**Figure 4-2** Permeation profiles of **caffeine** through heat-separated epidermis. Black circles: Relative cumulative caffeine amount per applied dose *normalized to total incubation area* (**uncorrected**). Red triangles: Relative cumulative caffeine amount per applied dose *normalized to application area* (**inclusion of application area**). Donor: caffeine 1 mg/ml. A: punch application, n=7. B: disc application, n=6. Mean, SD (provided only in one direction for the sake of clarity).

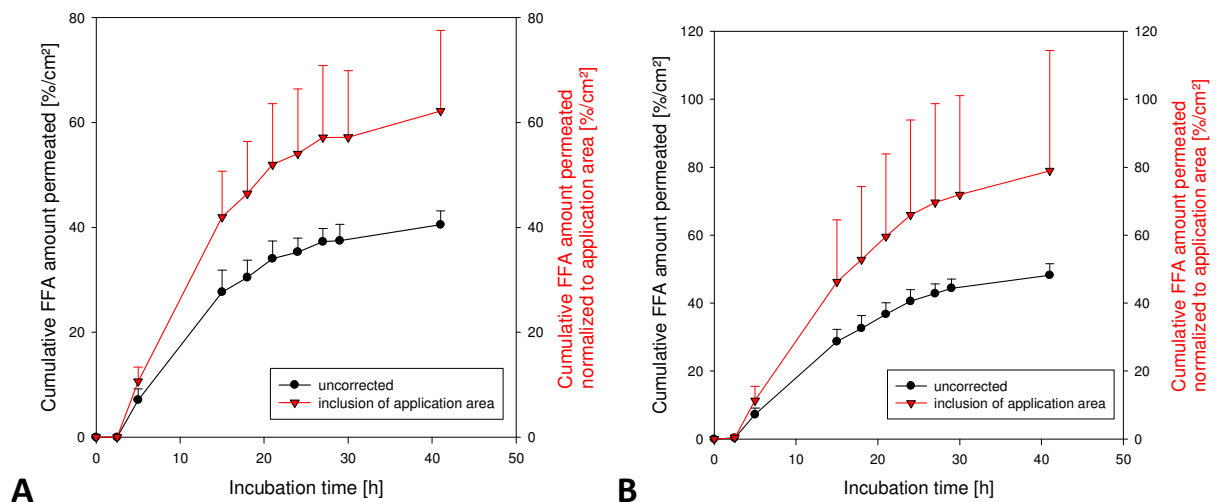


**Figure 4-3** Permeation profiles of **FFA** through heat-separated epidermis. Black circles: Relative cumulative FFA amount per applied dose *normalized to total incubation area* (**uncorrected**). Red triangles: Relative cumulative caffeine amount per applied dose *normalized to application area* (**inclusion of application area**). Donor: FFA 1 mg/ml. A: punch application, n=8. B: disc application, n=8. Mean, SD (provided only in one direction for the sake of clarity).

#### 4.4.3 Permeation data combined with calculated application area/coverage

To find out whether the application area had an effect on permeation, the previously obtained permeation profiles for caffeine and FFA were normalized to the application area of each single experiment.

Inclusion of the application area led to a decrease in variability of the permeation profiles of caffeine (**fig. 4-2**, red triangles). The relative standard deviation decreased strongly, too, and was slightly reduced over the incubation time (e.g. after 41 h for the punch 24% before and 11% after correction).

The permeation experiments with FFA exhibited a much lower variability between the different experiments compared to caffeine, even though the coverage was similar to the caffeine experiments. After including the application area, the variability between the experiments (**fig. 4-3**, red triangles), as well as the relative standard deviation (e.g. after 41 h for the punch 7% before and 25% after correction) increased highly.

#### 4.4.4 Lateral drug distribution

After 2 h incubation with FFA, only in the skin parts in contact with the donor formulation FFA could be detected (**fig. 4-4**). With increasing incubation time, the FFA amount in the stained skin parts decreased while in the non-stained parts it increased. After 20 h no significant difference between stained and non-stained skin could be detected any more ( $2.33 \pm 2.52\%$  of applied dose vs.  $0.31 \pm 0.05\%$  of applied dose, mean  $\pm$  SD), and after 41 h the amount of FFA in biopsies with or without staining was similar ( $0.28 \pm 0.04\%$  of applied dose vs.  $0.26 \pm 0.01\%$  of applied dose, mean  $\pm$  SD).

For caffeine, no lateral distribution could be observed after 41 h incubation.

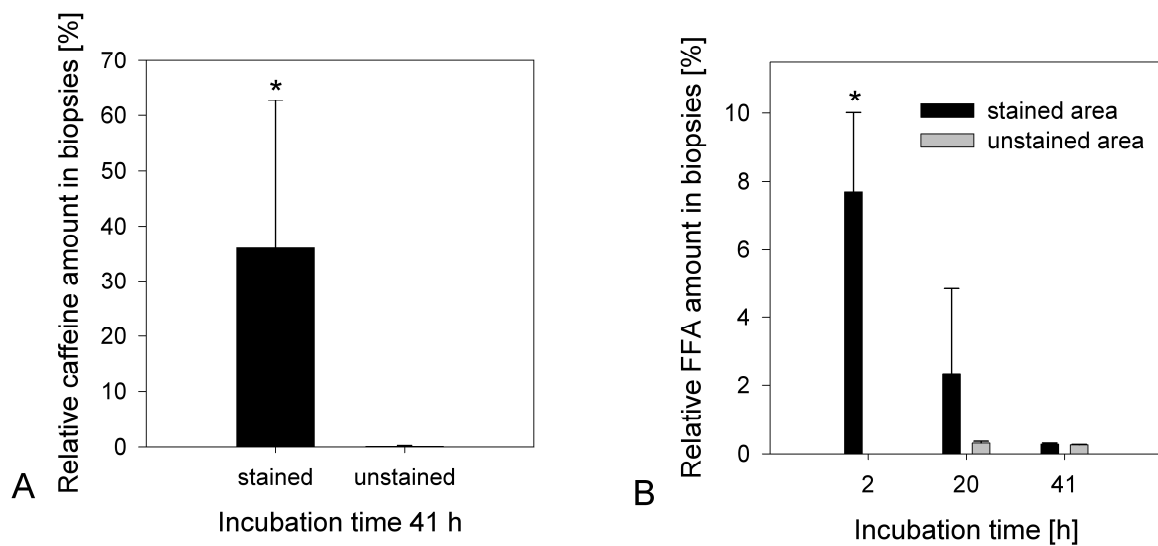


**Figure 4-4** Relative drug amount determined in 5 mm diameter skin biopsies of stained or non-stained skin parts after incubation in FD-C. Donor application as drop: A: Caffeine after 41 h incubation, n=7. B: FFA after 2 h, 20 h, 41 h incubation, n=3. T-test: \*: p<0.01. Mean  $\pm$  SD.

## 4.5 Discussion

The goal of this study was to evaluate the influence of drug distribution of the application area on the results of finite dose permeation experiments using aqueous donor solutions. Therefore, two different application methods were tested and an automated detection system for surface distribution based on dyes was developed.

### 4.5.1 Dye as a marker for skin contact with the donor formulation

The aqueous donor phase employed in this study shows a high contact angle on the skin surface and therefore does not spread easily. The highly water soluble dyes employed in this study can be assumed to remain in the aqueous donor solution and are not distributed laterally over the lipophilic stratum corneum, making them an ideal compound for marking the contact area of the hydrophilic formulation with the skin (application area).

### 4.5.2 Suitability of the automated computer-assisted approach for determination of coverage

Based on the analysis of hue values and z-scores by an automated computer-assisted method the determination of coverage and homogeneity is an objective method to characterize the formulation distribution on skin's surface. However, since the HSV colour space is a cylindrical-coordinate representation, two thresholds to define the blank skin (hue range) have to be determined. Within this range all pixels from the sample skin image will count as blank skin and all pixels outside this range will count as stained skin. Hue values between 0.02 and 0.35 were chosen empirically to identify non-stained skin pixels from a non-stained skin sample (**fig. 4-1 G**). These thresholds did guarantee a conservative prediction of staining since no false positive pixels were detected in a negative test set with only blank skin samples. Changing these parameters can significantly impact the definition of the coverage. Thus, for every batch of experiments a blank reference skin sample image (**fig. 4-1 G**) should be used to gather appropriate thresholds. The original sample images of skin (**fig. 4-1 A, C**) showed excellent consistency with the determined application areas (**fig. 4-1 B, D**).

Calculation of the absolute robust z-score requires a median intensity level and the median absolute deviation of the RGB colour channel of a perfectly stained reference skin sample



image (**fig. 4-1 E, F**). Since eosin Y showed z-scores near zero, this indicates that the dye distribution was close to a perfect staining (**table 4-1**). For methylene blue, the values are reasonable.

Besides increasing the speed of the evaluation process, the great benefits from using this automated approach is objectivity and stability of coverage, and colour distribution analysis for finite dose experiments that is not possible using a manual inspection method. In addition, the transfer of this method to evaluate formulation distribution *in vivo* is possible, if digital images made by photography were used instead of the scanned.

#### **4.5.3 Permeation profiles and lateral drug distribution**

The permeation profiles for caffeine do not resemble the typical finite dose characteristics (**fig. 4-2**). It is possible that after 41 h the effect of donor depletion is just not yet visible in the permeation profiles due to slower permeation of caffeine.

The effect of the application area on the permeation profiles depends on the drug employed. For FFA, the variability between the experiments increased after including the application area, leading to the assumption that other additional effects may influence the drug absorption. These effects may be explained by lateral distribution of the lipophilic FFA ( $\log D \sim 2.2$  at pH 7.4, estimated). Skin biopsies taken after different incubation intervals from stained and unstained skin resulted in information about the time profile of lateral distribution of FFA, which was distributed homogeneously over the whole incubation area after 41 h. As caffeine is a relatively hydrophilic compound ( $\log K_{o/w} -0.08$ ) [18,50] it cannot be transported into the lipid bilayers as easily as FFA.

Lateral distribution was investigated from aqueous solution. This medium was chosen to gain general data for a substance and make the data comparable to the extended Flynn database [157,158]. Moreover, penetration enhancing effects, e.g. of oils or ethanol, or even plasma [159], were excluded. In addition, using excised human skin in aqueous surrounding led to exclusion of the follicular route due to closure of the follicles during hydration [160].

A direct visualization of lateral drug distribution over time would be preferred. For fluorescent dyes, the fluorescent recovery after photo bleaching (FRAP) technique can be employed [117] to analyze lateral diffusion. However, quantitative results are difficult to obtain for non-fluorescent drugs due to the low amount of drug actually diffusing laterally

---

and thus of analytics. This problem is even increased by finite dose application. Thus, lateral distribution in our study was investigated by means of skin biopsies.

#### **4.5.4 Clinical relevance**

*In vivo* experiments are quite expensive and their number will be reduced in the future. Therefore, *in vitro* skin absorption studies are important to gain first information about the absorption kinetics of a substance. Correlations between *in vitro* and *in vivo* experiments have been shown previously [32-34,36]. Thus, for example for bioequivalence studies *in vitro* experiments are beneficial to determine e.g. the difference between two vehicles [82].

Finite dose experiments are even closer to the real-life scenario of a patient applying a small amount of a topical formulation. Due to that similarity, finite dose experiments are of major interest to predict the drug absorption. During *in vivo* application, differences in the homogeneity of donor formulation distribution are also possible, thus an analysis of the influence of inhomogeneous donor distribution is important, too.

## **4.6 Conclusion**

As shown in this paper, including the application area does not automatically improve the results from skin permeation studies using aqueous solutions, leading to more consistent results. Depending on the physicochemical characteristics of the drug, the substance behaves differently. For the more hydrophilic substances (e.g. caffeine) the degree of contact to the skin is crucial for permeation and this parameter should be included in the analysis of finite dose experiments. For lipophilic substances, e.g. FFA, however, the application area has less effect on the permeation of the drug.

It can be assumed that the lipophilicity of the drug plays a role on the degree of distribution over the lipophilic stratum corneum. One question that remains is whether a limit of lipophilicity exists up to where distribution has an influence on permeation. To answer this question, another study with substances covering a wide range of lipophilicity would be required.



## **5 Finite dose skin absorption – Comparison between simulation, pharmacokinetic modelling, and experiment**

This chapter is suggested for publication in Journal of Controlled Release in an adapted version.

The author of the thesis made the following contributions to this chapter: Performed and interpreted all experiments. Contributed to the development of the pharmacokinetic model.

Dominik Selzer made the following contributions to this chapter: Developed the pharmacokinetic model and the data correction with the stretching factor.

The Wittum group in Frankfurt made the following contributions to this chapter: Developed the detailed diffusion model and adapted it to finite dose, and performed the simulations.

## 5.1 *Abstract*

Skin absorption experiments are of great interest for determining the absorption of a compound to the skin. The mass profiles in each compartment give detailed information about the actual distribution of the drug in each compartment. As finite dose experiments are closer to the *in vivo* situation, they are of special interest.

In this thesis, finite dose has already been applied to permeation experiments with heat-separated epidermis. In the following chapter, the focus is on finite dose skin absorption experiments with full-thickness skin to obtain mass profiles in the different compartments. The experiments performed in this chapter include the finite dose application and analysis method previously established in the permeation experiments. The experimental mass profiles were investigated with respect to experimental data, pharmacokinetic modelling, and with a 2D diffusion model.

The pharmacokinetic model developed in this study included the lateral skin part compressed in the Franz diffusion cell during incubation and could fit the experimental profiles correctly, also in the lateral compartment.

Furthermore, the diffusion model adapted to finite dose reasonably predicted the mass profiles in the different compartments.

## 5.2 Introduction

As transdermal delivery of drug through the skin is gaining more relevance nowadays, the pharmaceutical industry is interested in evaluating the absorption of chemicals to the skin. Besides, the cosmetic industry is also interested in evaluating the systemic availability of cosmetically used substances, which normally should be avoided. To achieve this, usually infinite dose skin absorption experiments are performed. However, these experiments mainly give information about the steady-state conditions, but are not suitable for obtaining detailed information about the actual absorption process in the transient state. For the latter situation finite dose experiments are better suited.

As defined in the OECD guideline 428 [27] and the guidance document 28 [28], finite dose experiments are characterized by an application volume of  $10 \mu\text{l}/\text{cm}^2$  or less to the skin. This donor volume is much closer to the dermal application situation *in vivo*, where usually only a small amount of a topical formulation is evenly distributed on the skin surface. Finite dose experiments allow for estimation of the absorption of chemicals from a patient situation, a working environment, or a cosmetic application.

Most studies investigate the permeation of a drug through a membrane, and do not focus on the drug amount in the skin. To obtain a higher resolution of the drug in the different skin layers, penetration experiments are performed, separating the skin into different surface parallel sections. Thus, the concentration of the drug in the different skin layers can be determined. From this analysis, information about the absorption behaviour of the substance to the skin can be gained, e.g. the formation of a drug depot in the upper skin layers [8,9].

However, as skin absorption experiments are generally time consuming, mathematical descriptions are useful tools to investigate the absorption behaviour and to reduce the number of experiments. Mathematical predictions of substance absorption can significantly reduce the number of experiments. Different models are available, most of them however solely regard the permeation profiles of a drug through a skin membrane [101,128] and not the drug amount in each skin layer.

To account for finite dose application and the analysis of the drug amount in each skin layer, in this study finite dose skin penetration experiments were performed and the drug amount in each skin layer was determined.

As mathematical descriptions are not applicable without proper differentiation between the compartments, in this study the different compartments were carefully evaluated. In our study, a highly standardized method for tape-stripping the SC was employed, which required stretching of the skin before tape-stripping. To correct the experimental data for this setup, a stretching factor was necessary. When applying another tape-stripping technique, this correction may not be required. For example Lademann et al. [135] applied a roller to apply the pressure, which ensures that the complete surface of the SC can be stripped *in vivo*. Due to this setup, stretching of the skin is not necessary.

Furthermore, a pharmacokinetic model was developed to describe the mass profiles of the drug in each compartment in this setup. The novelty of this model was the separation of the skin into not only the stratum corneum (SC) and the deeper skin layers (DSL), but also into an additional lateral skin part. This compartment is usually completely neglected during mathematical descriptions of experimental data.

To simulate the mass profiles in the different compartments, a detailed diffusion model previously developed for infinite dose [19] was adapted to the finite dose scenario. The input parameters for this model were previously derived from infinite dose experiments [18], and the same parameters were used for the finite dose case. It has been shown previously that parameters derived from infinite dose can be employed to predict finite dose kinetics [128], whereas estimation from finite dose experiments may show great intraindividual variability [161].



## **5.3 Materials and methods**

### **5.3.1 Materials and instruments**

The following chemicals were used: potassium dihydrogen phosphate, citric acid x H<sub>2</sub>O (Merck, Darmstadt, Germany), caffeine, flufenamic acid, acetonitrile, methanol (Sigma-Aldrich, Steinheim, Germany), orthophosphoric acid, sodium hydrogen phosphate dihydrate (Riedel-de Haën, Sigma-Aldrich, Seelze, Germany). Purified water was prepared by a Millipore Synthesis device (Millipore GmbH, Schwalbach, Germany).

Static Franz diffusion cells type 6G-01-00-15-12 with a acceptor volume of 12.1 ml and an incubation area of 1.767 cm<sup>2</sup> were provided by Perme Gear, Riegelsville, PA, USA; tesa® Film kristall-klar, (t-tape, 33 m x 19 mm, #57330-00000-02, cut to pieces of 16 x 19 mm) was provided by tesa AG, Hamburg, Germany; cryomicrotome (MEV) was provided by SLEE, Mainz, Germany; centrifuge (Rotina 420R) was provided by Hettich Zentrifugen, Tuttlingen, Germany.

### **5.3.2 Skin**

Excised human full-thickness skin was obtained from three female Caucasian donors undergoing abdominal plastic surgery at the Department of Plastic and Hand surgery, Caritaskrankenhaus, Lebach, Germany. The study was approved by the Ethical Committee of the Aerztekammer des Saarlandes no. 204/08.

The skin was treated according to [32] and stored in the freezer at -26°C for a maximum of six months. When taking a skin punch on the day of the experiment, care was taken to strictly avoid repeated freezing and thawing of the skin. It has been shown that this treatment does not impair the barrier function of the skin [38-41].

### **5.3.3 Skin absorption experiments**

To conduct a skin absorption experiment, a 25 mm punch of the frozen skin was taken on the day of the experiment and allowed to thaw. After cleaning the skin with distilled water and drying it with cotton balls, the skin was mounted in a Franz diffusion cell with the epidermis side up. The acceptor compartment was filled with Soerensen phosphate buffer pH 7.4, and the skin was equilibrated for one hour with the acceptor solution with a sealed

donor chamber (with parafilm and aluminium foil) to avoid water evaporation. Preliminary experiments showed that longer equilibration time did not change the results.

The donor consisted of the respective drug dissolved in Soerensen phosphate buffer pH 7.4 in concentrations of 1 mg/ml for flufenamic acid (FFA), and 1 mg/ml and 12.5 mg/ml for caffeine.

25  $\mu$ l of the donor solution was applied to the skin by means of a positive displacement pipette. The donor formulation was spread evenly over the incubation area by means of a teflon punch with a diameter of 14 mm, which was turned through 360°. After removal of the punch, a teflon disc with a diameter of 14 mm was placed onto the donor solution to enhance the contact to the skin surface during incubation. The actual amount of donor formulation remaining on the skin was later determined from the washing of the punch.

In all experiments, a finite dose was achieved according to [27,28] (donor volume remaining on the skin surface less than 10  $\mu$ l/cm<sup>2</sup>). After application of the donor solution, the donor compartment was sealed again with parafilm and aluminium foil. The whole setup was incubated at 32  $\pm$  1 °C.

#### 5.3.4 Isolation of the different skin compartments

After incubation, the skin was cleaned of remaining donor formulation by cotton balls. Then, tape-stripping was performed *in vitro* with tesa® Film kristall-klar under highly standardized conditions according to *chapter 10 Appendix*.

After complete removal of the SC by tape-stripping, the rest of the skin was frozen using expanding carbon dioxide. Then, a punch of 13 mm diameter was taken from the stripped area of the frozen deeper skin layers (*DSL*) and cut by cryo-sectioning.

The lateral skin parts were leftover and were treated as explained in *chapter 5.3.5*.

#### 5.3.5 Determination of the stretching factor for data correction

The experimental methodology (skin stretching before tape-stripping and the usage of a smaller punch to separate the *DSL*) does promote the formation of a »pseudo-lateral« skin part in addition to an actual lateral skin part (**fig. 5-1**). Since this effect does falsify mass recovery results and the degree of stretching of the skin is typically unknown, the stretching factor  $f$  (Eq. 5-1) was introduced to scale mass  $f$  recovery data from the experiment.

We assumed a horizontal uniform drug distribution within each model compartment (Donor, SC, DSL, Lateral, and Acceptor) and used a first order mass balance model to estimate the stretching factor  $f$ .

$$f = \frac{A_{\text{Stretched}} - A_{\text{Incubated}}}{A_{\text{Incubated}}} \quad (\text{Equation 5-1})$$

$f$  is the ratio of the difference between stretched area  $A_{\text{Stretched}}$  and incubated area  $A_{\text{Incubated}}$  normalized to  $A_{\text{Incubated}}$ . We assumed an artificial flux from the donor compartment directly to the lateral compartment via the »pseudo-lateral« compartment that corresponds to skin stretching induced by the used tape-stripping procedure (**fig. 5-1 B**). In this mass balance model the rate constants of the flux through the stretched skin part outside of the stripped area to the lateral skin part should commensurate with the rate constants to the skin parts of the incubated area. The proportionality factor should correspond to the scaling factor  $f$ . The set of ordinary differential equations (ODEs) of the model was solved numerically and the rate equations as well as the stretching factor  $f$  were fitted to the mass over time curves by minimizing the root mean square deviation (RMSD) of the fitted results and experimental data points. The procedure was implemented using Python 2.7.1 and the SciPy package [162].

The amount of drug in the SC, DSL and the lateral skin part was scaled according to the ratio of surface area of the stretched skin and the area of incubation.

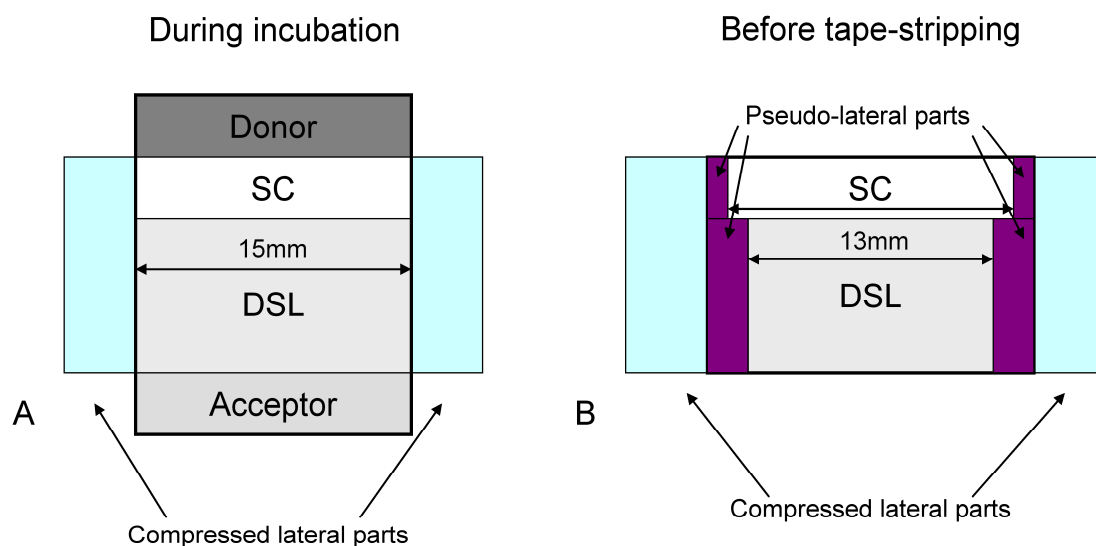


**Figure 5-1** Schematic visualization of the geometric problems associated with stretching the skin before tape-stripping. A: skin during incubation. B: skin stretched before tape-stripping.

### 5.3.6 Validation of the stretching factor

To validate the stretching factor, full-thickness skin was incubated in a Franz diffusion cell with the donor formulation. After incubation, the skin was not stretched in preparation for tape-stripping. Instead, a 16 mm biopsy was taken to remove all incubated skin parts. The remaining skin rest was regarded as lateral skin parts without any contact to the donor formulation. All skin compartments (Donor, Incubated skin (*SC+DSL*), Lateral skin parts, Acceptor) were quantified for their drug content.

For each drug the longest incubation time of the experimental range was chosen, for FFA 6 h and for caffeine 12 h. The same concentration of 1 mg/ml was applied for both drugs.

### 5.3.7 Mass balance

After incubation, the different compartments of the setup were thoroughly examined. The remaining donor on the surface of the skin, including remaining formulation on the upper part of the Franz diffusion cell was removed by means of cotton and extracted with the respective extraction fluid for two hours. The tape-strips (*SC*), the cryo-cuts (*DSL*), and the lateral skin parts were treated identically, with an additional centrifugation step for 10 min at 1000 rpm for the *DSL* extracts and removal of the supernatant for analysis. The samples from the acceptor were measured without further dilution steps.

FFA was extracted using 0.05 N sodium hydroxide solution and caffeine with phosphate buffer pH 2.6 for 2 h. For all experiments, the obtained total recovery for FFA ranged from 83.8% to 96.8% and for caffeine from 87.9% to 107.3%.

### 5.3.8 Quantification

Samples were analyzed by Reversed-phase high performance liquid chromatography (RP-HPLC) using an isocratic Dionex HPLC system with a Lichrospher® 100/RP-18 column with a Lichrocart 4-4 Lichrospher® 100/RP-18 guard column (Merck-Hitachi, Darmstadt). Software: Chromeleon 6.60 SP1 Build 1449.

For caffeine, the mobile phase was composed of phosphate buffer pH 2.6 (1.16 ml/l orthophosphoric acid, 2.04 g/l potassium dihydrogen phosphate): acetonitrile (90:10), (v/v). Injection volume: 50 µl; flow rate: 1.4 ml/min; retention time: 4.9 ± 0.2 min; detection wavelength: 262 nm; detection limit: 20 ng/ml; quantification limit: 30 ng/ml.

For FFA, the mobile phase was composed of methanol: buffer pH 2.2 (22.75 g/l citric acid monohydrate, 0.4 g/l  $\text{Na}_2\text{HPO}_4 \times 2\text{H}_2\text{O}$ ) (80:20), (v/v). Injection volume: 50  $\mu\text{l}$ ; flow rate: 1.2 ml/min; retention time:  $3.3 \pm 0.2$  min; detection wavelength: 284 nm; detection limit: 30 ng/ml; quantification limit: 50 ng/ml.

The detection limit was determined as the threefold standard deviation of the y-axis intercept divided by the mean of the slope. The quantification limit was determined by the fivefold standard deviation of the y-axis intercept divided by the mean of the slope.

For calibration, both substances were dissolved in the respective extraction medium in concentrations of 0.03 – 20  $\mu\text{g/ml}$ . Stability tests in Soerensen buffer showed that both drugs were stable in this buffer up to 30 h incubation at 32°C.

### 5.3.9 Pharmacokinetic modelling

Pharmacokinetic (PK) modelling was applied to analyze mass profiles in the different compartments for FFA and caffeine finite dose experiments. The model treats the different skin layers as well stirred compartments. First-order kinetics was assumed to describe the substance mass flux for every compartment, which yielded a set of ODEs. An explicit lateral compartment was modeled as an extension of the classical models. The set of ODEs was numerically integrated and fitted (nonlinear least squares regression) to experimental data using the Python programming language with the SciPy package (scientific python). The root mean square deviation (RMSD) was used as an indicator for accuracy. A grid search was applied to find appropriate starting values in order to avoid sticking in a local minimum.

In the PK model a lateral compartment was added, into which the drug can enter through the *SC* or the *DSL* compartment (**fig. 5-2**). In this model the transport constants  $k_5$  and  $k_6$  display an averaged transport via the *SC* and *DSL* to the lateral compartment.

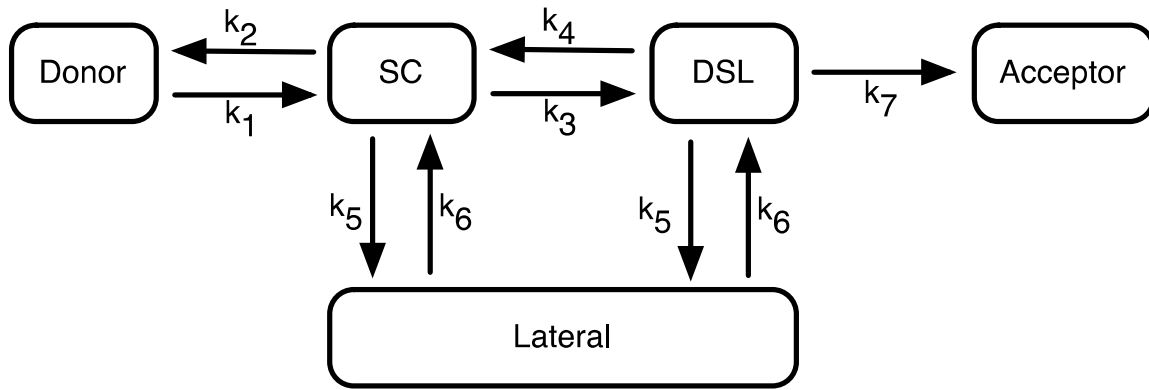


**Figure 5-2** Pharmacokinetic model developed to analyze the drug distribution between various relevant compartments in the setup.

### 5.3.10 Detailed diffusion model

The transport is modeled by a diffusion process in an idealized, two-dimensional model membrane. The model has been described previously for an infinite dose setting [18,19]. The core part of the model is a brick-and-mortar like structure, which represents the SC. On top and bottom side of this structure two additional compartments were added. These model the donor chamber (don) of the diffusion cell and the DSL, respectively. The heights for donor and DSL compartments are  $h_{\text{don}}=0.1$  mm and  $h_{\text{DSL}}=3$  mm, respectively. Initially, no substance is present in SC and DSL, and a defined concentration matching the experimental setup is provided in the donor. A lateral compartment was not included in the model. A schematic graph of the diffusion model can be found in *chapter 1 Introduction fig. 1-9*.

The model relies on a variety of diffusion and partition coefficients, which are provided in **table 5-1**. All parameters employed in this model were taken from infinite dose experiments performed previously [18], except  $D_{\text{don}}$ , which has been calculated for the finite dose scenario. A relationship to predict the diffusion coefficient  $D_a$  in an aqueous solution from the solute molecular weight was proposed by Anderson et al. [163] with

$$D_a = D_a^0 \cdot MW^{-n} \quad (\text{Equation 5-2})$$

where  $D_a$  is the diffusion coefficient in a certain medium,  $n$  and  $D_a^0$  are constants associated with the medium at a defined temperature, and  $MW$  the molecular weight in Da. Using 37 substances and their corresponding molecular weight and diffusion coefficient in water at a given temperature [164] the previous equation was fitted using a linear model.

**Table 5-1** Input parameters for simulation of skin absorption with 2D diffusion model from [18,19] and the calculated values for  $D_{don}$ .

Parameter		FFA	Caffeine
$D_{don}$	$[\mu\text{m}^2/\text{s}]$	686.33	809.92
$D_{lip}$	$[\mu\text{m}^2/\text{s}]$	3.055	5.833
$D_{cor}$	$[\mu\text{m}^2/\text{s}]$	0.014166	0.003888
$D_{DSL}$	$[\mu\text{m}^2/\text{s}]$	136.11	63.89
$K_{lip/don}$		20.32	2.15
$K_{cor/lip}$		0.21	2.22
$K_{DSL/lip}$		0.1	0.08

### 5.3.11 Statistics

Graph Pad Prism was used for calculating student t-test. Significant differences were found at  $p < 0.05$ .

## 5.4 Results

### 5.4.1 Validation of the stretching factor

By scaling of the experimental data the drug amount in the lateral skin parts decreased and in the *SC+DSL* compartments it increased. Experiments with unstretched skin resulted in similar drug amounts in the *SC+DSL* and in the lateral skin compartments as the scaled experimental data set (fig. 5-3). No significant differences could be found between the scaled experimental data and the data obtained from the experiments with unstretched skin (Reference) both for FFA and caffeine. The difference between Reference and Original in the lateral part was significant for both drugs.

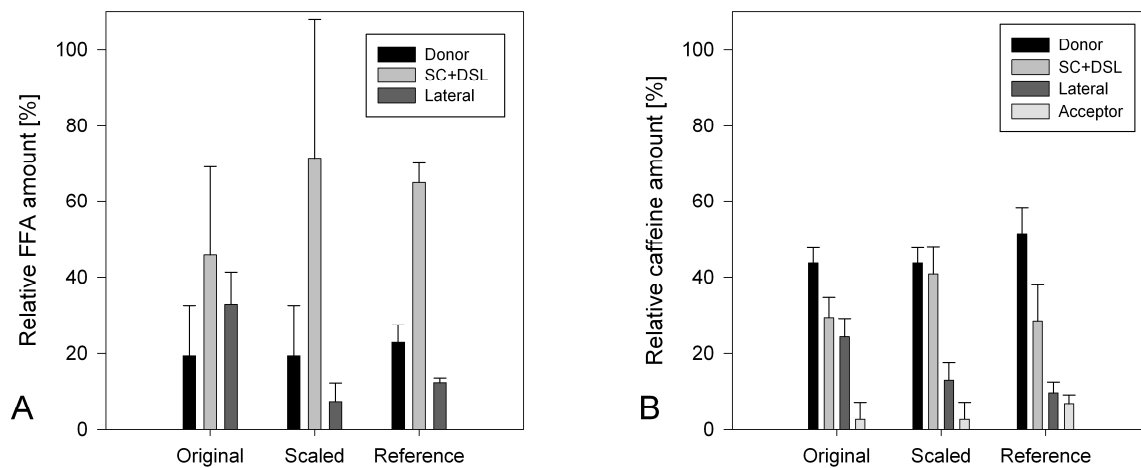


**Figure 5-3** Relative drug amount recovered from the different compartments. Donor: Formulation recovered from the skin surface and surface of donor compartment. *SC+DSL*: incubated skin parts. Lateral: Skin outside of the incubated area. Acceptor: drug in acceptor compartment. Original: data from tape-stripping experiments. Scaled: data from tape-stripping experiments scaled with stretching factor. Reference: data from experiments without stretching. A: FFA: n=5. B: caffeine: n=4.



### 5.4.2 FFA mass profiles

#### - Experimental data

FFA finite dose experiments resulted in a relatively fast decrease of drug in the donor. Already after 15 min the drug amount in the donor was reduced to around 60% of the applied dose (**fig. 5-4 A**). After this quick donor reduction, the donor continued to deplete more slowly, reaching around 20% remaining in the donor compartment after 6 h incubation. In the *SC* around 30% of the applied dose was found after 15 min and a plateau was reached and maintained until 2 h after application (**fig. 5-4 B**). Afterwards, the FFA amount decreased to 10-20% with high variability at the 4 h and 6 h data points. The drug amount in the *DSL* increased constantly, reaching a plateau at approximately 50% after 4 h of incubation (**fig. 5-4 C**). No FFA could be quantified in the acceptor compartment until 6 h of incubation due to analytical reasons (**fig. 5-4 D**). The drug amount determined in the lateral skin part appeared to increase after longer incubation (**fig. 5-4 E**). However, data is affected by high variability, especially for later time points, a tendency comparable to the other compartments.

#### - Pharmacokinetic model

The donor could be correctly fitted by the PK model, decreasing rapidly in the first hour to around 50%, and then decreasing slowly to around 20% after 6 h (**fig. 5-4 A**). The *SC* profile could also be correctly fitted; however the drug amount in the *SC* for the 30 min and 60 in time points was slightly over predicted, but clearly in the range of the standard deviation (**fig. 5-4 B**). The *DSL* was correctly fitted by the PK model, too (**fig. 5-4 C**). Since no FFA was obtained in the acceptor compartment (**fig. 5-4 D**), it was obviously not possible to fit the efflux rate constant  $k_7$ . In the lateral compartment, the profile was fitted reasonably with the PK model (**fig. 5-4 E**). Values for rate constants of the PK model are provided in **table 5-2**.

#### - Detailed diffusion model

The donor decreased more slowly than in the experiment and the PK model over the whole experimental period (**fig. 5-4 A**). Values range from slightly less than 80% after 15 minutes to roughly 30% after 6 h, and the deviation after 4 h and 6 h is well within the range of the standard deviations. In the *SC*, the consistency between experiment and simulation was

reasonable (**fig. 5-4 B**). After an initial phase with no substance present until 30 minutes, the amount in the *DSL* increased to reach a maximum at 50%, corresponding to the experimental data (**fig. 5-4 C**). The plot shows an inflection point at roughly 2 h indicating the finite dose character of the experiment. In the acceptor low FFA amount (less than 3%) was simulated after 6 h (**fig. 5-4 D**).

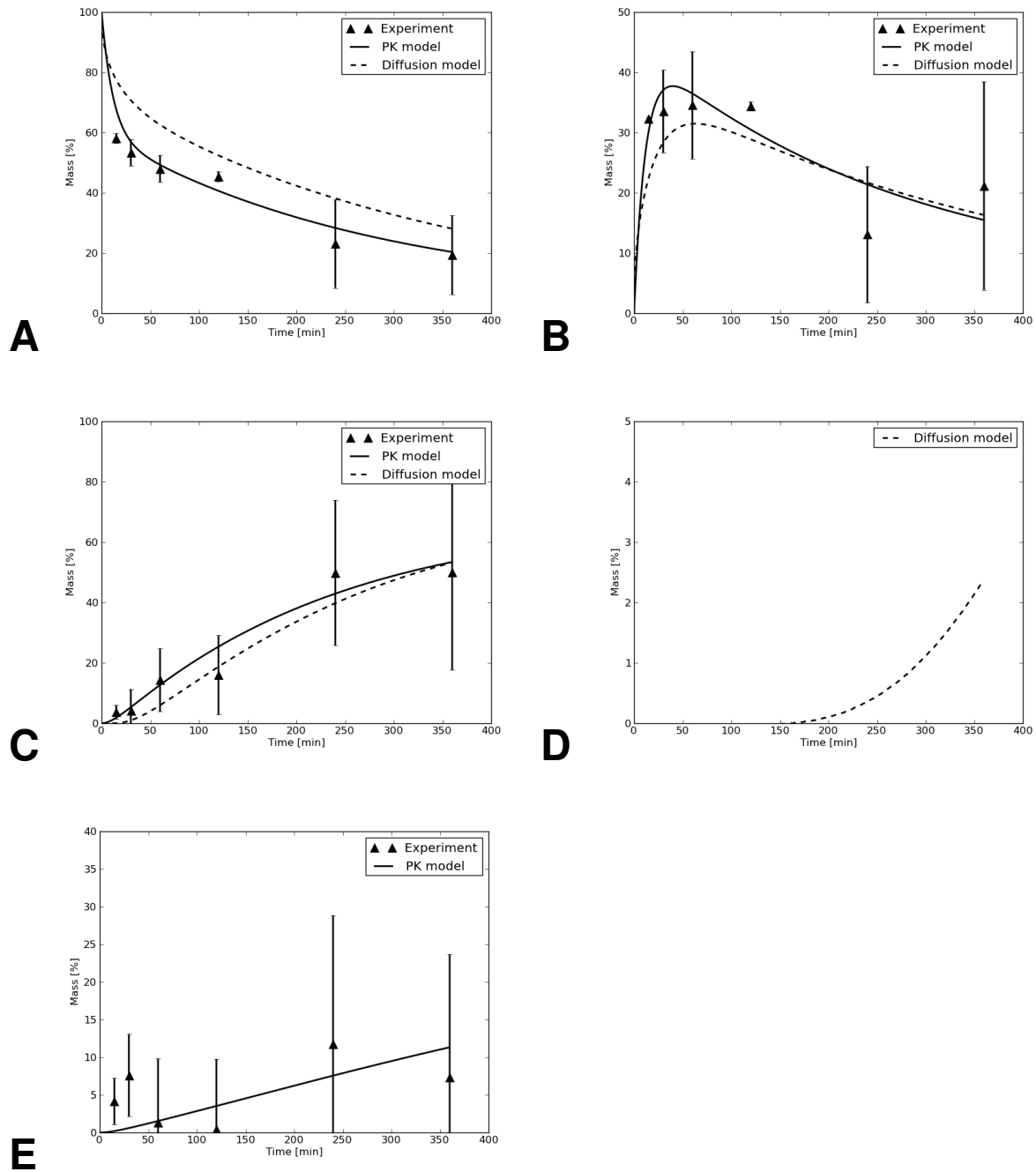


**Figure 5-4** FFA mass profiles over time: experimental data, PK fitting, and detailed diffusion simulation. A: Mass profile of the Donor compartment. B: Mass profile of the SC compartment. C: Mass profile of the DSL compartment. D: Mass profile of the Acceptor compartment (diffusion model with mass leaving the system). E: Mass profile of the Lateral compartment (diffusion model data not available).

### 5.4.3 Caffeine mass profiles

#### - Experimental data

In the **1 mg/ml** caffeine experiments, the drug in the donor did not decrease as fast as for FFA. After 5 min, still more than 85% of the initial dose could be found, decreasing slowly and reaching around 60% remaining on the skin after 6 h (**fig. 5-5 A**). At the last measuring time point after 12 h, still more than 40% of the drug was found in the donor. In the *SC*, a plateau at around 25% was reached after 2 h and maintained until 6 h, then slowly increasing to around 35% at the end of incubation after 12 h (**fig. 5-5 B**). The amount of drug in the *DSL* remained very low until 6 h due to values close to the LLOQ, and then increased to around 10% after 12 h (**fig. 5-5 C**). Only after the longest incubation at 12 h, caffeine was found in the acceptor (**fig. 5-5 D**). However, the variation was quite high due to concentration values close to the LLOQ. The caffeine amount in the lateral compartment slowly increased, reaching around 10% of the applied dose after 12 h incubation (**fig. 5-5 E**).

For the **12.5 mg/ml** experiments, the course of relative drug amount in the donor was similar to the 1 mg/ml data (**fig. 5-6 A**). In the *SC*, a plateau was immediately reached between 10% and 15% and maintained until 6 h after application (**fig. 5-6 B**). The amount of caffeine in the *DSL* increased slowly, reaching around 10% after 6 h (**fig. 5-6 C**). After 6 h incubation, around 5% of the applied caffeine was found in the acceptor phase (**fig. 5-6 D**). No caffeine was found at earlier time points. In the lateral compartment the caffeine amount increased to around 15% after 6 h (**fig. 5-6 E**).

#### - Pharmacokinetic model

The PK model showed a good agreement with the donor profile of caffeine **1 mg/ml** (**fig. 5-5 A**). Both *SC* and *DSL* profiles were reasonably fitted (**fig. 5-5 B, C**). The acceptor was also nicely fitted (**fig. 5-5 D**), as well as the lateral compartment (**fig. 5-5 E**).

For the **12.5 mg/ml** experiments the donor profile was excellently fitted by the PK model (**fig. 5-6 A**). The same was true for the *SC* compartment (**fig. 5-6 B**) and the *DSL* compartment (**fig. 5-6 C**). The acceptor was correctly fitted (**fig. 5-6 D**), as well as the lateral skin parts (**fig. 5-6 E**).

- Detailed diffusion model

As relative drug amounts in the diffusion model are independent of the concentration in the donor, **fig. 5-5 and 5-6** show identical plots, with the exception of the longest incubation times (12 h for 1 mg/ml, 6 h for 12.5 mg/ml). The donor depletes more slowly than for FFA with values of 60% after 6 h and 40% after 12 h. The SC diagrams show a characteristic plateau slightly below 30% after 150 minutes. Mass transfer into the DSL increased to more than 20% after 12 h. About 5% of the drug left the membrane into the acceptor after 12 h.

For **1 mg/ml**, the experimental data is simulated well in the donor compartment, the SC, and the acceptor. However, the amount in the DSL is highly over predicted with the model for longer incubation times.

For **12.5 mg/ml**, the donor compartment and the DSL are well simulated. The caffeine amount in the SC is however over predicted, whereas in the acceptor it is under predicted.

**Table 5-2** Rate constants and standard errors (SE) of the pharmacokinetic model

Parameter	FFA		Caffeine1mg		Caffeine 12.5 mg	
	Mean [%/min]	SE	Mean [%/min]	SE	Mean [%/min]	SE
$k_1$	3,70E-02	3,45E-03	3,81E-03	2,09E-04	5,92E-03	5,68E-04
$k_2$	4,52E-02	5,29E-03	5,73E-03	4,66E-04	2,11E-02	3,08E-03
$k_3$	6,78E-03	2,80E-04	2,76E-04	3,14E-04	4,35E-03	1,55E-03
$k_4$	2,29E-04	2,42E-04	1,52E-03	1,90E-03	2,38E-03	2,68E-03
$k_5$	1,00E-03	8,42E-04	1,96E-03	7,79E-04	4,52E-03	1,78E-03
$k_6$	7,12E-04	1,15E-04	1,50E-03	4,06E-04	5,53E-03	1,61E-03
$k_7$	-	-	1,05E-03	4,30E-04	2,13E-03	4,37E-04

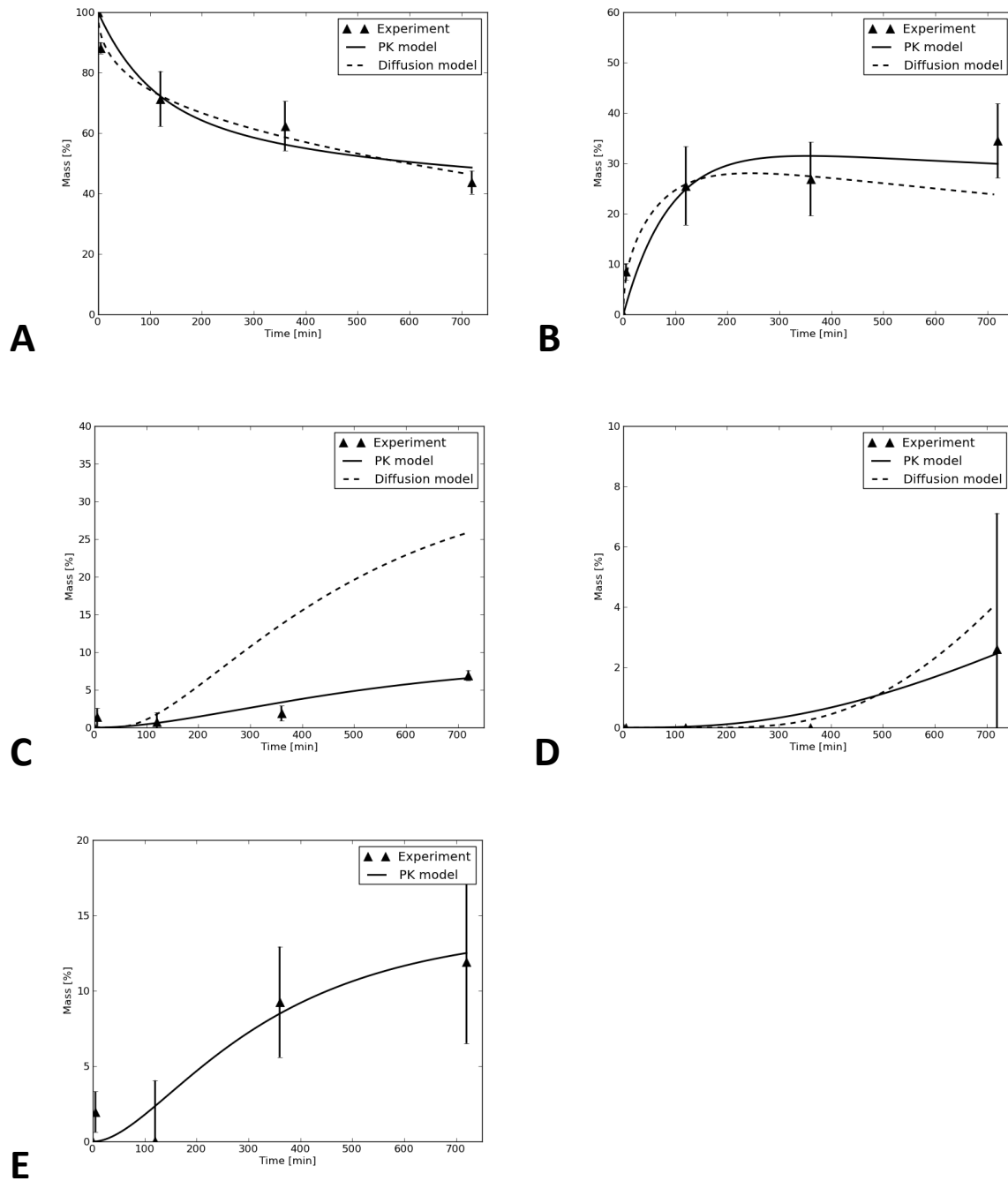


**Figure 5-5** Caffeine (1 mg/ml) mass profiles over time: experimental data, PK fitting, and detailed diffusion simulation. A: Mass profile of the Donor compartment. B: Mass profile of the SC compartment. C: Mass profile of the *DSL* compartment. D: Mass profile of the Acceptor compartment (diffusion model with mass leaving the system). E: Mass profile of the Lateral compartment (diffusion model data not available).

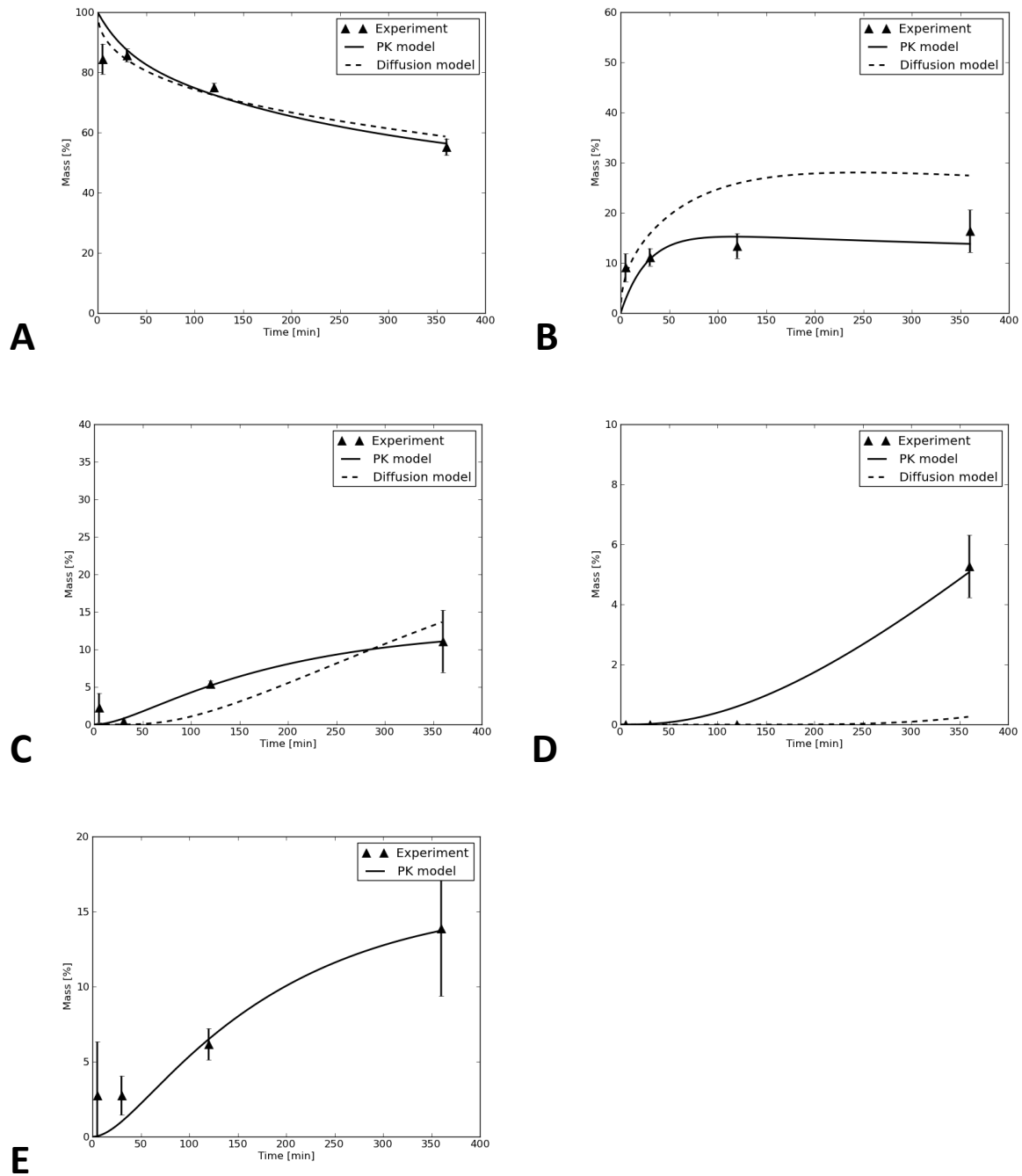


**Figure 5-6** Caffeine (12.5 mg/ml) mass profiles over time: experimental data, PK fitting, and detailed diffusion simulation. A: Mass profile of the Donor compartment. B: Mass profile of the SC compartment. C: Mass profile of the *DSL* compartment. D: Mass profile of the Acceptor compartment (diffusion model with mass leaving the system). E: Mass profile of the Lateral compartment (diffusion model data not available).

## 5.5 Discussion

### 5.5.1 Experimental data

Validation of the stretching factor showed that this method is a suitable method to correct the experimental data for the conditions during incubation and tape-stripping.

The experimental mass profiles of caffeine in the *SC* are clearly different between the different concentrations. For caffeine 1 mg/ml around 25 to 35% of the drug can be found in the *SC*, whereas for the higher concentration the values reach only up to 15%. One explanation for the different profiles is a saturable effect in the *SC*, allowing only a certain caffeine amount to be taken up by the *SC*, e.g. reversible protein binding to keratin [95,165,166].

### 5.5.2 Pharmacokinetic model

The PK model is a model to completely describe finite dose absorption of the drugs employed in this study using a reasonable mass transport model. PK models using first-order rate constants were typically used as *in vivo* prediction tools [167,168] and a lot of effort was spent trying to relate rate constants to physicochemical properties of the diffusant and to fit a model to plasma-level curves or *in vitro* absorption [169,170]. Overview articles relating to one or two compartment PK models can be found in the literature [171-173].

It has been shown that for *in vitro* skin absorption multi compartment modelling, a two compartment model is providing the best compromise of accuracy and complexity for a great variety of substances [78]. Thus, we developed a two compartment model and extended it to mass transport into the lateral part, which to the best of our knowledge has never been investigated before. However, the PK model is not able to predict mass profiles since it was not promising to relate rate constants to physicochemical properties of the diffusant and vehicle.

To reduce the number of rate constants for the fitting procedure, an averaged transport (rate constants  $k_5$  and  $k_6$ ) between *SC* and Lateral compartment as well as between *DSL* and Lateral compartment, was assumed.



### 5.5.3 Detailed diffusion model

The detailed diffusion model relies on input parameters, which are accessible in an experimental framework. In principle all parameters can be related directly to physico-chemical properties of the substance. This is an advantage as the model has a predictive character. Although optimization of parameters is possible, it was not applied in this case. Since the presented model consists of 16 cell layers arranged in a fully aligned way, it is not possible to consider lateral diffusion in this case.

Some differences between experiment and diffusion model were found, which can be easily explained by analytical reasons, e.g. concentration below the LLOQ in the acceptor for FFA.

In general, the detailed diffusion model reasonably predicted the mass profiles in each compartment for both drugs over the experimental time of 6 h or 12 h.

### 5.5.4 Comparison of the models

The models employed in this study are very different and serve different purposes.

The PK model is a compartmental model adapted to fit the entire experimental data, including the lateral compartment. In this approach the whole experimental setup and not just a small part of the experiment is modelled to gain insight into all effects occurring during incubation.

The detailed diffusion model is a strongly divergent model, simulating the SC at a high resolution level of single corneocytes and the lipid phase. The major advantage of this model is the possibility of actually predicting finite dose mass profiles.

### 5.5.5 Lateral skin parts

Even after correction of the data, still a high amount of drug can be found in the lateral skin parts. Thus, it is essential to regard the lateral skin parts in the mass balance during finite dose skin absorption studies. Most studies investigating finite dose experiments do not discuss the lateral drug amount found in their studies. Lateral diffusion of benzyl alcohol into the clamped parts of the diffusion cell has been assumed previously [174].

From microscopic pictures (**fig. 5-7**) taken both from untreated skin and from skin squeezed in a FD-C for 20 h, no significant difference was found for the SC thickness ( $p=0.218$ ). The dermis, however, appeared much denser than before. The geometry of the skin is clearly

changed, reducing the possibility of using measured diffusivity and partition behaviour from fully hydrated skin experiments.

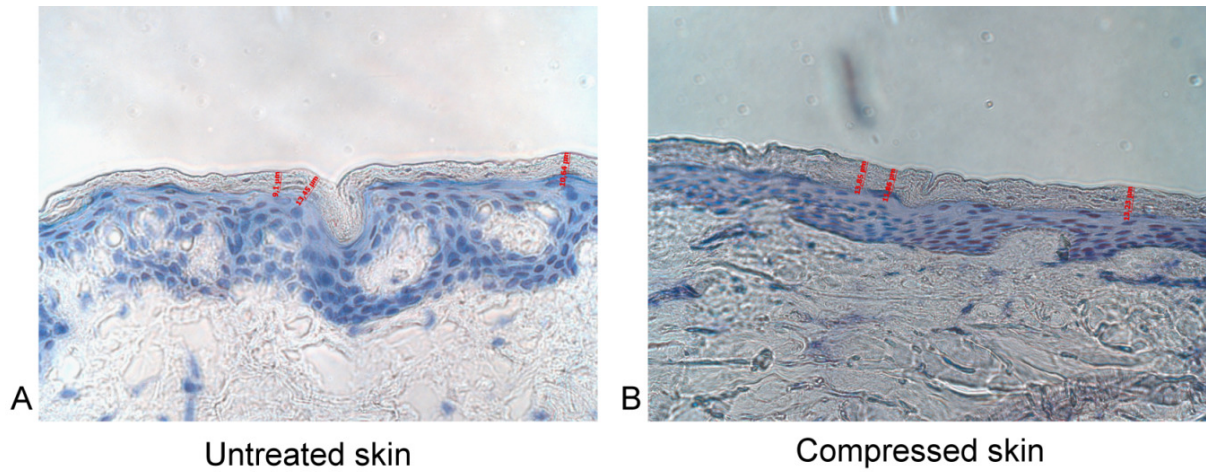


**Figure 5-7** Cross sections of skin biopsies from untreated skin (A), and from the lateral, compressed part of a skin sample squeezed in a Franz diffusion cell during incubation with buffer for 20 h (B). Stained with haematoxylin. Magnification 200 x.

## **5.6 Conclusion and outlook**

With the help of both mathematical models the experimental setup of finite dose skin absorption experiments in a Franz diffusion cell can be thoroughly investigated. The PK model is suitable for describing the whole setup and gives information about the diffusion process also into the lateral skin parts. This approach may expand the knowledge about the whole absorption process in a Franz diffusion cell.

The detailed diffusion model on the other hand can predict the diffusion of FFA and caffeine into the different skin compartments in a finite dose setup. If this model can be applied to further substances, in the future only infinite dose preliminary experiments to determine the input parameters would be required to predict the finite dose profiles.

In the future, a homogenized model will be applied to the same experimental data to simulate the mass profiles in the different compartments. In this model, the SC structure is homogenized and transport over a wider area compared to the detailed diffusion model can be simulated. Furthermore, a lateral compartment is added. Thus, simulation of the drug transport into the different compartments including the lateral part is possible with one model.



## **6 Finite dose skin penetration: Concentration depth profiles – Comparison between experiment and simulation**

The author of the thesis made the following contributions to this chapter: Performed and interpreted all experiments. Wrote the chapter.

The Wittum group in Frankfurt made the following contributions to this chapter: Developed the detailed diffusion model and adapted it to finite dose, and performed the simulations.

## 6.1 *Abstract*

This chapter focuses on finite dose skin penetration experiments with a detailed resolution of the drug concentration over depth in the *SC* and in the *DSL* and comparison of the experimental concentration depth profiles with simulations of a 2D diffusion model.

The detailed diffusion model for the prediction of concentration depth profiles in the *SC* and the *DSL* had previously been developed for infinite dose and was now adapted to finite dose. The concentration depth profiles of the model drugs Flufenamic acid (FFA) and caffeine were obtained experimentally and were compared to the detailed diffusion model.

The detailed diffusion model could predict the concentration depth profiles of FFA well, both in the *SC* and the *DSL*. The concentration depth profiles of caffeine on the other hand were not predicted quite as well as for FFA, but the order of magnitude between experiment and simulation was the same.

## 6.2 Introduction

As already described before in *chapter 1 Introduction*, skin penetration experiments give more information about the actual distribution of the drug in the different skin layers after a certain incubation time. For instance, the systemic absorption of a compound can be estimated from the drug content recovered in the SC [9].

However, due to extensive laboratory work and mathematical challenges, only few publications regard the concentration depth profiles of a substance in the skin layers, e.g. in the SC. When it comes to finite dose experiments, the number decreases even more due to analytical challenges.

In some publications concentration depth profiles were simulated, but no comparison between the obtained results to experimental data was done [112,121,175,176].

Thus, in our study both experiment and simulation were investigated, and the results of the two methods were compared. Finite dose skin penetration experiments with the model drugs Flufenamic acid (FFA) and caffeine from aqueous solution pH 7.4 were performed and the obtained concentration depth profiles were compared to the simulated profiles.

The diffusion model employed for simulation predicted the finite dose profiles with the input parameters derived from infinite dose experiments.

## **6.3 Materials and Methods**

### **6.3.1 Penetration experiments**

Penetration experiments were performed with full-thickness skin in a Franz diffusion cell as described in *chapter 5*.

### **6.3.2 Tape-stripping procedure**

Tape-stripping and SC quantification on tape-strips were performed under highly standardized conditions according to *chapter 10 Appendix* with tesa® Film kristall-klar. The first two tapes were extracted individually, and then always two tapes were pooled together.

### **6.3.3 Cryo-sectioning of the deeper skin layers**

After removal of the SC by tape-stripping, the rest of the skin was segmented according to [32]. In short, after freezing of the tape-stripped skin, 25 µm slices of the DSL were cut by a cryo-microtome. The cuts were collected in pre-weighed glass tubes and the thickness of the skin layers was determined by their mass.

### **6.3.4 Mass balance**

Mass balance was ensured by extraction of the drug from all skin parts and all devices in contact with the drug. Flufenamic acid (FFA) was extracted using 0.05 N sodium hydroxide solution, and caffeine with phosphate buffer pH 2.6, both under shaking for two hours at room temperature. The deeper skin layer extracts were centrifuged for 10 min at 1000 rpm and the supernatant carefully removed for analysis. A total recovery of 83.8% to 96.8% for FFA and 87.9% to 107.3% for caffeine for the single experiments was obtained.

### **6.3.5 Quantification by HPLC**

FFA and caffeine were quantified according to *chapter 5*. For calibration, both substances were dissolved in the respective extraction medium in concentrations of 0.03 – 20 µg/ml.



### 6.3.6 Concentration depth profiles

Concentration depth profiles were calculated from the drug amount in the different skin pools, the thickness of each pool and the depth inside the skin according to *chapter 10 Appendix*.

### 6.3.7 Detailed diffusion model

The detailed diffusion model adapted to the finite dose case of *chapter 5* was used to predict the concentration depth profiles of both drugs in the *SC* and the *DSL*. The input parameters employed in the simulation are given in **table 5-1**.

## 6.4 Results

### 6.4.1 FFA

#### - Experiment

The shape of the experimental concentration depth profiles appeared as a two-phase shape with a steep decrease in drug concentration in the outermost *SC* layers and then a slower decrease from around 0.1 relative depth (**fig. 6-1**). The concentration depth profiles of FFA in the *SC* at the different time points resembled each other.

The amount of drug in the *DSL* increased with increasing incubation time, from around  $4 \mu\text{g}/\text{cm}^3$  after 15 minutes to around 50 to  $100 \mu\text{g}/\text{cm}^3$  after 6 h in the uppermost part of the *DSL* (**fig. 6-2**). The profiles decreased quickly after the first *DSL* layers and then decreased more slowly.

#### - Simulation

In the *SC* the shape of the simulated concentration depth profiles resembled an exponential decay for the shortest incubation time, and at longer incubation times the concentration depth profiles became linear. The simulation predicted the *SC* concentration depth profiles well, especially at the shorter incubation points. Afterwards, the correlation was still reasonable with only the first tape-strips varying from the simulation.

In the *DSL*, the simulation under predicted the experimental concentration depth profiles for the incubation times 15 min and 30 min (**fig. 6-2**). Afterwards, for the time points 60 min and 4 h the concentration depth profiles were well predicted. The shape of the simulation curve was similar to the experimental data. However, for 4 h and 6 h incubation time the simulation predicted a linearly decreasing depth profile in contrast to experimental data.

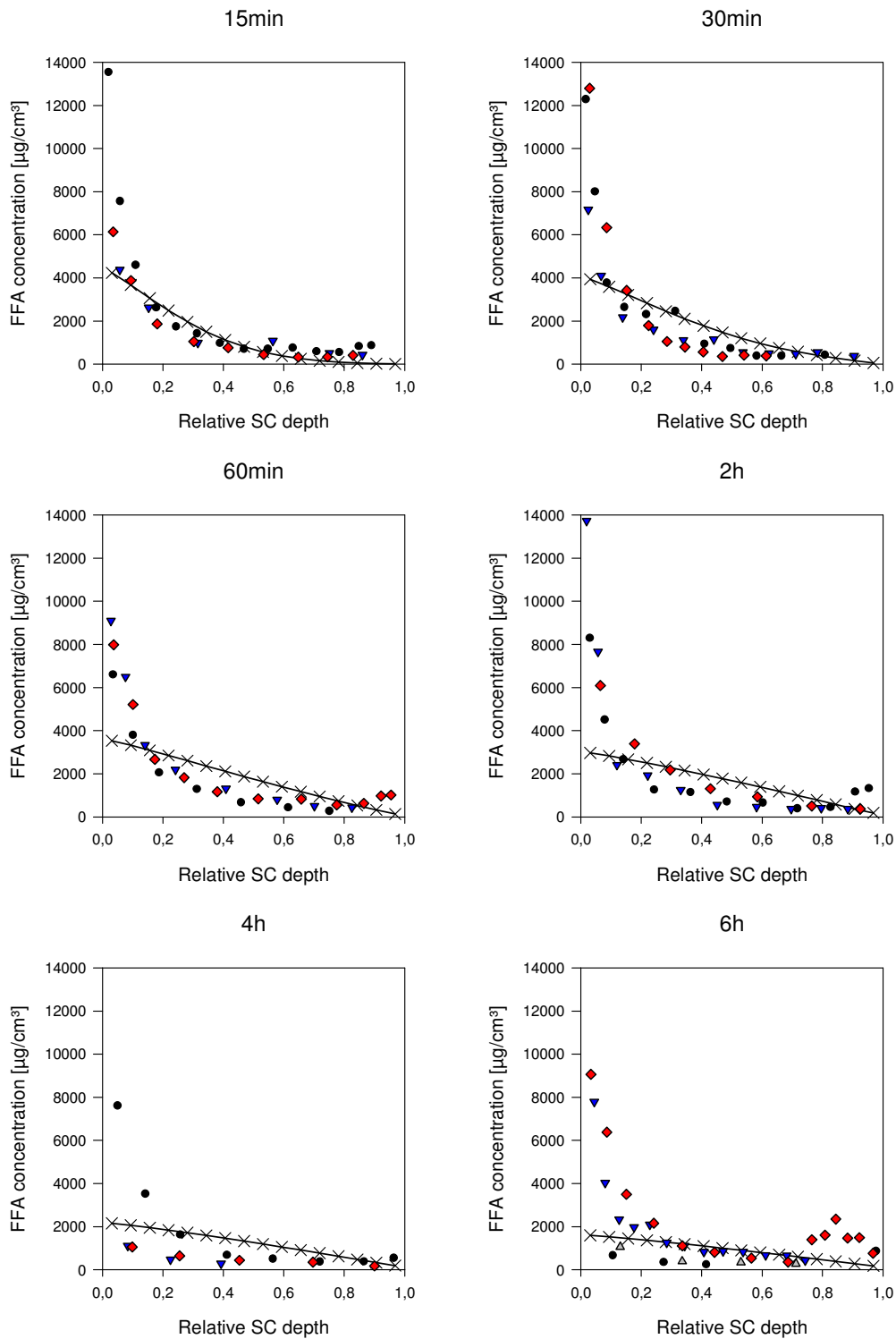


**Figure 6-1** FFA concentration depth profiles in SC for different incubation times. Crosses and the line as a guide to the eye represent the simulated depth profiles. The experimental data points are plotted according to the individual experiment: A: black circles, B: blue triangles down, C: red diamonds, D: grey triangles up. N=3 for experiments 15 min to 4 h. For 6 h: N=4.

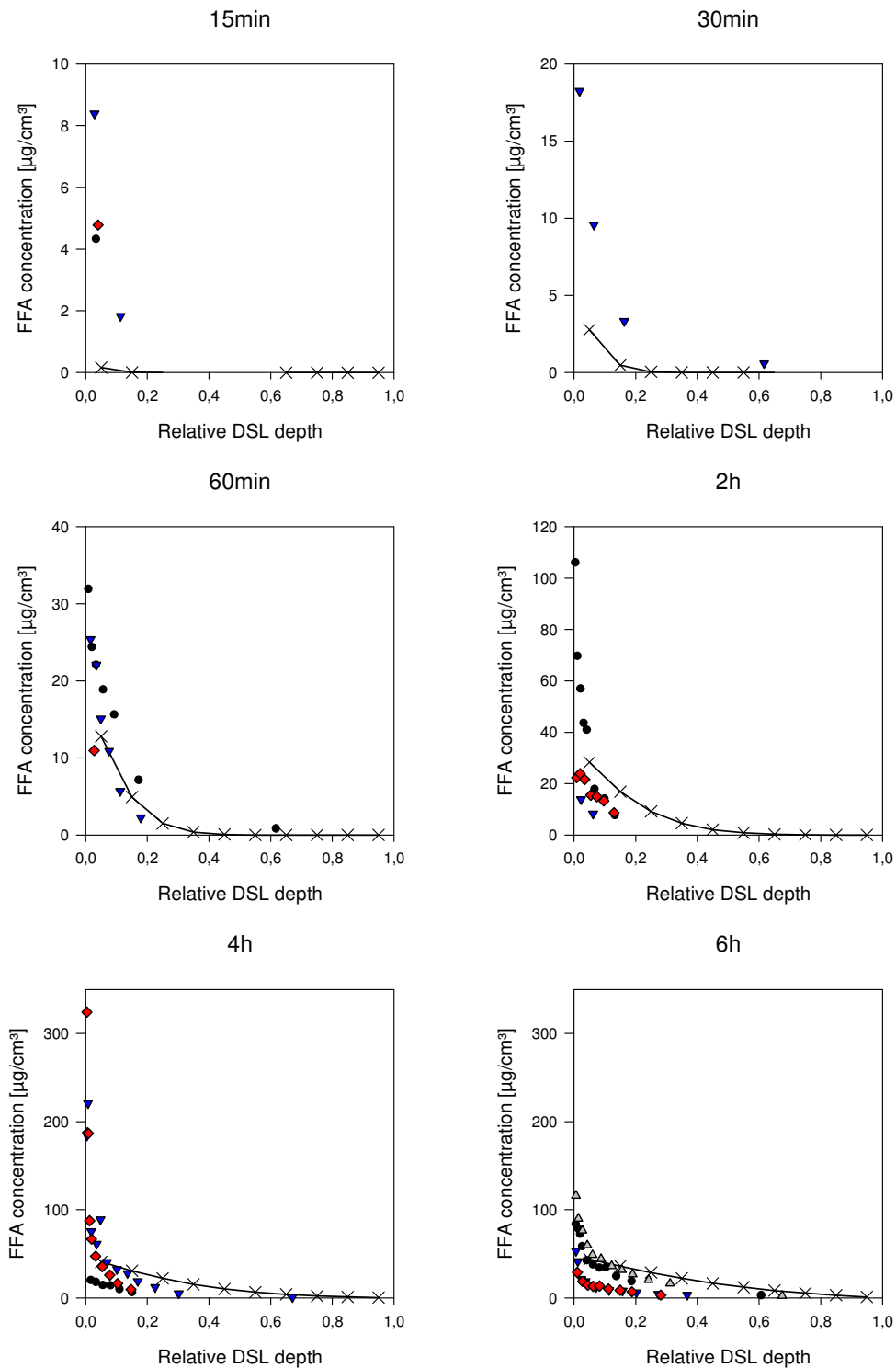


**Figure 6-2** FFA concentration depth profiles in *DSL* after different incubation times. Crosses and the line as a guide to the eye represent the simulated depth profiles. The experimental data points are plotted according to the individual experiment: A: black circles, B: blue triangles down, C: red diamonds, D: grey triangles up. N=3 for experiments 15 min to 4 h. For 6 h: N=4.

### 6.4.2 Caffeine

#### - Experiment

For **1 mg/ml** the caffeine amount in the *SC* was low after the shortest incubation time of 5 min compared to the other incubation times (**fig. 6-3**). Afterwards, the concentration increased slowly over the whole depth of the *SC*. The shape of the concentration depth profiles appeared more or less linear for all time points.

The drug amount in the *DSL* was very low for the 1 mg/ml experiments, and scattered around the limit of quantification. Too few data points above the LLOQ were available to create concentration depth profiles. Thus, the results are not shown and no simulation was performed.

When applied at the high concentration of **12.5 mg/ml**, the caffeine concentration in the *SC* strongly increased, leading to a caffeine concentration of over  $10000 \mu\text{g}/\text{cm}^3$  in the first *SC* layers for all time points (**fig. 6-4**). Interestingly, the concentration values were roughly a factor of 12.5 higher than the data of the lower concentration of 1 mg/ml. The concentration depth profiles at the earlier time points slowly decreased over depth. At the later time points at 2 h and 6 h, however, the caffeine concentration appeared to remain constant over the whole *SC* depth.

After application of the 12.5 mg/ml donor, caffeine could also be found in the *DSL* (**fig. 6-5**). After 30min, only few data points could be generated experimentally, whereas after 2 h and 6 h reasonable depth profiles could be plotted. The caffeine concentration increased from around  $4 \mu\text{g}/\text{cm}^3$  after 30 minutes to around  $100 \mu\text{g}/\text{cm}^3$  in the outer *DSL* layers after 6 h. The profiles slowly decreased over depth.

#### - Simulation

As the diffusion model is calculating relative concentrations only, the simulated profiles for the different caffeine concentrations are connected by a factor of 12.5.

For the low caffeine concentration, the depth profile in the *SC* was reasonably predicted for all time points (**fig. 6-3**). The shape of the experimental curves was reasonably simulated, with an exponential decay curve at shorter incubation times and linear decrease at longer incubation times.

The simulation of the high caffeine concentration was modelled not quite as well (**fig. 6-4**). After 5 minutes, the simulation over predicted the concentration in the outermost SC layer, but then decreased rapidly to below the experimental data. For 30 minutes incubation, also the outer SC layers were over predicted. The 2 h and 6 h data of the outer half of the SC was over predicted.

The prediction of the *DSL* of the 12.5 mg/ml experiments corresponded moderately with the experimental data (**fig. 6-5**). After 30 minutes, the drug concentration was under predicted, after 2 h it was reasonably predicted, and after 6 h it was over predicted.

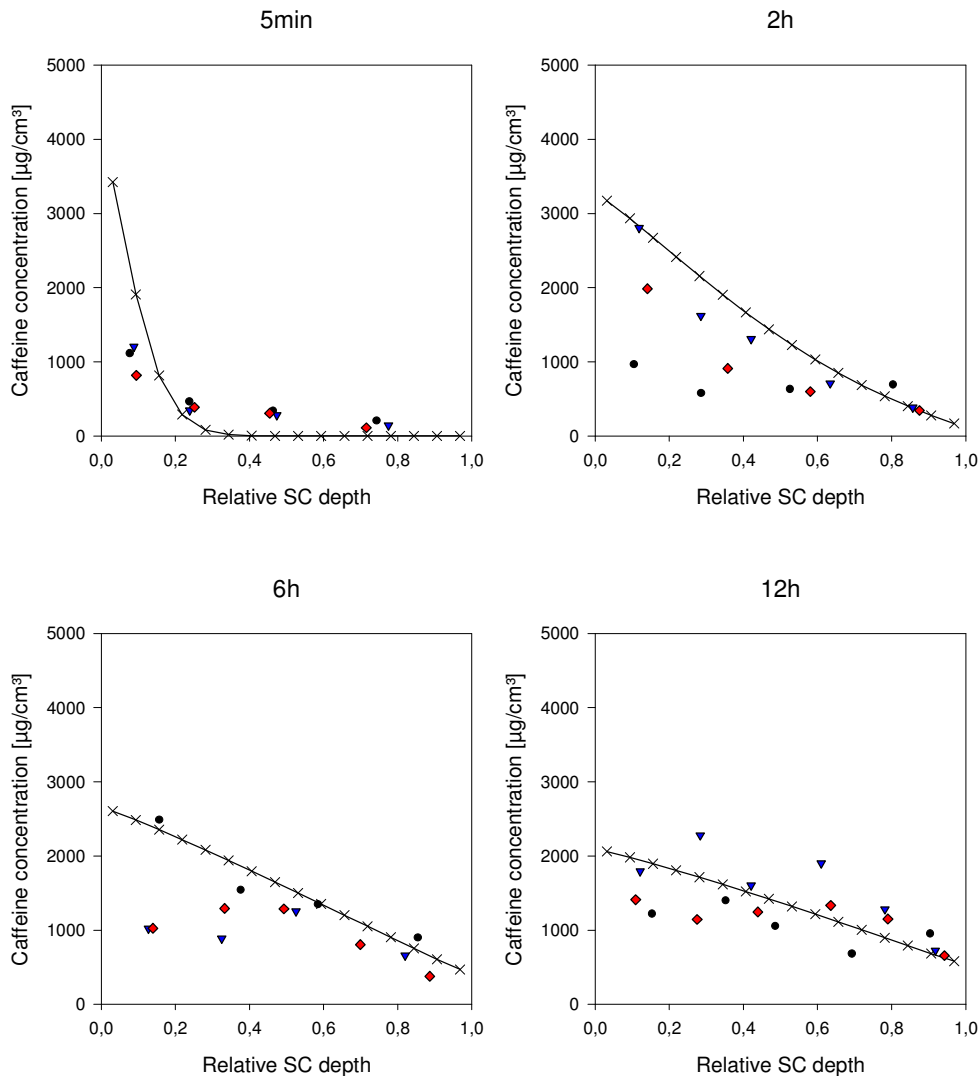


**Figure 6-3** Caffeine 1 mg/ml concentration depth profiles in SC. Crosses and the line as a guide to the eye represent the simulated depth profiles. The experimental data points are plotted according to the individual experiment: A: black circles, B: blue triangles down, C: red diamonds. N=3 for each time point.

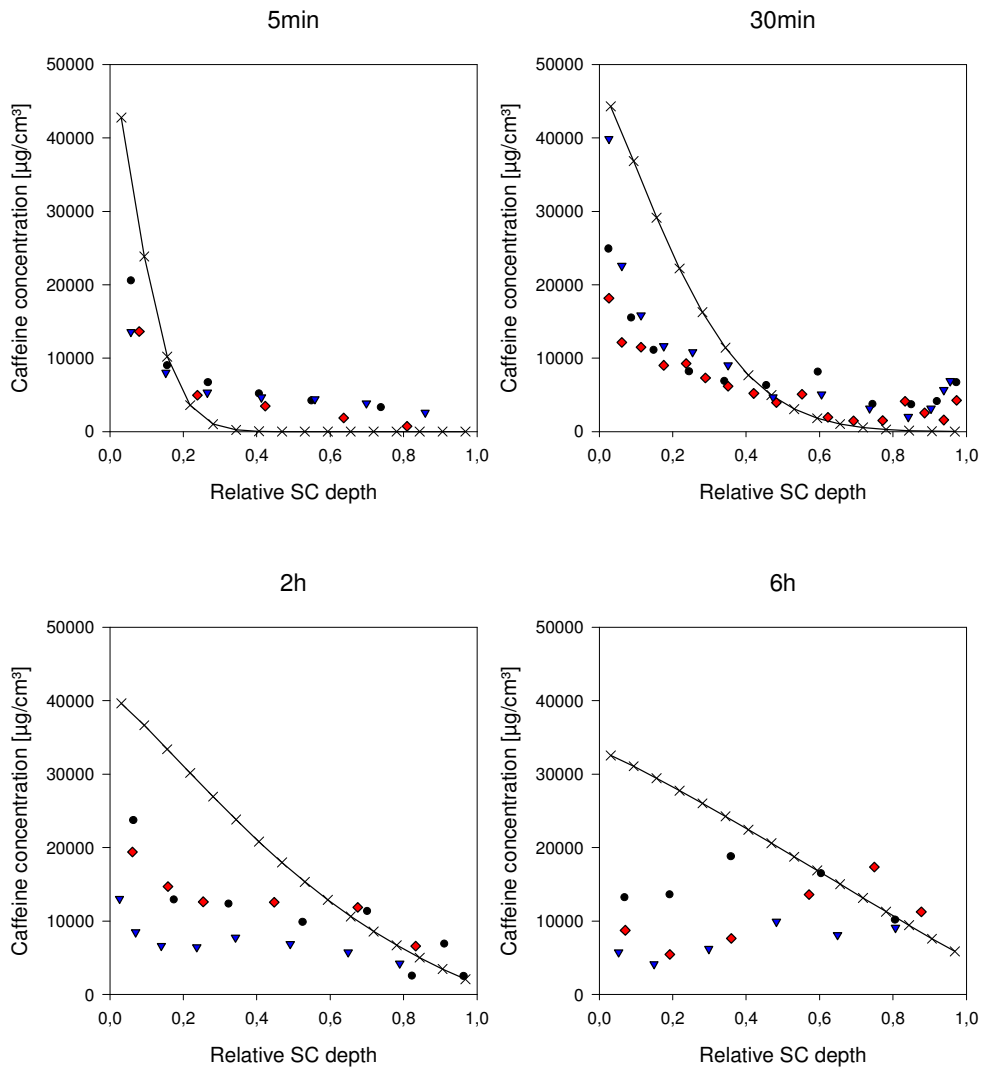


**Figure 6-4** Caffeine 12.5 mg/ml concentration depth profiles in SC. Crosses and the line as a guide to the eye represent the simulated depth profiles. The experimental data points are plotted according to the individual experiment: A: black circles, B: blue triangles down, C: red diamonds. N=3 for each time point.

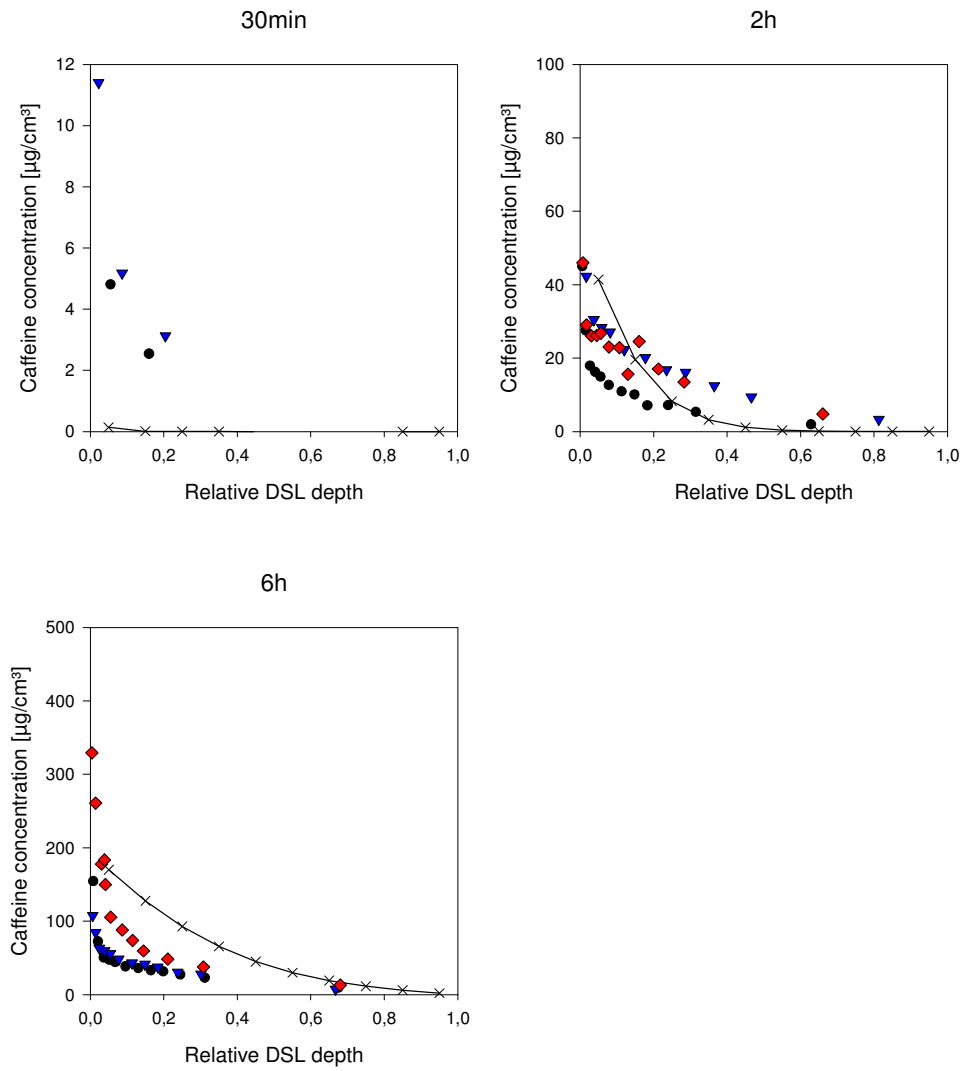


**Figure 6-5** Caffeine 12.5 mg/ml concentration depth profiles in *DSL*. Crosses and the line as a guide to the eye represent the simulated depth profiles. The experimental data points are plotted according to the individual experiment: A: black circles, B: blue triangles down, C: red diamonds. N=3 for each time point.



## 6.5 Discussion

### 6.5.1 Experimental data

The FFA concentration depth profiles exhibit a strong decrease in drug concentration from the first strips, then reaching a slower decay rate. The shape of the FFA concentration depth profiles appears to have a biphasic character, which previously has also been found for other drugs, e.g. clobetasol propionate [177] and nortriptyline [178].

The concentration depth profiles of FFA in the *SC* are not very different at the various incubation times. This is very different to previously presented infinite dose experiments [18], where usually for longer incubation times the drug concentration in the skin increases, and after reaching the steady-state, a linear decrease of drug concentration over the *SC* depth can be found. For finite dose experiments, it should be expected that *SC* concentration depth profiles first increase and after a certain time, when drug depletion of the donor affects the drug delivery to the *SC*, decrease. This tendency might be detected comparing the profiles after 15 min and 4 h. It might be speculated that the experimental setup is not sensitive enough to discriminate such differences in *SC* concentration depth profiles for FFA. The FFA concentration depth profiles in the *DSL* increase over time. Thus, it can be assumed that the donor depletion might not yet have an influence on the profiles in the *DSL*.

The *SC* concentration depth profiles of caffeine on the other hand seem to be dependent on time. At the early time points, the concentration in the first *SC* layers is higher than for the deeper *SC* layers. After longer incubation, however, the decrease is not so strong any more and the profiles appear linear over depth. This is in accordance to what was expected according to finite dose kinetics.

The concentration of caffeine in the *SC* of the higher concentration (12.5 mg/ml) is roughly 12.5 times higher than for the lower concentration (1mg/ml). This is in correlation to previously published data, where the concentration in the skin increases with increasing donor concentration [179]. The caffeine concentrations in the *DSL* increase over time and no impact of the donor depletion can be seen, yet.

Recently, other non-destructive methods are being investigated at the moment to replace the tape-stripping procedure, e.g. Raman spectroscopy [180,181]. However, this method is

only suitable for Raman-active substances and the problem of correct determination of the depth inside the skin is still under investigation. Also, this method is not able to give quantitative results, yet. Therefore, tape-stripping is still the method of choice for determination of concentration depth profiles in the SC.

### **6.5.2 Correlation between experiment and simulation**

A reasonable agreement between the concentration depth profiles of experiment and simulation was found both for FFA and for caffeine. Although simulation of concentration depth profiles deviate at some time points from experimental data the agreement between in-silico and experiment altogether is reasonable. Especially, if considered that input parameters from infinite dose experiments with skin of other donors were employed [18]. This is a major advantage as infinite dose experiments are much easier and can be faster performed, thus reducing the experimental effort.

## **6.6 Conclusion**

The detailed diffusion model could reasonably predict the concentration depth profiles of FFA and caffeine. Thus, this model has the potential to reduce the number of finite dose experiments and still give reasonable calculations of the drug concentration in the skin layers.



## 7 Summary

*In vivo*, the usually employed formulation volume applied to the skin is quite small. Per definition, this dose is called a finite dose. As this application scheme is much closer to the *in vivo* situation, finite dose experiments are of special interest also for *in vitro* experiments.

In this thesis, finite dose skin absorption experiments were investigated with respect to the experimental procedure and setup. Furthermore, mathematical modelling was employed to describe or predict the experimental profiles. Most publications dealing with mathematical modelling do not compare their results to experimental data. Thus, in this thesis both experiment and mathematics are included to elucidate the absorption process to the skin.

For comparison of experimental data with computational results, correct experimental setup and analysis are generally required. To improve the accuracy of the experimental data, the tape-stripping procedure was investigated with respect to SC quantification on tape-strips. Infrared densitometry proved to be a suitable tool for determining the SC depth reached after each strip *in vitro*, and also to determine the endpoint for complete SC removal. With this method, not only the depth resolution was improved, allowing for more precise determination of the depth inside the SC, but also the drug concentration in the skin was normalized to the actual skin volume removed by each tape-strip. Thus, more accurate concentration depth profiles can be obtained for future experiments. Besides, this method is easy and not expensive, thus suitable for most laboratories. A widespread use of this method would allow for better comparison between results of different working groups. Recently, the use of infrared densitometry has been broadened to porcine ear SC [182], allowing for the use on animal models.

The first question resulting from the finite dose experimental setup that was addressed in this thesis was the influence of the donor surface distribution on the absorption of the substance under investigation. Permeation experiments with the model drugs caffeine and flufenamic acid (FFA) with stained aqueous donor solution to delimit the area actually in contact with the donor formulation (application area) showed that the application area had a great influence on the permeation of the hydrophilic caffeine, but not on the lipophilic FFA. Furthermore, in contrast to caffeine, FFA could be found distributed homogeneously over the whole incubation area after 41 h. Thus, it can be assumed that the lipophilic FFA distributed well over the lipophilic SC and from there was absorbed homogeneously into and

through the skin. It can be further presumed that the lipophilicity of the drug may influence the effect on the permeation. However, this was actually the first study to investigate the influence of the application area on the absorption of solely two compounds to the skin. Further studies with more substances are needed to ensure the lipophilicity is indeed responsible for this effect and, if possible, determine a limit for lipophilicity until an effect on the permeation can be seen.

Finite dose skin penetration experiments were performed to investigate the mass profiles in the different compartments and the concentration depth profiles in the *SC* and the *DSL*. The experimental setup was thoroughly evaluated and the different skin compartments were carefully separated.

Due to the highly standardized tape-stripping method, the skin was stretched before tape-stripping to obtain a flat skin surface, thereby increasing the incubated skin area. Thus, the incubation area did not correspond to the stripped skin area, requiring a correction of the experimental data by a newly-developed stretching factor. This factor could properly correct the experimental data for this setup.

A pharmacokinetic model was developed for the finite dose skin penetration setup in the Franz diffusion cell, and a lateral compartment was included, representing the skin parts compressed by the device during incubation. The model could describe the mass profiles in all compartments for FFA and caffeine reasonably well, also in the lateral compartment. This was the first time the mass profiles in the lateral skin part had ever been investigated.

Furthermore, a 2D diffusion model previously developed for infinite dose was adapted to finite dose conditions. The input parameters of this model had previously been derived from infinite dose experiments. After adaptation of the model to finite dose, the model could predict the finite dose mass profiles relatively well and the concentration depth profiles more or less reasonably. Even though the simulated depth profiles not always resulted in the same shape as the experiments, the order of magnitude was the same. Thus, the model is suitable to predict finite dose profiles.

As the input parameters remained identical to the infinite dose simulations, it was shown that input parameters derived from infinite dose experiments can also be applied to finite dose experiments and reasonably predict drug kinetics.

## 8 Zusammenfassung

*In vivo* wird üblicherweise ein recht kleines Volumen der Formulierung zur Anwendung auf der Haut eingesetzt. Diese Dosis wird per Definition finite dose genannt. Da dieses Applikationsvolumen näher an der *in vivo* Situation ist, sind finite dose Hautabsorptionsversuche von besonderem Interesse auch *in vitro*.

In dieser Dissertation wurden finite dose Hautabsorptionsversuche durchgeführt und untersucht im Hinblick auf den experimentellen Ablauf und den Aufbau. Des Weiteren wurden mathematische Modellierungen eingesetzt, um die experimentellen Profile zu beschreiben oder vorherzusagen. Die meisten Publikationen, die sich mit mathematischer Modellierung beschäftigen, vergleichen die berechneten Daten nicht mit experimentellen Daten. Aus diesem Grund wurden in dieser Dissertation sowohl Experimente als auch Mathematik eingesetzt, um den Absorptionsprozess in die Haut aufzuklären.

Ein genauer experimenteller Aufbau und eine exakte Auswertung sind erforderlich, um experimentelle Daten mit rechenbetonten Ergebnissen vergleichen zu können. Um die Genauigkeit der experimentellen Daten zu erhöhen, wurde die Durchführung des Tape-strippings im Hinblick auf die Quantifizierung von SC auf Tape-strips untersucht. Hierbei zeigte sich Infrarot Densitometrie geeignet, die erreichte SC Tiefe nach jedem Strip *in vitro*, sowie den Endpunkt für die Entfernung des kompletten SC zu bestimmen. Mit dieser Methode wurde nicht nur die Tiefenauflösung verbessert, was eine genauere Bestimmung der Tiefe im SC erlaubt; zudem wurde die Arzneistoffkonzentration in der Haut normalisiert auf das tatsächlich entfernte Hautvolumen je Strip. Folglich können genauere Konzentrationsschichttiefenprofile für zukünftige Versuche erhalten werden. Außerdem ist diese Methode einfach und preiswert und deshalb geeignet für die meisten Labore. Ein weitverbreiteter Gebrauch dieser Methode würde zu einer besseren Vergleichsmöglichkeit zwischen den Ergebnissen verschiedener Arbeitsgruppen führen. Vor kurzem wurde gezeigt, dass Infrarot Densitometrie auch für die Anwendung am Schweineohr geeignet ist [182], was die mögliche Anwendung auf Tiermodelle ausweitet.

Die erste Frage bezogen auf das experimentelle Setup von finite dose Versuchen, die im Rahmen dieser Dissertation untersucht wurden, war der Einfluss der Donorverteilung auf der Hautoberfläche auf die Absorption der untersuchten Substanz. Permeationsversuche mit den Modell-Arzneistoffen Coffein und Flufenaminsäure (FFA), die in angefärbter wässriger

Donorlösung gelöst waren, erlaubten die Bestimmung der tatsächlich mit Donorformulierung inkubierten Fläche (Applikationsfläche). Die Versuche zeigten, dass die Applikationsfläche einen großen Einfluss auf die Permeation des hydrophilen Coffeins hatte, aber nicht auf die der lipophilen FFA. Des Weiteren war FFA im Gegensatz zu Coffein nach 41 h homogen über die ganze Inkubationsfläche verteilt. Demzufolge kann vermutet werden, dass die lipophile FFA sich gut über das lipophile SC verteilt und von dort dann homogen in und durch die Haut aufgenommen wird. Es wurde angenommen, dass die Lipophilie des Arzneistoffs den Einfluss auf die Permeation bestimmt. Allerdings war dies die erste Studie, welche tatsächlich den Einfluss der Applikationsfläche auf die Hautabsorption von zwei Substanzen untersucht hat. Weitere Studien mit mehreren Substanzen sind nötig, um sicherzugehen, dass die Lipophilie tatsächlich verantwortlich für diesen Effekt ist und, wenn möglich, eine Grenze zu bestimmen, bis wann ein Effekt auf die Permeation sichtbar ist.

Finite dose Hautpenetrationsversuche wurden durchgeführt, um die Massenprofile in den verschiedenen Kompartimenten und die Konzentrationsschichttiefenprofile im SC und den tieferen Hautschichten (*DSL*) zu untersuchen. Der experimentelle Aufbau wurde sorgfältig beurteilt und die verschiedenen Hautkompartimente vorsichtig voneinander getrennt.

Bedingt durch die hochstandardisierte Tape-stripping Methode wurde die Haut vor dem Strippen aufgespannt, um eine glatte Hautoberfläche zu erreichen, wodurch die Inkubationsfläche vergrößert wurde. Demzufolge entspricht die Inkubationsfläche nicht der gestrippten Hautfläche, was eine Korrektur der experimentellen Daten durch einen neu entwickelten Stretching Faktor nötig machte. Dieser Faktor konnte die experimentellen Daten für diesen Aufbau nachgewiesenermaßen korrigieren.

Das pharmakokinetische Modell konnte die Massenprofile von FFA und Coffein in allen Kompartimenten angemessen beschreiben, auch im lateralen Kompartiment. Dies war der bisher erste Versuch, die Massenprofile im lateralen Hautteil zu untersuchen.

Außerdem wurde ein zuvor für infinite dose entwickeltes 2D Diffusionsmodell angepasst an finite dose Bedingungen. Die Parameter dieses Modells waren zuvor von infinite dose Versuchen abgeleitet worden. Nach Anpassung des Modells auf finite dose konnte dieses finite dose Massenprofile relativ gut und Konzentrations-Schichttiefenprofile annehmbar vorhersagen. Obwohl die simulierten Tiefenprofile nicht immer die gleiche Form wie die



Experimente zeigten, war die Größenordnung die gleiche. Deshalb ist das eingesetzte Modell geeignet, finite dose Profile vorherzusagen.

Da die Input Parameter identisch zu den infinite dose Simulationen blieben, wurde gezeigt, dass die aus infinite dose Versuchen erhaltenen Input Parameter auch auf finite dose Versuche angewendet werden können und Arzneistoffkinetiken richtig vorhersagen können.



## 9 References

- 1 Roberts MS, Walters KA: Human Skin Morphology and Dermal Absorption; in Roberts MS, Walters KA (eds): Dermal Absorption and Toxicity Assessment. New York, Informa Healthcare, 2008, vol 177.
- 2 Hahn T, Selzer D, Neumann D, Schaefer UF: Das geht unter die Haut - Aufbau der humanen Haut und mögliche Invasionswege. PZ Prisma 2011;1:35-43.
- 3 Wagner H, Zghoul N, Lehr CM, Schaefer UF: Human skin and skin equivalents to study dermal penetration and permeation; Cell Culture Models of Biological Barriers. London, Taylor & Francis, 2002.
- 4 Environmental Health Criteria 235. Guidance Document on Dermal Absorption. World Health Organization. 2004.
- 5 Elias PM, Cooper ER, Korc A, Brown BE: Percutaneous transport in relation to stratum corneum structure and lipid composition. Journal of Investigative Dermatology 1981;76:297-301.
- 6 Elias PM: Epidermal lipids, barrier function, and desquamation. Journal of Investigative Dermatology 1983;80 (Suppl.):44s-49s.
- 7 Bronaugh RL, Maibach HI: Percutaneous Absorption. New York, Basel, Marcel Dekker, 1999.
- 8 Roberts MS, Cross SE, Anissimov YG: Factors Affecting the Formation of a Skin Reservoir for Topically Applied Solutes. Skin Pharmacology and Physiology 2004;17:3-16.
- 9 Rougier A, Dupuis D, Lotte C: In vivo correlation between stratum corneum reservoir function and percutaneous absorption. Journal of Investigative Dermatology 1983;81:275-278.
- 10 Vickers CF: Existence of Reservoir in the Stratum corneum. Experimental Proof. Archives of dermatology 1963;88:20-23.
- 11 Pershing LK, Corlett J, Jorgensen C: In vivo pharmacokinetics and pharmacodynamics of topical ketoconazole and miconazole in human stratum corneum. Antimicrobial Agents and Chemotherapy 1994;38:90-95.

- 12 Lademann J, Richter H, Schaefer UF, Blume-Peytavi U, Teichmann A, Otberg N, Sterry W: Hair Follicles - A Long-Term Reservoir for Drug Delivery. *Skin Pharmacology and Physiology* 2006;19:232-236.
- 13 Lademann J, Richter H, Teichmann A, Otberg N, Blume-Peytavi U, Luengo J, Weiß B, Schaefer UF, Lehr CM, Wepf R, Sterry W: Nanoparticles - An efficient carrier for drug delivery into the hair follicles. *European Journal of Pharmaceutics and Biopharmaceutics* 2007;66:159-164.
- 14 Scheuplein RJ, Blank IH: Permeability of the skin. *Physiological Reviews* 1971;51:702-747.
- 15 Otberg N, Richter H, Schaefer H, Blume-Peytavi U, Sterry W, Lademann J: Variations of Hair Follicle Size and Distribution in Different Body Sites; in Bronaugh RL, Maibach HI (eds): *Percutaneous Absorption*. Boca Raton, Taylor & Francis, 2005, vol 155.
- 16 Heisig M, Lieckfeldt R, Wittum G, Mazurkevich G, Lee G: Non steady-state descriptions of drug permeation through stratum corneum. I. The biphasic brick-and-mortar model. *Pharmaceutical Research* 1996;13:421-426.
- 17 Johnson ME, Blankschtein D, Langer R: Evaluation of solute permeation through the stratum corneum: Lateral bilayer diffusion as the primary transport mechanism. *Journal of Pharmaceutical Sciences* 1997;86:1162-1172.
- 18 Hansen S, Henning A, Naegel A, Heisig M, Wittum G, Neumann D, Kostka KH, Zbytovska J, Lehr CM, Schaefer UF: In-silico model of skin penetration based on experimentally determined input parameters. Part I: Experimental determination of partition and diffusion coefficients. *European Journal of Pharmaceutics and Biopharmaceutics* 2008;68:352-367.
- 19 Naegel A, Hansen S, Neumann D, Lehr CM, Schaefer UF, Wittum G, Heisig M: In-silico model of skin penetration based on experimentally determined input parameters. Part II: Mathematical modelling of in-vitro diffusion experiments. Identification of critical input parameters. *European Journal of Pharmaceutics and Biopharmaceutics* 2008;68:368-379.
- 20 Hansen S, Naegel A, Heisig M, Wittum G, Neumann D, Kostka KH, Meiers P, Lehr CM, Schaefer UF: The role of corneocytes in skin transport revised-a combined computational and experimental approach. *Pharmaceutical Research* 2009;26:1379-1397.
- 21 Hahn T, Winkler K, Lehr CM, Schaefer UF: Salbengrundlagen und die Wasserabgaberrate der Haut. *Deutsche Apotheker Zeitung* 2010;150:59-62.

- 22 Pinnagoda J, Tupker RA, Agner T, Serup J: Guidelines for transepidermal water loss (TEWL) measurement. A report from the Standardization Group of the European Society of Contact Dermatitis. *Contact Dermatitis* 1990;22:164-178.
- 23 Farahmand S, Tien L, Hui X, Maibach HI: Measuring transepidermal water loss: A comparative in vivo study of condenser-chamber, unventilated-chamber and open-chamber systems. *Skin Research and Technology* 2009;15:392-398.
- 24 Russell LM, Wiedersberg S, Begoña Delgado-Charro M: The determination of stratum corneum thickness. An alternative approach. *European Journal of Pharmaceutics and Biopharmaceutics* 2008;69:861-870.
- 25 Regulation (EC) No 1907/2006 of the European Parliament concerning the Registration, Evaluation, Authorisation and Restriction of Chemicals (REACH). 2006.
- 26 Eskes C, Zuang V: Alternative (Non-Animal) Methods for Cosmetics Testing: Current Status and Future Prospects. A report prepared in the context of the 7th Amendment to the Cosmetics Directive for establishing the timetable for phasing out animal testing. *ATLA Alternatives to Laboratory Animals* 2005;33 (Suppl. 1).
- 27 OECD: Guideline for the Testing of Chemicals. Skin Absorption: in vitro Method. 428. 2004.
- 28 OECD: Guidance document for the conduct of skin absorption studies. OECD series on testing and assessment. Number 28. 2004.
- 29 European Commission. Scientific Committee on Consumer Products: Basic criteria for the in vitro assessment of dermal absorption of cosmetic ingredients, 2006.
- 30 FDA: Guidance for industry: SUPAC-SS In vitro release testing and in vivo bioequivalence documentation. 1997.
- 31 Franz TJ: Percutaneous absorption. On the relevance of in vitro data. *Journal of Investigative Dermatology* 1975;64:190-195.
- 32 Wagner H, Kostka KH, Lehr CM, Schaefer UF: Drug Distribution in Human Skin Using Two Different In Vitro Test Systems: Comparison with In Vivo Data. *Pharmaceutical Research* 2000;17:1475-1481.
- 33 Lehman PA, Raney SG, Franz TJ: Percutaneous Absorption in Man: In vitro-in vivo Correlation. *Skin Pharmacology and Physiology* 2011;24:224-230.
- 34 Hotchkiss SA, Chidgey MAJ, Rose S, Caldwell J: Percutaneous absorption of benzyl acetate through rat skin in vitro. 1. Validation of an in vitro model against in vivo data. *Food and Chemical Toxicology* 1990;28:443-447.

- 35 Hotchkiss SAM, Hewitt P, Caldwell J, Chen WL, Rowe RR: Percutaneous absorption of nicotinic acid, phenol, benzoic acid and triclopyr butoxyethyl ester through rat and human skin in vitro: Further validation of an in vitro model by comparison with in vivo data. *Food and Chemical Toxicology* 1992;30:891-899.
- 36 Wagner H, Kostka KH, Lehr CM, Schaefer UF: Human skin penetration of flufenamic acid: In vivo/in vitro correlation (deeper skin layers) for skin samples from the same subject. *Journal of Investigative Dermatology* 2002;118:540-544.
- 37 Feldmann RJ, Maibach HI: Regional variation in percutaneous penetration of 14C cortisol in man. *Journal of Investigative Dermatology* 1967;48:181-183.
- 38 Swarbrick J, Lee G, Brom J: Drug Permeation through Human Skin: I. Effect of Storage Conditions of Skin. *Journal of Investigative Dermatology* 1982;78:63-66.
- 39 Harrison SM, Barry BW, Dugard PH: Effects of freezing on human skin permeability. *Journal of Pharmacy and Pharmacology* 1984;36:261-262.
- 40 Schreiber S, Mahmoud A, Vuia A, Ruebbelke MK, Schmidt E, Schaller M, Kandárová H, Haberland A, Schaefer UF, Bock U, Korting HC, Liebsch M, Schaefer-Korting M: Reconstructed epidermis versus human and animal skin in skin absorption studies. *Toxicology in Vitro* 2005;19:813-822.
- 41 Schaefer U: An ex-vivo model for the study of drug penetration into human skin. *Pharmaceutical Research* 1996;13 (Suppl.).
- 42 Cross SE, Magnusson BM, Winckle G, Anissimov Y, Roberts MS: Determination of the effect of lipophilicity on the in vitro permeability and tissue reservoir characteristics of topically applied solutes in human skin layers. *J Invest Dermatol* 2003;120:759-764.
- 43 Henning A, Neumann D, Kostka KH, Lehr CM, Schaefer UF: Influence of Human Skin Specimens Consisting of Different Skin Layers on the Result of in vitro Permeation Experiments. *Skin Pharmacology and Physiology* 2008;21:81-88.
- 44 Howes D, Guy R, Hadgraft J, Heylings J, Hoeck U, Kemper F, Maibach H, Marty JP, Merk H, Parra J, Rekkas D, Rondelli I, Schaefer H, Taeuber U, Verbiere N: Methods for Assessing Percutaneous Absorption: The Report and Recommendations of ECVAM Workshop 13. *ATLA Alternatives to Laboratory Animals* 1996;24:81-106.
- 45 Kligman AM, Christophers E: Preparation of isolated sheets of human stratum corneum. *Archives of Dermatological Research* 1963;88:702-705.

- 
- 46 Pitman IH, Rostas SJ: A Comparison of Frozen and Reconstituted Cattle and Human Skin as Barriers to Drug Penetration. *Journal of Pharmaceutical Sciences* 1982;71:427-430.
- 47 Bartek MJ, LaBudde JA, Maibach HI: Skin permeability in vivo: comparison in rat, rabbit, pig and man. *Journal of Investigative Dermatology* 1972;58:114-123.
- 48 Van Ravenzwaay B, Leibold E: A comparison between in vitro rat and human and in vivo rat skin absorption studies. *Human and Experimental Toxicology* 2004;23:421-430.
- 49 Bronaugh RL, Stewart RF, Congdon ER: Methods for in vitro percutaneous absorption studies. II. Animal models for human skin. *Toxicology and Applied Pharmacology* 1982;62:481-488.
- 50 Schaefer-Korting M, Bock U, Diembeck W, Duesing HJ, Gamer A, Haltner-Ukomadu E, Hoffmann C, Kaca M, Kamp H, Kersen S, Kietzmann M, Korting HC, Kraechter HU, Lehr CM, Liebsch M, Mehling A, Mueller-Goymann C, Netzlaff F, Niedorf F, Ruebhelke MK, Schaefer U, Schmidt E, Schreiber S, Spielmann H, Vuia A, Weimer M: The use of reconstructed human epidermis for skin absorption testing: Results of the validation study. *ATLA Alternatives to Laboratory Animals* 2008;36:161-187.
- 51 Netzlaff F, Lehr CM, Wertz PW, Schaefer UF: The human epidermis models EpiSkin<sup>®</sup>, SkinEthic<sup>®</sup> and EpiDerm<sup>®</sup>: An evaluation of morphology and their suitability for testing phototoxicity, irritancy, corrosivity, and substance transport. *European Journal of Pharmaceutics and Biopharmaceutics* 2005;60:167-178.
- 52 OECD: Guideline for the Testing of Chemicals. In Vitro Skin Corrosion: Human Skin Model Test. 431. 2004.
- 53 Chilcott RP, Barai N, Beezer AE, Brain SI, Brown MB, Bunce AL, Burgess SE, Cross S, Dalton CH, Dias M, Farinha A, Finnin BC, Gallacher SJ, Green DM, Gunt H, Gwyther RL, Heard CM, Jarvis CA, Kamiyama F, Kasting GB, Ley EE, Lim ST, McNaughton GS, Morris A, Nazemi MH, Pellett MA, Du Plessis J, Quan YS, Rachavan SL, Roberts M, Romonchuk W, Roper CS, Schenk D, Simonsen L, Simpson A, Traversa BD, Trottet L, Watkinson A, Wilkinson SC, Williams FM, Yamamoto A, Hadcraft J: Inter- and intralaboratory variation of in vitro diffusion cell measurements: An international multicenter study using quasi-standardized methods and materials. *Journal of Pharmaceutical Sciences* 2005;94:632-638.
- 54 Cevc G, Blume G: Lipid vesicles penetrate into intact skin owing to the transdermal osmotic gradients and hydration force. *Biochimica et Biophysica Acta - Biomembranes* 1992;1104:226-232.

- 
- 55 Bronaugh RL, Stewart RF: Methods for In Vitro Percutaneous Absorption Studies. IV: The Flow-Through Diffusion Cell. *Journal of Pharmaceutical Sciences* 1985;74:64-67.
- 56 Bronaugh RL, Maibach H: In vitro percutaneous absorption: principles, fundamentals, and applications. Boca Raton, CRC Press, 1991.
- 57 Holland JM, Kao JY, Whitaker MJ: A Multisample Apparatus for Kinetic Evaluation of Skin Penetration in Vitro: The Influence of Viability and Metabolic Status of the Skin. *Toxicology and Applied Pharmacology* 1984;72:272-280.
- 58 Wester RC, Christoffel J, Hartway T, Poblete N, Maibach H: Human Cadaver Skin Viability for In Vitro Percutaneous Absorption: Storage and Detrimental Effects of Heat-Separation and Freezing; in Bronaugh RL, Maibach H (eds): *Percutaneous Absorption*. Boca Raton, Taylor & Francis Group, 2005, vol 155.
- 59 Loth H, Hauck G, Borchert D, Theobald F: Statistical testing of drug accumulation in skin tissues by linear regression versus contents of stratum corneum lipids. *International Journal of Pharmaceutics* 2000;209:95-108.
- 60 Kasting GB, Miller MA: Kinetics of finite dose absorption through skin 2: Volatile compounds. *Journal of Pharmaceutical Sciences* 2006;95:268-280.
- 61 Fasano WJ, Baer KN: The in vitro permeability coefficient and short-term absorption rates for vinyl toluene using human cadaver skin mounted in a static diffusion cell model. *Drug and Chemical Toxicology* 2006;29:39-55.
- 62 Elewski BE: Percutaneous absorption kinetics of topical metronidazole formulations in vitro in the human cadaver skin model. *Advances in Therapy* 2007;24:239-246.
- 63 Grice JE, Ciotti S, Weiner N, Lockwood P, Cross SE, Roberts MS: Relative uptake of minoxidil into appendages and stratum corneum and permeation through human skin in vitro. *Journal of Pharmaceutical Sciences* 2009;99:712-718.
- 64 Gupta VK, Zatz JL, Rerek M: Percutaneous absorption of sunscreens through micro-Yucatan pig skin in vitro. *Pharmaceutical Research* 1999;16:1602-1607.
- 65 Simonsen L, Petersen MB, Groth L: In vivo skin penetration of salicylic compounds in hairless rats. *European Journal of Pharmaceutical Sciences* 2002;17:95-104.
- 66 Nicolazzo JA, Morgan TM, Reed BL, Finnin BC: Synergistic enhancement of testosterone transdermal delivery. *Journal of Controlled Release* 2005;103:577-585.
- 67 Viegas TX, Van Winkle LL, Lehman PA, Franz SF, Franz TJ: Evaluation of creams and ointments as suitable formulations for peldesine. *International Journal of Pharmaceutics* 2001;219:73-80.



- 
- 68 Laugel C, Baillet A, Youenang Piemi MP, Marty JP, Ferrier D: Oil-water-oil multiple emulsions for prolonged delivery of hydrocortisone after topical application: Comparison with simple emulsions. *International Journal of Pharmaceutics* 1998;160:109-117.
- 69 Walters KA, Brain KR, Dressler WE, Green DM, Howes D, James VJ, Kelling CK, Watkinson AC, Gettings SD: Percutaneous penetration of N-nitroso-N-methyldodecylamine through human skin in vitro: Application from cosmetic vehicles. *Food and Chemical Toxicology* 1997;35:705-712.
- 70 Brain KR: Percutaneous penetration of dimethylnitrosamine through human skin in vitro: Application from cosmetic vehicles. *Food and Chemical Toxicology* 1995;33:315-322.
- 71 Chen M, Liu X, Fahr A: Skin penetration and deposition of carboxyfluorescein and temoporfin from different lipid vesicular systems: In vitro study with finite and infinite dosage application. *International Journal of Pharmaceutics* 2011;408:223-234.
- 72 Van De Sandt JJM, Van Burgsteden JA, Cage S, Carmichael PL, Dick I, Kenyon S, Korinth G, Larese F, Limasset JC, Maas WJM, Montomoli L, Nielsen JB, Payan JP, Robinson E, Sartorelli P, Schaller KH, Wilkinson SC, Williams FM: In vitro predictions of skin absorption of caffeine, testosterone, and benzoic acid: A multi-centre comparison study. *Regulatory Toxicology and Pharmacology* 2004;39:271-281.
- 73 Wester RC, Hui X, Hartway T, Maibach HI, Bell K, Schell MJ, Northington DJ, Strong P, Culver BD: In vivo percutaneous absorption of boric acid, borax, and disodium octaborate tetrahydrate in humans compared to in vitro absorption in human skin from infinite and finite doses. *Toxicological Sciences* 1998;45:42-51.
- 74 Sarpotdar PP, Zatz JL: Evaluation of penetration enhancement of lidocaine by nonionic surfactants through hairless mouse skin in vitro. *Journal of Pharmaceutical Sciences* 1986;75:176-181.
- 75 Buist HE, van Burgsteden JA, Freidig AP, Maas WJM, van de Sandt JJM: New in vitro dermal absorption database and the prediction of dermal absorption under finite conditions for risk assessment purposes. *Regulatory Toxicology and Pharmacology* 2010;57:200-209.
- 76 Wilkinson SC, Williams FM: Effects of experimental conditions on absorption of glycol ethers through human skin in vitro. *International Archives of Occupational and Environmental Health* 2002;75:519-527.

- 
- 77 Traynor MJ, Wilkinson SC, Williams FM: The influence of water mixtures on the dermal absorption of glycol ethers. *Toxicology and Applied Pharmacology* 2007;218:128-134.
- 78 Davies M, Pendlington RU, Page L, Roper CS, Sanders DJ, Bourner C, Pease CK, MacKay C: Determining epidermal disposition kinetics for use in an integrated nonanimal approach to skin sensitization risk assessment. *Toxicological Sciences* 2011;119:308-318.
- 79 Wilkinson SC, Maas WJM, Nielsen JB, Greaves LC, van de Sandt JJM, Williams FM: Interactions of skin thickness and physicochemical properties of test compounds in percutaneous penetration studies. *International Archives of Occupational and Environmental Health* 2006;79:405-413.
- 80 Walker M, Chambers LA, Hollingsbee DA, Hadgraft J: Significance of vehicle thickness to skin penetration of Halcinonide. *International Journal of Pharmaceutics* 1991;70:167-172.
- 81 Simonsen L, Petersen MB, Benfeldt E, Serup J: Development of an in vivo animal model for skin penetration in hairless rats assessed by mass balance. *Skin Pharmacology and Applied Skin Physiology* 2002;15:414-424.
- 82 Dreher F, Fouchard F, Patouillet C, Andrian M, Simonnet JT, Benech-Kieffer F: Comparison of cutaneous bioavailability of cosmetic preparations containing caffeine or alpha-tocopherol applied on human skin models or human skin ex vivo at finite doses. *Skin Pharmacology and Applied Skin Physiology* 2002;15:40-58.
- 83 Youenang Piemi MP, De Luca M, Grossiord JL, Seiller M, Marty JP: Transdermal delivery of glucose through hairless rat skin in vitro: Effect of multiple and simple emulsions. *International Journal of Pharmaceutics* 1998;171:207-215.
- 84 Franz TJ, Lehman PA, Franz SF, North-Root H, Demetrulias JL, Kelling CK, Moloney SJ, Gettings SD: Percutaneous Penetration of N-Nitrosodiethanolamine through Human Skin (in Vitro): Comparison of Finite and Infinite Dose Applications from Cosmetic Vehicles. *Fundamental and Applied Toxicology* 1993;21:213-221.
- 85 Walters KA, Brain KR, Howes D, James VJ, Kraus AL, Teetsel NM, Toulon M, Watkinson AC, Gettings SD: Percutaneous penetration of octyl salicylate from representative sunscreen formulations through human skin in vitro. *Food and Chemical Toxicology* 1997;35:1219-1225.
- 86 Jarvis CA, McGuigan C, Heard CM: In vitro delivery of novel, highly potent anti-varicella Zoster virus nucleoside analogues to their target site in the skin. *Pharmaceutical Research* 2004;21:914-919.

- 
- 87 Richards H, Thomas CP, Bowen JL, Heard CM: In-vitro transcutaneous delivery of ketoprofen and polyunsaturated fatty acids from a pluronic lecithin organogel vehicle containing fish oil. *Journal of Pharmacy and Pharmacology* 2006;58:903-908.
- 88 Pendlington RU, Minter HJ, Stupart L, MacKay C, Roper CS, Sanders DJ, Pease CK: Development of a modified in vitro skin absorption method to study the epidermal/dermal disposition of a contact allergen in human skin. *Cutaneous and Ocular Toxicology* 2008;27:283-294.
- 89 Crank J: *The Mathematics of Diffusion*, ed 2nd. Oxford, Oxford University Press, 1975.
- 90 Franz TJ: Kinetics of cutaneous drug penetration. *International Journal of Dermatology* 1983;22:499-505.
- 91 Potts RO, Guy RH: Predicting skin permeability. *Pharmaceutical Research* 1992;9:663-669.
- 92 Bos JD, Meinardi MMHM: The 500 Dalton rule for the skin penetration of chemical compounds and drugs. *Experimental Dermatology* 2000;9:165-169.
- 93 Hadgraft J: Skin deep. *European Journal of Pharmaceutics and Biopharmaceutics* 2004;58:291-299.
- 94 Hansen S, Selzer D, Schaefer UF, Kasting GB: An extended database of keratin binding. *Journal of Pharmaceutical Sciences* 2010;100:1712-1726.
- 95 Anissimov YG, Roberts MS: Diffusion modelling of percutaneous absorption kinetics: 4. Effects of a slow equilibration process within stratum corneum on absorption and desorption kinetics. *Journal of Pharmaceutical Sciences* 2009;98:772-781.
- 96 Michaels AS, Chandrasekaran SK, Shaw JE: Drug Permeation Through Human Skin: Theory and In Vitro Experimental Measurement. *AIChE Journal* 1975;21:985-996.
- 97 Wagner H, Kostka KH, Adelhardt W, Schaefer UF: Effects of various vehicles on the penetration of flufenamic acid into human skin. *European Journal of Pharmaceutics and Biopharmaceutics* 2004;58:121-129.
- 98 Cross SE, Jiang R, Benson HAE, Roberts MS: Can increasing the viscosity of formulations be used to reduce the human skin penetration of the sunscreen oxybenzone? *Journal of Investigative Dermatology* 2001;117:147-150.
- 99 El Maghraby GMM, Williams AC, Barry BW: Skin hydration and possible shunt route penetration in controlled estradiol delivery from ultradeformable and standard liposomes. *Journal of Pharmacy and Pharmacology* 2001;53:1311-1322.

- 
- 100 Kasting GB, Barai ND, Wang TF, Nitsche JM: Mobility of Water in Human Stratum Corneum. *Journal of Pharmaceutical Sciences* 2003;92:2326-2340.
- 101 Kasting GB: Kinetics of finite dose absorption through skin 1. Vanillylnonanamide. *Journal of Pharmaceutical Sciences* 2001;90:202-212.
- 102 Scheuplein RJ, Ross LW: Mechanism of percutaneous absorption. V. Percutaneous absorption of solvent deposited solids. *Journal of Investigative Dermatology* 1974;62:353-360.
- 103 Mitragotri S, Anissimov YG, Bunge AL, Frasch HF, Guy RH, Hadgraft J, Kasting GB, Lane ME, Roberts MS: Mathematical models of skin permeability: An overview. *International Journal of Pharmaceutics* 2011;418:115-129.
- 104 Flynn GL: Physicochemical determinates of skin absorption; in Gerrity, J.R. H, C.J (eds): *Principles of Route-to-Route Extrapolation for Risk Assessment*. Amsterdam, Elsevier, 1990, pp 93-127.
- 105 Wilschut A, Ten Berge WF, Robinson PJ, McKone TE: Estimating skin permeation. The validation of five mathematical skin permeation models. *Chemosphere* 1995;30:1275-1296.
- 106 Roberts MS, Pugh WJ, Hadgraft J: Epidermal permeability: Penetrant structure relationships. 2. The effect of H-bonding groups in penetrants on their diffusion through the stratum corneum. *International Journal of Pharmaceutics* 1996;132:23-32.
- 107 Potts RO, Guy RH: A predictive algorithm for skin permeability: The effects of molecular size and hydrogen bond activity. *Pharmaceutical Research* 1995;12:1628-1633.
- 108 McCarley KD, Bunge AL: Pharmacokinetic models of dermal absorption. *Journal of Pharmaceutical Sciences* 2001;90:1699-1719.
- 109 McCarley KD, Bunge AL: Physiologically relevant two-compartment pharmacokinetic models for skin. *Journal of Pharmaceutical Sciences* 2000;89:1212-1235.
- 110 Guy RH, Hadgraft J, Maibach HI: A pharmacokinetic model for percutaneous absorption. *International Journal of Pharmaceutics* 1982;11:119-129.
- 111 Anissimov YG, Roberts MS: Diffusion modeling of percutaneous absorption kinetics. 1. Effects of flow rate, receptor sampling rate, and viable epidermal resistance for a constant donor concentration. *Journal of Pharmaceutical Sciences* 1999;88:1201-1209.

- 
- 112 Anissimov YG, Roberts MS: Diffusion modeling of percutaneous absorption kinetics: 2. Finite vehicle volume and solvent deposited solids. *Journal of Pharmaceutical Sciences* 2001;90:504-520.
- 113 Wang TF, Kasting GB, Nitsche JM: A multiphase microscopic diffusion model for stratum corneum permeability. I. Formulation, solution, and illustrative results for representative compounds. *Journal of Pharmaceutical Sciences* 2006;95:620-648.
- 114 Wang TF, Kasting GB, Nitsche JM: A multiphase microscopic diffusion model for stratum corneum permeability. II. Estimation of physicochemical parameters, and application to a large permeability database. *Journal of Pharmaceutical Sciences* 2007;96:3024-3051.
- 115 Muha I, Naegel A, Stichel S, Grillo A, Heisig M, Wittum G: Effective diffusivity in membranes with tetrakaidekahedral cells and implications for the permeability of human stratum corneum. *Journal of Membrane Science* 2010;368:18-25.
- 116 Rim JE, Pinsky PM, van Osdol WW: Using the method of homogenization to calculate the effective diffusivity of the stratum corneum. *Journal of Membrane Science* 2007;293:174-182.
- 117 Johnson ME, Berk DA, Blankschtein D, Golan DE, Jain RK, Langer RS: Lateral diffusion of small compounds in human stratum corneum and model lipid bilayer systems. *Biophysical Journal* 1996;71:2656-2668.
- 118 Tajreja PS, Kleene NK, Pickens WL, Wang TF, Kasting GB: Visualization of the lipid barrier and measurement of lipid pathlength in human stratum corneum. *AAPS PharmSci* 2001;3(2):1-9.
- 119 Barbero AM, Frasch HF: Transcellular route of diffusion through stratum corneum: Results from finite element models. *Journal of Pharmaceutical Sciences* 2006;95:2186-2194.
- 120 Mitragotri S: Modeling skin permeability to hydrophilic and hydrophobic solutes based on four permeation pathways. *Journal of Controlled Release* 2003;86:69-92.
- 121 Barbero AM, Frasch HF: Modeling of diffusion with partitioning in stratum corneum using a finite element model. *Annals of Biomedical Engineering* 2005;33:1281-1292.
- 122 Chandrasekaran SK, Campbell PS, Watanabe T: Application of the 'Dual Sorption' Model to Drug Transport through Skin. *Polymer Engineering and Science* 1980;20:36-39.

- 
- 123 Bommannan D, Potts RO, Guy RH: Examination of stratum corneum barrier function in vivo by infrared spectroscopy. *Journal of Investigative Dermatology* 1990;95:403-408.
- 124 Watkinson AC, Bunge AL, Hadgraft J, Naik A: Computer simulation of penetrant concentration-depth profiles in the stratum corneum. *International Journal of Pharmaceutics* 1992;87:175-182.
- 125 Bouwstra JA, De Graaff A, Gooris GS, Nijse J, Wiechers JW, Van Aelst AC: Water distribution and related morphology in human stratum corneum at different hydration levels. *Journal of Investigative Dermatology* 2003;120:750-758.
- 126 Anissimov YG, Roberts MS: Diffusion Modeling of Percutaneous Absorption Kinetics: 3. Variable Diffusion and Partition Coefficients, Consequences for Stratum Corneum Depth Profiles and Desorption Kinetics. *Journal of Pharmaceutical Sciences* 2004;93:470-487.
- 127 Reddy MB, Guy RH, Bunge AL: Does epidermal turnover reduce percutaneous penetration? *Pharmaceutical Research* 2000;17:1414-1419.
- 128 Krüse J, Golden D, Wilkinson S, Williams F, Kezic S, Corish J: Analysis, interpretation, and extrapolation of dermal permeation data using diffusion-based mathematical models. *Journal of Pharmaceutical Sciences* 2007;96:682-703.
- 129 Mitragotri S: A theoretical analysis of permeation of small hydrophobic solutes across the stratum corneum based on Scaled Particle Theory. *Journal of Pharmaceutical Sciences* 2002;91:744-752.
- 130 Cleek RL, Bunge AL: A new method for estimating dermal absorption from chemical exposure. 1. General approach. *Pharmaceutical Research* 1993;10:497-506.
- 131 Kalia YN, Pirot F, Guy RH: Homogeneous Transport in a Heterogeneous Membrane: Water Diffusion Across Human Stratum Corneum In Vivo. *Biophysical Journal* 1996;71:2692-2700.
- 132 Netzlaff F, Kostka KH, Lehr CM, Schaefer UF: TEWL measurements as a routine method for evaluating the integrity of epidermis sheets in static Franz type diffusion cells in vitro. Limitations shown by transport data testing. *European Journal of Pharmaceutics and Biopharmaceutics* 2006;63:44-50.
- 133 Darlenski R, Sassning S, Tsankov N, Fluhr JW: Non-invasive in vivo methods for investigation of the skin barrier physical properties. *European Journal of Pharmaceutics and Biopharmaceutics* 2009;72:295-303.

- 
- 134 Herkenne C, Alberti I, Naik A, Kalia YN, Mathy FX, Pr at V, Guy RH: In vivo methods for the assessment of topical drug bioavailability. *Pharmaceutical Research* 2008;25:87-103.
- 135 Lademann J, Jacobi U, Surber C, Weigmann HJ, Fluhr JW: The tape stripping procedure - evaluation of some critical parameters. *European Journal of Pharmaceutics and Biopharmaceutics* 2009;72:317-323.
- 136 Weigmann HJ, Lademann J, Meffert H, Schaefer H, Sterry W: Determination of the Horny Layer Profile by Tape Stripping in Combination with Optical Spectroscopy in the Visible Range as a Prerequisite to Quantify Percutaneous Absorption. *Skin Pharmacology and Applied Skin Physiology* 1999;12:34-45.
- 137 Jacobi U, Weigmann HJ, Ulrich J, Sterry W, Lademann J: Estimation of the relative stratum corneum amount removed by tape stripping. *Skin Research and Technology* 2005;11:91-96.
- 138 Schwindt DA, Wilhelm KP, Maibach HI: Water diffusion characteristics of human stratum corneum at different anatomical sites in vivo. *Journal of Investigative Dermatology* 1998;111:385-389.
- 139 Pellanda C, Strub C, Figueiredo V, Ruffli T, Imanidis G, Surber C: Topical bioavailability of triamcinolone acetonide: Effect of occlusion. *Skin Pharmacology and Physiology* 2007;20:50-56.
- 140 Bashir SJ, Chew AL, Anigbogu A, Dreher F, Maibach HI: Physical and physiological effects of stratum corneum tape stripping. *Skin Research and Technology* 2001;7:40-48.
- 141 Pelchrzım RV, Weigmann HJ, Schaefer H, Hagemester T, Linscheid M, Shah VP, Sterry W, Lademann J: Determination of the formation of the stratum corneum reservoir for two different corticosteroid formulations using tape stripping combined with UV/VIS spectroscopy. *JDDG - Journal of the German Society of Dermatology* 2004;2:914-919.
- 142 Voegeli R, Heiland J, Doppler S, Rawlings AV, Schreier T: Efficient and simple quantification of stratum corneum proteins on tape strippings by infrared densitometry. *Skin Research and Technology* 2007;13:242-251.
- 143 Jacobi U, Kaiser M, Richter H, Audring H, Sterry W, Lademann J: The Number of Stratum corneum Cell Layers Correlates with the Pseudo-Absorption of the Corneocytes. *Skin Pharmacology and Physiology* 2005;18:175-179.
- 144 Dreher F, Arens A, Host nyek JJ, Mudumba S, Ademola J, Maibach HI: Colorimetric Method for Quantifying Human Stratum Corneum Removed by Adhesive-Tape-Stripping. *Acta Dermato-Venereologica* 1998;78:186-189.

- 
- 145 Weigmann HJ, Lindemann U, Antoniou C, Tsikrikas GN, Stratigos AI, Katsambas A, Sterry W, Lademann J: UV/VIS Absorbance Allows Rapid, Accurate, and Reproducible Mass Determination of Corneocytes Removed by Tape Stripping. *Skin Pharmacology and Applied Skin Physiology* 2003;16:217-227.
- 146 Marttin E, Neelissen-Subnel MTA, DeHaan FHN, Boddé HE: A critical comparison of methods to quantify stratum corneum removed by tape stripping. *Skin Pharmacology* 1996;9:69-77.
- 147 Lademann J, Ilgevicius A, Zurbau O, Liess HD, Schanzer S, Weigmann HJ, Antoniou C, Pelchrzim RV, Sterry W: Penetration studies of topically applied substances: optical determination of the amount of stratum corneum removed by tape stripping. *Journal of Biomedical Optics* 2006;11.
- 148 Lindemann U, Weigmann HJ, Schaefer H, Sterry W, Lademann J: Evaluation of the Pseudo-Absorption Method to Quantify Human Stratum corneum Removed by Tape Stripping Using Protein Absorption. *Skin Pharmacology and Applied Skin Physiology* 2003;16:228-236.
- 149 Breternitz M, Flach M, Praessler J, Elsner P, Fluhr JW: Acute barrier disruption by adhesive tapes is influenced by pressure, time and anatomical location: integrity and cohesion assessed by sequential tape stripping; a randomized, controlled study. *British Journal of Dermatology* 2007;156:231-240.
- 150 Dreher F, Modjtahedi BS, Modjtahedi SP, Maibach HI: Quantification of stratum corneum removal by adhesive tape stripping by total protein assay in 96-well microplates. *Skin Research and Technology* 2005;11:97-101.
- 151 Anderson RL, Cassidy JM: Variations in physical dimensions and chemical composition of human stratum corneum. *Journal of Investigative Dermatology* 1973;61:30-32.
- 152 Holbrook KA, Odland GF: Regional differences in the thickness (cell layers) of the human stratum corneum: an ultrastructural analysis. *Journal of Investigative Dermatology* 1974;62:415-422.
- 153 Lademann J, Rudolph A, Jacobi U, Weigmann HJ, Schaefer H, Sterry W, Meinke M: Influence of nonhomogeneous distribution of topically applied UV filters on sun protection factors. *Journal of Biomedical Optics* 2004;9:1358-1362.
- 154 Teichmann A, Pissavini M, Ferrero L, Dehais A, Zastrow L, Ritcher H, Lademann J: Investigation of the homogeneity of the distribution of sunscreen formulations on the human skin: Characterization and comparison of two different methods. *Journal of Biomedical Optics* 2006;11.



- 
- 155 Lademann J, Richter H, Golz K, Zastrow L, Sterry W, Patzelt A: Influence of microparticles on the homogeneity of distribution of topically applied substances. *Skin Pharmacology and Physiology* 2008;21:274-282.
- 156 Joblove GH, Greenberg D: Color spaces for computer graphics. *SIGGRAPH Comput Graph* 1978;12:20-25.
- 157 Majumdar S, Thomas J, Wasdo S, Sloan KB: The effect of water solubility of solutes on their flux through human skin in vitro. *International Journal of Pharmaceutics* 2007;329:25-36.
- 158 Thomas J, Majumdar S, Wasdo S, Majumdar A, Sloan KB: The effect of water solubility of solutes on their flux through human skin in vitro: An extended Flynn database fitted to the Roberts-Sloan equation. *International Journal of Pharmaceutics* 2007;339:157-167.
- 159 Lademann O, Richter H, Meinke MC, Patzelt A, Kramer A, Hinz P, Weltmann KD, Hartmann B, Koch S: Drug delivery through the skin barrier enhanced by treatment with tissue-tolerable plasma. *Experimental Dermatology* 2011;20:488-490.
- 160 Trauer S, Lademann J, Knorr F, Richter H, Liebsch M, Rozycki C, Balizs G, Buettmeyer R, Linscheid M, Patzelt A: Development of an in vitro modified skin absorption test for the investigation of the follicular penetration pathway of caffeine. *Skin Pharmacology and Physiology* 2010;23:320-327.
- 161 Kubota K, Yamada T: Finite dose percutaneous drug absorption: Theory and its application to in vitro timolol permeation. *Journal of Pharmaceutical Sciences* 1990;79:1015-1019.
- 162 Jones E, Oliphant T, Peterson P: *SciPy: Open source scientific tools for Python*, 2001.
- 163 Anderson BD, Raykar PV: Solute structure-permeability relationships in human stratum corneum. *Journal of Investigative Dermatology* 1989;93:280-286.
- 164 Lide DR: *Handbook of Chemistry and Physics*. CRC Press Inc, 2008.
- 165 Frasch HF, Barbero AM, Hettick JM, Nitsche JM: Tissue binding affects the kinetics of theophylline diffusion through the stratum corneum barrier layer of skin. *Journal of Pharmaceutical Sciences* 2011;100:2989-2995.
- 166 Nitsche JM, Frasch HF: Dynamics of diffusion with reversible binding in microscopically heterogeneous membranes: General theory and applications to dermal penetration. *Chemical Engineering Science* 2011;66:2019-2041.

- 
- 167 Guy R, Hadgraft J, Maibach H: A pharmacokinetic model for percutaneous absorption. *International Journal of Pharmaceutics* 1982;11:119-129.
- 168 Kubota K: A compartment model for percutaneous drug absorption. *Journal of pharmaceutical sciences* 1991;80:502-504.
- 169 Guy RH, Hadgraft J: Transdermal drug delivery: A simplified pharmacokinetic approach. *International Journal of Pharmaceutics* 1985;24:267-274.
- 170 Wallace SM, Barnett G: Pharmacokinetic analysis of percutaneous absorption: evidence of parallel penetration pathways for methotrexate. *Journal of Pharmacokinetics and Biopharmaceutics* 1978;6:315-325.
- 171 McCarley K, Bunge A: Pharmacokinetic models of dermal absorption. *Journal of pharmaceutical sciences* 2001;90:1699-1719.
- 172 Reddy M, McCarley K, Bunge A: Physiologically relevant one-compartment pharmacokinetic models for skin. 2. Comparison of models when combined with a systemic pharmacokinetic model. *Journal of pharmaceutical sciences* 2000;87:482-490.
- 173 McCarley K, Bunge A: Physiologically relevant two-compartment pharmacokinetic models for skin. *Journal of pharmaceutical sciences* 2000;89:1212-1235.
- 174 Miller MA, Bhatt V, Kasting GB: Dose and airflow dependence of benzyl alcohol disposition on skin. *Journal of Pharmaceutical Sciences* 2006;95:281-291.
- 175 George K, Kubota K, Twizell EH: A two-dimensional mathematical model of percutaneous drug absorption. *BioMedical Engineering Online* 2004;3:18:1-13.
- 176 George K: A two-dimensional mathematical model of non-linear dual-sorption of percutaneous drug absorption. *BioMedical Engineering Online* 2005;4:40:1-15.
- 177 Mueller B, Anissimov YG, Roberts MS: Unexpected Clobetasol Propionate Profile in Human Stratum Corneum after Topical Application in Vitro. *Pharmaceutical Research* 2003;20:1835-1837.
- 178 Melero A, Garrigues TM, Alós M, Kostka KH, Lehr CM, Schaefer UF: Nortriptyline for smoking cessation: Release and human skin diffusion from patches. *International Journal of Pharmaceutics* 2009;378:101-107.
- 179 Wagner H, Kostka KH, Lehr CM, Schaefer UF: Interrelation of permeation and penetration parameters obtained from in vitro experiments with human skin and skin equivalents. *Journal of Controlled Release* 2001;75:283-295.

- 
- 180 Tfayli A, Piot O, Pitre F, Manfait M: Follow-up of drug permeation through excised human skin with confocal Raman microspectroscopy. *European Biophysics Journal* 2007;36:1049-1058.
- 181 Tfayli A, Piot O, Manfait M: Confocal Raman microspectroscopy on excised human skin: uncertainties in depth profiling and mathematical correction applied to dermatological drug permeation. *Journal of biophotonics* 2008;1:140-153.
- 182 Klang V, Schwarz JC, Hartl A, Valenta C: Facilitating in vitro tape stripping: Application of infrared densitometry for quantification of porcine stratum corneum proteins. *Skin Pharmacology and Physiology* 2011;24:256-268.



## 10 Appendix: A detailed description of skin segmentation

Parts of this chapter have been published in:

Melero A, Hahn T, Schaefer U F, Schneider M

*In vitro* Human Skin Segmentation and Drug Concentration-Skin Depth Profiles

Methods Mol Biol 763 (2011) 33-50

The author of the thesis made the following contributions to the publication: Wrote major parts of the manuscript and refined the equations.

## 10.1 *Abstract*

Penetration experiments are characterized by segmentation of the skin to separate the different skin layers. Generally, skin segmentation is performed in two consecutive procedures: First, the major barrier of the skin, the *SC*, is removed by tape-stripping. Afterwards, the deeper skin layers are cut parallel to the skin surface by *cryo*-sectioning. In this chapter, a detailed description of the skin segmentation technique employed in the experiments in this thesis is given. This highly standardized segmentation method has been described previously by [32].

Skin segmentation is required in order to investigate the concentration depth profile of a drug in the skin. Two parameters are essential for the correct investigation of skin depth profiles: first, the amount of skin removed with each sample is required and secondly the amount of drug contained in each sample. The determination of the first is described below, and the latter is determined by extraction of the drug from the samples.

From these parameters, the *SC* depth and the normalized drug concentration (drug amount per skin volume of the sample) can be calculated.

## 10.2 Tape-stripping

Human skin is obtained from abdominal plastic surgery and prepared for storage. For performing the experiments, 25 mm diameter pieces of skin are used. After incubation for different time intervals with the formulation under study, the SC is removed by successive application of adhesive tapes onto the surface of the skin. The corneocytes and intercellular lipids adhere to the tape and can be easily removed by this technique.

For reproducible stripping, the incubated skin specimen is transferred onto a special stripping apparatus. To avoid the influence of wrinkles the skin is moderately stretched and fixed with small pins on a cork disk. Afterwards, a pre-cut tape is placed on the stripping area restricted by a stripping mask made from an inert material. To enhance the contact between tape and skin surface the tape is charged with a weight of 2 kg for 10 seconds (**fig. 10-1**). Subsequently, the tape is removed in one swift move. For analytical reasons tapes from several strips may be advantageously pooled in corresponding fractions.

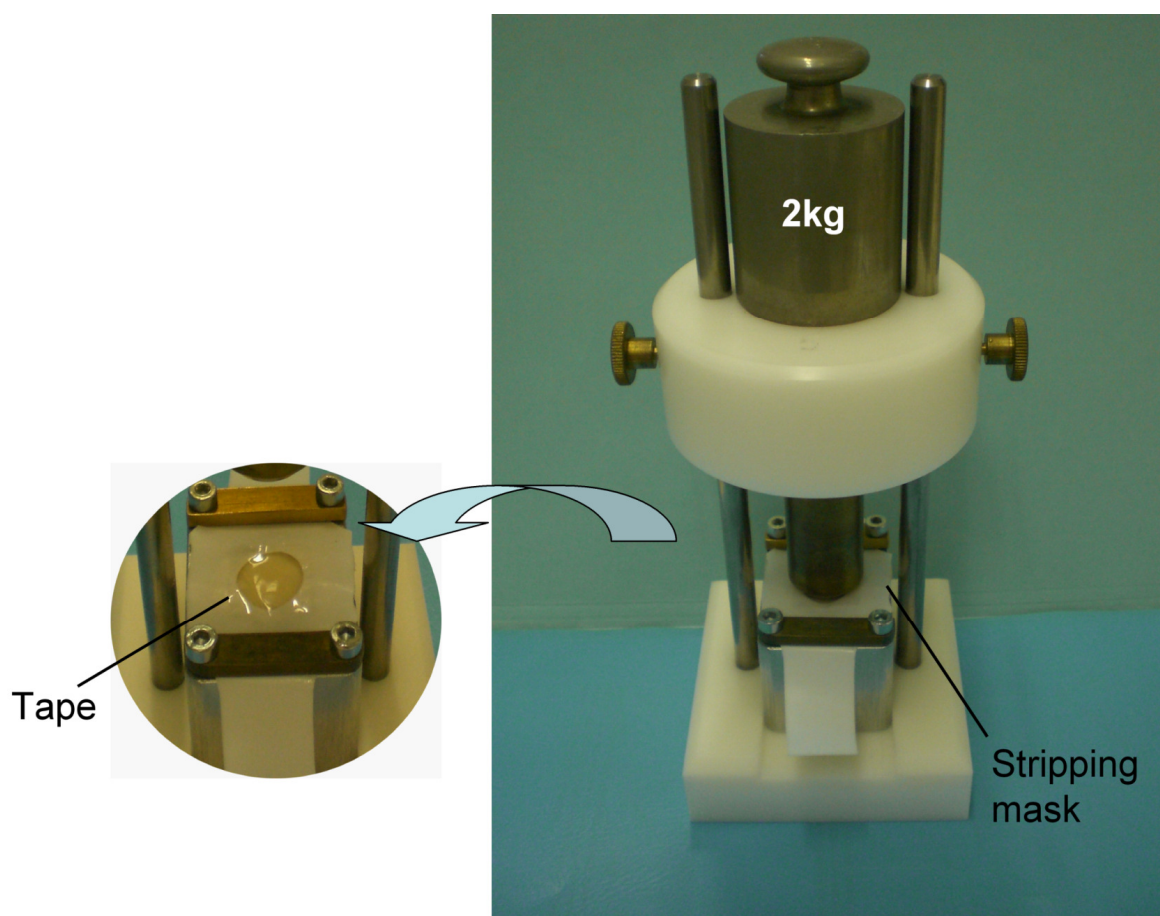


**Figure 10-1** *In vitro* tape-stripping apparatus.

---

*Procedure*

1. The tesa® Film tape (tesa® Film kristall-klar Nr. 57330-00000, Tesa AG, Hamburg, Germany) is cut into strips of 16 mm length each with clean scissors
2. The infrared densitometer (Squame Scan™ 850A, Heiland electronic GmbH, Wetzlar, Germany) is put to auto zero with the provided 0% standard filter, and the provided grey filter is measured, which should give 33.8% absorption.
3. An empty tape-strip is placed on the sample holder of the infrared densitometer with the adhesive side facing up and the optical density is measured. This value is taken as background and will be later subtracted from the values obtained for the samples.
4. The skin is fixed to the aluminium block filled with cork discs with the help of needles (Prym, Stolberg, Germany) and forceps. The skin is properly stretched to eliminate wrinkles.
5. The skin is covered with a Teflon mask with the hole of 15 mm diameter centred on the skin to define the stripping area. Then, the setup is fixed by tightening the screws.
6. One tape-strip is placed centrally on the stripping area with the forceps and pressed slightly with the back side of the forceps to assure full contact between the tape and the skin.
7. The aluminium block is placed under the stamp of the stripping device and charged with a weight of 2 kg for exactly 10 seconds.
8. The adhesive tape is removed rapidly with forceps in one swift move.
9. Directly after stripping, each strip is transferred to the sample holder with the adhesive side facing up. After three minutes equilibration time, the tape-strip in the sample holder is placed under the measuring head. The optical absorption of each tape is directly displayed. The tape-strips should always be handled with forceps and only the corners of the tape-strip, which will not be measured by infrared densitometry, should be touched.
10. The skin is stripped until the SC is removed completely. This endpoint has to be determined previously, for tesa® Film kristall-klar this is the case, when the lower limit of quantification (LLOQ) of the IR-D is reached. The LLOQ can be calculated from the five fold background noise of an empty tape. Reaching this endpoint no further strips are applied.



11. The sticky side of the tape-strips are covered with some glass pearls (Merck, Darmstadt, Germany) and the tapes are transferred to scintillation vials (20 mL, neoLab Migge Laborbedarf-Vertriebs GmbH, Heidelberg, Germany) with the sticky side facing up. The glass pearls should prevent the strips from sticking to each other and to the vials.
12. Depending on the nature of the analyzed drug it may be necessary to combine several tapes into pools (e.g. "pool 1": tape n° 1. "pool 2": tape n° 2. "pool 3": tapes n° 3-5. "pool 4": tapes n° 6-10. "pool 5": tapes n° 11-15. "pool 6": tapes n° 16-20).

### 10.3 *Cryo-sectioning of the deeper skin layers*

After removal of the complete SC by tape-stripping, the stripped skin is frozen by expanding carbon dioxide, and slices of 25  $\mu\text{m}$  thickness are cut parallel to the skin surface by means of a *cryo*-microtome (**fig. 10-2**). The skin segments are transferred into suitable containers for drug extraction. For analytical reasons the cuts may be pooled in several fractions.

#### *Procedure*

1. After complete removal of the SC the rest of the skin is frozen, still fixed on the aluminium block, in a stream of expanding carbon dioxide until achieving a pale appearance. Carbon dioxide is normally used because it is the quickest way to freeze skin as it is important to stop drug diffusion. This method is not suitable for volatile drugs.
2. A 13 mm diameter (*cryo*-section area) biopsy is taken and allowed to thaw.
3. A drop of water is used to assure the contact between the closed part of the *cryo*-bloc and the skin.
4. The biopsy is mounted (epidermis up) on the drop on the self made aluminium tube. This tube with the skin can then be fixed in the *cryo*-microtome. It has a ring that can be moved to different positions.
5. The spacer ring is placed in the upper position, at the same height as the skin and the skin is covered with a glass slide.
6. The skin is frozen using expanding carbon dioxide again, while retaining the glass slide in the same position to obtain a flat surface.

7. The glass slide is removed, and the ring put in the lowest position to uncover the skin. Then, the tube is fixed with the frozen skin in the *cryo*-microtome.
8. All cuts are performed parallel to the skin's surface (thickness of the skin cuts: 25  $\mu\text{m}$ ).
9. The cuts are collected in pre-weighed centrifuge tubes and combined in a suitable scheme, e.g. incomplete cuts, 4 x 2 cuts, 4 x 4 cuts, 2 x 8 cuts and skin rest.
10. The centrifuge tubes containing the samples are weighed. The weight of the skin samples is later related to the skin thickness.

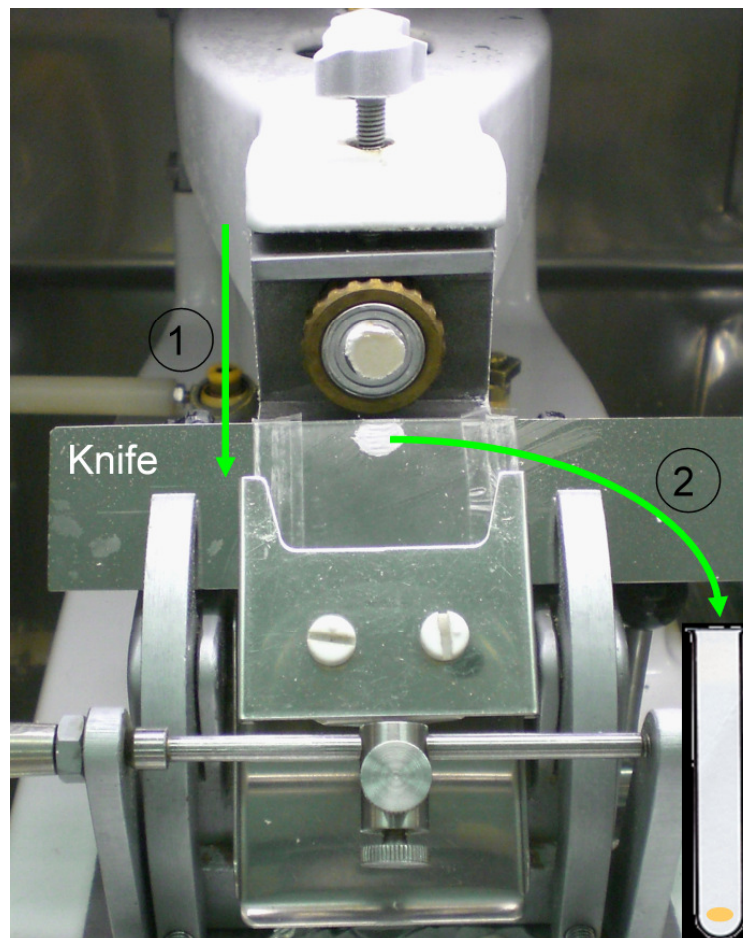


**Figure 10-2** Cryo-sectioning of the deeper skin layers. Step 1: The knife moves down and cuts a slice of the skin biopsy. Step 2: The skin slice is transferred into a test-tube for extraction and quantification.

#### **10.4 Extraction of drug from tape-strips and deeper skin layers**

The selection of the extraction medium has to be carefully evaluated for each drug. The selected solvent should not remove the glue of the tapes or skin components, as they might interfere with the chromatogram or damage the HPLC column.

To assure the recovery effectiveness in finite dose experiments, a mass balance should be carried out. For doing so, the whole absorption experiment is performed as usual and every part of the setup in contact with the formulation is extracted with the medium, including the rest of the applied formulation. After extraction and analysis of all these samples, a mass balance is performed. The recovery should always be between 85 and 115% of the applied amount of drug [29] to allow for reliable and comparable results.

#### **10.5 Measurement of the skin thickness**

After segmentation of the skin and extraction of the drug from each segment, the next step towards generating concentration-depth profiles is the measurement of both the total thickness of the whole skin and also of the thickness of the intact SC.

##### *Complete skin thickness*

The calliper gauge is calibrated to 0 using a glass slide and a cover slip. The skin disc is placed on a glass slide and a cover slip is put on the top. The whole skin thickness is measured with a tactile probe. The total skin thickness is the mean of five measurements on different positions on the skin.

##### *Stratum corneum thickness*

A 4 mm biopsy is punched out of frozen full-thickness skin. A drop of Tissue-Tek® (Sakura Finetek, Torrance, CA, USA) is put on a pre-tempered aluminium tube and placed in the cryo-microtome (Slee, Mainz, Germany) until it starts to freeze. The biopsy is carefully embedded in Tissue-Tek® with the SC arranged perpendicular to the metal block surface. Then, the whole metal block is placed in the cryo-microtome to allow complete freezing of the biopsy. The skin is cut vertically to the surface of the skin in 8 µm thick slices. These slices are mounted directly on glass by melting the frozen skin slices to the slides. To achieve this, the slides need to be warmer than the slices, e.g. room temperature.

Staining of the skin samples, e.g. with haematoxylin, improves the contrast. Afterwards, a drop of Fluor Save™ (Calbiochem, San Diego, CA, USA) is applied to the sample and a cover slip is placed onto it to protect the sample.

A conventional light microscope (Leica, Wetzlar, Germany) equipped with a graduate scale bar, and a digital camera (Jenoptik, Jena, Germany) are used to visualize the cuts at 400x magnification. Image software is used to analyze the pictures (Carl Zeiss Axio Vision Rel. 4.7, Carl Zeiss Imaging Solutions GmbH, Göttingen, Germany).

The mean SC thickness for each skin donor is calculated from microscopic pictures of histological cross-sections on at least 10 different positions (**fig. 10-3**).

Skin should not be used after 6 months storage at -26°C as not only the permeability characteristics might be changed, but also the SC thickness [39,41].

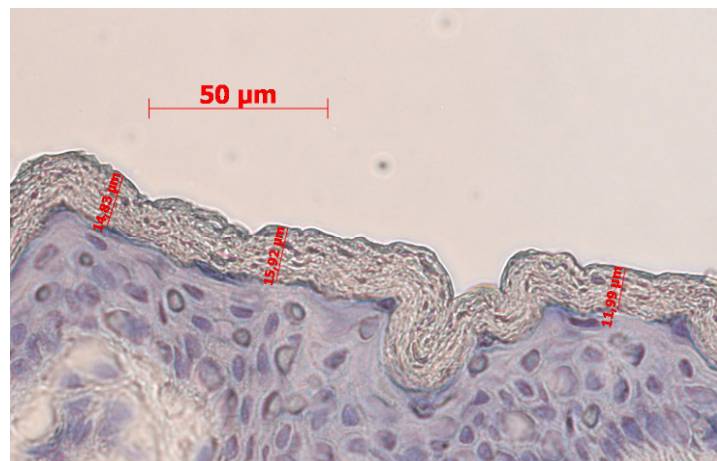


**Figure 10-3** Histological cross-section of human skin at 400x magnification.

## 10.6 Data treatment and plotting

Normalized drug concentration can be plotted versus skin depth to see the drug distribution within the different skin layers after the selected incubation times. The concentration depth profiles provide information about:

- the influence of the incubation time, drug concentration, and the vehicle on drug distribution
- saturation of the SC
- formation of depots in the different skin layers

Please note that the first tape-strip also removes rests of formulation that can be left on the skin surface after cleaning. Therefore, the first strip is usually not plotted in drug concentration skin depth profiles [135]. However, it has to be taken into account for determining the SC depth as well as for mass balance.

A step-by-step calculation of the depth in the SC and in the *DSL* is presented below:

- *Corrected absorption value for a single tape-strip*

$$x_i = x_i^* - x_0 \quad \text{(Equation 10-1)}$$

$x_i$ : absorption of a tape-strip measured by IR-D and corrected for absorption of empty tape

$x_i^*$ : absorption measured by IR-D, non-corrected value

$x_0$ : absorption of an empty tape measured by IR-D

$i$ : tape-strip number

- *Absorption value for pooled strips*

$$x_{pool(n)} = \sum_{i=h}^j x_i \quad (\text{Equation 10-2})$$

- $x_{pool(n)}$ : sum of absorption of strips in pool  $n$  containing strips  $h$ - $j$  measured by IR-D  
 $x_i$ : absorption of  $i$ -th tape-strip measured by IR-D and corrected for empty tape  
 $i$ : tape-strip number  
 $h$ : first strip belonging to the  $n$ -th pool  
 $j$ : last strip belonging to the  $n$ -th pool

- *Relative SC thickness removed per pool*

$$d_{rel(n)}^* = \sum_{i=h}^j x_i / X_{n_{max}} \quad \text{with } X_{n_{max}} = \sum_{i=1}^{n_{max}} x_i \quad (\text{Equation 10-3})$$

- $d_{rel(n)}^*$ : relative SC thickness removed per pool  $n$   
 $x_i$ : absorption of  $i$ -th tape-strip measured by IR-D and corrected for empty tape  
 $h$ : first strip belonging to the  $n$ -th pool  
 $j$ : last strip belonging to the  $n$ -th pool  
 $n_{max}$ : total number of tape-strips  
 $X_{n_{max}}$ : absorption of total number of tapes  $n_{max}$

- *Absolute SC thickness of the  $n$ -th pool*

$$d_n^* = d_{tot} \cdot d_{rel(n)}^* \quad (\text{Equation 10-4})$$

- $d_n^*$ : absolute SC thickness of the  $n$ -th pool  
 $d_{tot}$ : total SC thickness  
 $d_{rel(n)}^*$ : relative SC thickness removed per pool  $n$

- *SC depth after  $n_n$  pools of tape-strips*

$$d_{n_n} = \sum_{n=1}^{n_n} d_n^* \quad (\text{Equation 10-5})$$

- $d_{n_n}$ : SC depth after  $n_n$  pools of tape-strips  
 $d_n^*$ : thickness of the  $n$ -th pool

- *Absolute thickness of pool l of cuts*

$$L_l^* = L_{tot} \cdot \sum_{k=1}^l w_k / W_{N_{max}} \quad \text{with } W_{N_{max}} = \sum_{k=1}^{N_{max}} w_k \quad \text{(Equation 10-6)}$$

- $L_l^*$ : absolute thickness of pool l of cuts  
 $L_{tot}$ : total thickness of the stripped skin  
 $w_k$ : weight of the pool of cuts / rest of the skin  
 $k$ : lower number of pools of cuts  
 $l$ : upper number of pools of cuts  
 $N_{max}$ : total number of pools  
 $W_{N_{max}}$ : weight of total number of pools

- *Depth of deeper skin layers after pool l of cuts*

$$L_l = \sum_{k=l}^l L_k^* \quad \text{(Equation 10-7)}$$

- $L_l$ : depth into the deeper skin layers after pool l of cuts  
 $L_k^*$ : thickness of pool k of cuts

- *Drug amount in pool n*

$$m_{EX_n} = c_{EX_n} * V_{EX} \quad \text{(Equation 10-8)}$$

- $m_{EX_n}$ : extracted drug amount of pool n  
 $c_{EX_n}$ : drug concentration in the extract of n-th pool of tape-strips  
 $V_{EX}$ : volume of the extracting agent (e.g. 2.0 ml)

- *Normalized drug concentration in SC for n-th pool of tape-strips*

$$c_n = \frac{c_{EX_n} \cdot V_{EX}}{A_T \cdot d_n^*} \quad (\text{Equation 10-9})$$

- $c_n$ : normalized drug concentration in skin for  $n$ -th pool of tape-strips  
 $c_{EX_n}$ : drug concentration in the extract of  $n$ -th pool of tape-strips  
 $V_{EX}$ : volume of the extracting agent (e.g. 2.0 ml)  
 $A_T$ : area of tape-stripping (e.g. 1.767 cm<sup>2</sup>)  
 $d_n^*$ : thickness of SC removed by tape-strips of pool  $n$

- *Normalized drug concentration in deeper skin layers for l-th pool of cuts*

$$c_l = \frac{c_{EX_l} \cdot V_{EX}}{A_C \cdot L_l^*} \quad (\text{Equation 10-10})$$

- $c_l$ : normalized drug concentration in skin for  $l$ -th pool of cuts  
 $c_{EX_l}$ : drug concentration in the extract of  $l$ -th pool of cuts  
 $V_{EX}$ : volume of the extracting agent (2.0 ml)  
 $A_C$ : area of cryo cutting (1.327 cm<sup>2</sup>)  
 $L_l^*$ : thickness of viable skin removed by cuts of pool  $l$

- *Calculation of the middle of segment*

$$d_x = \frac{(d_h + d_j)}{2} \quad (\text{Equation 10-11})$$

- $d_x$ : middle of segment  
 $d_h$ : depth before first strip of the pool  
 $d_j$ : depth after last strip of the pool

- *Cumulative drug amount in SC*

$$Q = \sum_{i=2}^{n_{max}} m_{EX_n} \quad (\text{Equation 10-12})$$

- $Q$ : cumulative drug amount in SC without strip 1  
 $m_{EX_n}$ : extracted drug amount of pool  $n$   
 $n_{max}$ : total number of tapes



With these calculations, concentration depth profiles can be established, for an example see **fig. 10-4**. On the following pages, this example for the calculation of concentration skin depth profiles is given.

For the calculations the following values are used:

Stripping area ( $A_T$ ):	1.76 cm <sup>2</sup>
Area of cryo-cuts ( $A_C$ ):	1.327 cm <sup>2</sup>
Extraction volume for samples ( $m_{Ex}$ ):	2 ml

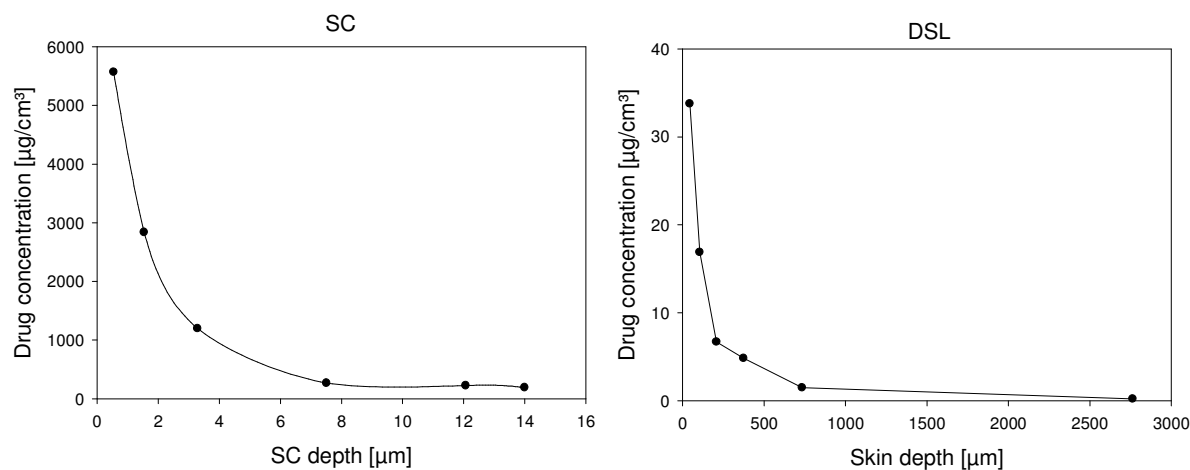


**Figure 10-4** Concentration depth profiles obtained from the example calculation in tables 10-1 to 10-3.

**Table 10-1** Determination of the depth within the SC

$i$	$x_i^*$	$x_i$	pool	$x_{pool(n)} = \sum_{i=h}^j x_i$	$d_{rel(n)}^* = \sum_{i=h}^j x_i / X_{n_{max}}$	$d_n^* = d_{tot} \cdot d_{rel(n)}^*$
	measured by IR-D	corrected (from IR-D)		sum of IR-D absorption of strips in pool $n$	relative amount of SC removed per pool	thickness of segment
	[%]	[%]		[%]	[%]	[ $\mu\text{m}$ ]
empty strip	6.7					
1	21.2	14.5	#1; ( $h=j=1$ )	14.5	7.2	1.08
2	18.8	12.1	#2; ( $h=j=2$ )	12.1	6.0	0.90
3	16.9	10.2	#3; ( $h=3$ ; $j=5$ )	34.7	17.3	2.59
4	19	12.3				
5	18.9	12.2				
6	22.3	15.6	#4; ( $h=6$ ; $j=10$ )	78.3	39.0	5.85
7	24.1	17.4				
8	20.1	13.4				
9	21.7	15				
10	23.6	16.9				
11	18.4	11.7	#5; ( $h=11$ ; $j=16$ )	43.5	21.7	3.25
12	17.8	11.1				
13	15.3	8.6				
14	12.3	5.6				

<b>15</b>	13.2	6.5				
<b>16</b>	11.8	5.1	#6; ( $h=15$ ; $j=20$ )	17.5	8.7	1.31
<b>17</b>	11.4	4.7				
<b>18</b>	10.4	3.7				
<b>19</b>	9.3	2.6				
<b>20</b>	8.1	1.4				
$\sum_{i=1}^{n_{\max}} x_i$	334.6	<b>200.6</b>				

**Table 10-2** Determination of the depth into the viable skin layers

<b>pool</b>	$w_k$	$L_l^* = L_{tot} \cdot \sum_{k=1}^l w_k / W_{N_{max}}$
	<b>weight of viable skin removed by pool</b>	<b>thickness of segment</b>
	<b>[mg]</b>	<b>[<math>\mu\text{m}</math>]</b>
<b>#7</b>	3.06	60.36
<b>#8</b>	3.07	60.55
<b>#9</b>	7.46	147.14
<b>#10</b>	9.29	183.24
<b>#11</b>	27.16	535.71
<b>#12 (rest of skin)</b>	178.53	3521.38
$\sum_{i=\#7}^{i=\#12} w_i$	228.57	<b>cumulative weight of viable skin removed by all pools</b>

**Table 10-3** Calculation of concentration-depth profiles in the SC and the viable skin layers

<b>pool</b>	$c_{EX}$	$m_{EX_n} = c_{EX_n} * V_{EX}$	$d_n^* = d_{tot} \cdot \sum_{i=h}^j x_i / X_{n_{max}}$	$d_n$	$(d_n + d_{n-1})/2$	$V_n = A_T \cdot d_{tot} \cdot \sum_{i=h}^j x_i / X_{n_{max}}$	$c_n = \frac{c_{EX_n} \cdot V_{EX}}{A_T \cdot d_n^*}$
	<b>experimental</b>	<b>extracted amount</b>	<b>thickness of segment</b>	<b>depth into the SC</b>	<b>middle of segment</b>	<b>volume of segment</b>	<b>concentration</b>
	<b>[µg/ml]</b>	<b>[µg]</b>	<b>[µm]</b>	<b>[µm]</b>	<b>[µm]</b>	<b>[cm<sup>3</sup>]</b>	<b>[µg/cm<sup>3</sup>]</b>
<b>#1</b>	0.5334	1.0668	1.08	1.08	<b>0.54</b>	1.916E-04	<b>5568.24</b>
<b>#2</b>	0.2268	0.4536	0.90	1.99	<b>1.54</b>	1.599E-04	<b>2837.21</b>
<b>#3</b>	0.2742	0.5484	2.59	4.58	<b>3.29</b>	4.585E-04	<b>1196.11</b>
<b>#4</b>	0.1377	0.2754	5.85	10.44	<b>7.51</b>	1.035E-03	<b>266.20</b>
<b>#5</b>	0.0645	0.1290	3.25	13.69	<b>12.07</b>	5.748E-04	<b>224.44</b>
<b>#6</b>	0.0220	0.0440	1.31	15	<b>14</b>	2.312E-04	<b>190.29</b>
	$Q = \sum_{i=2}^{n_{max}} m_{EX_n}$	$Q/A_T$					
	<b>amount in SC (without first strip)</b>	<b>normalized for stripping area</b>					
	<b>[µg]</b>	<b>[µg/cm<sup>2</sup>]</b>					
	1.4504	0.8208					

Table 10-3 second part

pool	$c_{EX}$	$m_{EX_n} = c_{EX_n} \cdot V_{EX}$	$L_l^* = l_{tot} \cdot w_k / W_{N_{max}}$	$d_{tot+l_i}$	$d_{tot} + (l_i + l_{i-1})/2$	$V_k = A_C \cdot L_{tot} \cdot w_k / W_{N_{max}}$	$c_l = \frac{c_{EX_l} \cdot V_{EX}}{A_C \cdot L_l^*}$
	<b>experimental</b>	<b>extracted amount</b>	<b>thickness of segment</b>	<b>depth inside the skin</b>	<b>middle of segment</b>	<b>volume of segment</b>	<b>concentration</b>
	[ $\mu\text{g/ml}$ ]	[ $\mu\text{g}$ ]	[ $\mu\text{m}$ ]	[ $\mu\text{m}$ ]	[ $\mu\text{m}$ ]	[ $\text{cm}^3$ ]	[ $\mu\text{g/cm}^3$ ]
#7	0.1352	0.2704	60.36	75	45	8.009E-03	33.76
#8	0.0678	0.1356	60.55	136	106	8.035E-03	16.88
#9	0.0654	0.1308	147.14	283	209	1.953E-02	6.70
#10	0.0589	0.1178	183.24	466	375	2.432E-02	4.84
#11	0.0532	0.1064	535.71	1002	734	7.109E-02	1.50
#12	0.0504	0.1008	3521.38	4523	2763	4.673E-01	0.22
	$\sum_{i=\#7}^{\#12} m_{EX_i}$	$\sum_{i=\#7}^{\#12} m_{EX_i} / A_C$					
	<b>amount in viable skin</b>	<b>normalized for cutting area</b>					
	[ $\mu\text{g}$ ]	[ $\mu\text{g/cm}^2$ ]					
	0.8618	0.6494					

## 11 Abbreviations

$A_C$ :	area of cryo-sectioning (1.327 cm <sup>2</sup> )
$A_T$ :	area of tape-stripping (e.g. 1.767 cm <sup>2</sup> )
BCA:	bicinchoninic acid
BSA:	bovine serum albumin
$C_{Ex_n}$ :	drug concentration in the extract of $n$ -th pool of tape-strips
$c_l$ :	drug concentration in skin for $l$ -th pool of cuts
$c_n$ :	drug concentration in skin for $n$ -th pool of tape-strips
$D$ :	diffusion coefficient
$d^*_{rel(n)}$ :	relative SC thickness removed per pool $n$
$d^*_n$ :	absolute SC thickness of the $n$ -th pool
$Da$ :	Dalton
$d_{nn}$ :	SC depth after $n_n$ pools of tape-strips
$DSL$ :	deeper skin layers
$d_{tot}$ :	total SC thickness
$d_x$ :	middle of segment
FFA:	flufenamic acid
$i$ :	tape-strip number
IR-D:	infrared densitometry
$h_s$ :	first strip belonging to the $n$ -th pool
$J$ :	flux through a membrane
$J_{ss}$ :	steady-state flux
$j_s$ :	last strip belonging to the $n$ -th pool
$K_{o/w}$ :	octanol/water partition coefficient
$k_p$ :	permeability coefficient
$l$ :	thickness of the membrane
$L^*_k$ :	depth in the deeper skin layers after pool $k$ of cuts
$L^*_l$ :	absolute thickness of pool $l$ of cuts
$L_l$ :	depth into the deeper skin layers after pool $l$ of cuts
LLOQ:	lower limit of quantification
$L_{tot}$ :	total thickness of the stripped skin

---

$m_{EXn}$ :	extracted amount of drug of pool $n$
$MW$ :	molecular weight
$n_{max}$ :	total number of tape-strips
$N_{max}$ :	total number of pools of cuts
$Q$ :	cumulative drug amount in SC without strip 1
$Q_t$ :	Cumulative permeated drug amount over time
$SC$ :	stratum corneum
$t$ :	time
$t_{lag}$ :	lag time
$TEWL$ :	transepidermal water loss
$V_{Ex}$ :	volume of the extracting agent (e.g. 2.0 ml)
$w_k$ :	weight of the pool of cuts / rest of the skin
$W_{Nmax}$ :	weight of total number of pools of cuts
$x_i$ :	absorption of a tape-strip measured by IR-D and corrected for absorption of empty tape
$x_i^*$ :	absorption measured by IR-D, non-corrected value
$X_{nmax}$ :	absorption of total number of tapes $n_{max}$
$x_0$ :	absorption of an empty tape measured by IR-D
$X_{pool(n)}$ :	sum of absorption of strips measured by IR-D in pool $n$ containing strips $h-j$ measured by IR-D



## 12 Curriculum vitae

### Personal data

Name	Tsambika Hahn
Address	Richard-Wagner-Str. 78, 66111 Saarbrücken
Date of birth	September 26th 1981
Place of birth	Mannheim
Nationality	German

### PhD studies

2008 - 2011	PhD thesis in the Department of Biopharmaceutics and Pharmaceutical Technology, Saarland University, Saarbruecken
-------------	---

### Academic studies

2007	License to practice pharmacy
2004 – 2005	Erasmus semester at University of Bath, England
2002 – 2006	Pharmacy studies at Johannes Gutenberg University, Mainz

### Internships/Work

2007	Marien pharmacy in Mainz
2006 – 2007	Leiden / Amsterdam Centre for Drug Research (LACDR) at Leiden University, Netherlands
2005	Student trainee at Sanofi-Aventis in Frankfurt Hoechst
2001	Internship in PCR laboratory of Klinikum der Stadt Ludwigshafen

### School

2001	Abitur at Johann-Sebastian-Bach-Gymnasium, Mannheim
------	---



## 13 List of publications

### Publications in peer-reviewed journals

Infrared densitometry: a fast and non-destructive method for exact stratum corneum depth calculation for in vitro tape-stripping

Hahn T, Hansen S, Neumann D, Kostka K-H, Lehr C-M, Muys L, Schaefer U F

Skin Pharmacol Physiol 2010;23:183–192

DOI: 10.1159/000288165

Influence of the application area on finite dose permeation in relation to drug type applied

Hahn T, Selzer D, Neumann D, Kostka K-H, Lehr C-M, Schaefer U F

Article in press in Experimental Dermatology

DOI:10.1111/j.1600-0625.2011.01424.x

### Book chapter

Melero A, Hahn T, Schaefer U F, Schneider M

In vitro Human Skin Segmentation and Drug Concentration-Skin Depth Profiles

Methods Mol Biol 763 (2011) 33-50

### Other publications

Measuring Skin Absorption in Vitro

Hahn T, Schaefer U F, Lehr C M

SOFW-Journal | 136 | 1/2-2010

Salbengrundlagen und die Wasserabgaberrate der Haut

Hahn T, Winkler K, Lehr C-M, Schaefer U F

Deutsche Apotheker Zeitung, 34; 59-62, 2010

Das geht unter die Haut – Aufbau der humanen Haut und mögliche Invasionswege

Hahn T, Selzer D, Neumann D, Schaefer U F

PZ Prisma, 1; 35-43, 2011

**Conference contributions – oral presentations**

Infrared densitometry for fast, non-destructive depth determination in the stratum corneum  
in vitro

Hahn T, Hansen S, Kostka K-H, Lehr C-M, Schaefer U F

European IP - Galenos Course on Skin Barrier Function, Lyon, September 27<sup>th</sup> – October 10<sup>th</sup>  
2009

Finite dose skin penetration – experiment and simulation

Hahn T, Naegel A, Heisig M, Kostka K-H, Lehr C-M, Schaefer U F

DPhG Jahrestagung, Braunschweig, October 4-7<sup>th</sup> 2010

Finite dose skin absorption analysis with respect to donor surface distribution

Hahn T, Selzer D, Neumann D, Lehr C-M, Schaefer U F

DPhG Doktorandentagung, Heringsdorf, March 30<sup>th</sup> – April 2<sup>nd</sup> 2011

**Conference contributions – poster presentations**

Infrared densitometry as a method for quantification of stratum corneum on tape

Hahn T, Hansen S, Kostka K-H, Lehr C-M, Schaefer U

Controlled Release Society Local Chapter Germany Annual Meeting, Halle, March 19-20<sup>th</sup>  
2009

Transfer of infrared densitometry to in vitro tape-stripping for determination of stratum corneum amount on tape

Hahn T, Hansen S, Neumann D, Kostka K-H, Lehr C-M, Schaefer, U F

Occupational and Environmental Exposure of Skin to Chemicals, Edinburgh, Scotland, June 14-17<sup>th</sup> 2009

Challenges associated with finite dose skin absorption experiments: Homogeneous drug distribution of liquid formulations on skin surface

Hahn T, Hansen S, Schneider M, Lehr C-M, Schaefer U F

8<sup>th</sup> International Conference and Workshop on Biological Barriers, Saarbruecken, March 21<sup>th</sup>  
- April 1<sup>st</sup> 2010

Challenges associated with finite dose skin absorption experiments: Homogeneous drug distribution of liquid formulations on skin surface

Hahn T, Hansen S, Schneider M, Lehr C-M, Schaefer U F

Perspectives in Percutaneous Penetration – 12<sup>th</sup> International Conference, La Grande Motte, France, April 7-10<sup>th</sup> 2010

The role of donor surface distribution in finite dose skin absorption experiments

Hahn T, Selzer D, Neumann D, Lehr C-M, Schaefer U F

Occupational and Environmental Exposure of Skin to Chemicals, Toronto, Canada, June 5-8<sup>th</sup>  
2011

*Co-author:*

One step further towards computer assisted simulation of percutaneous absorption to avoid animal experiments –the combination of experiment and simulation effectively helps to identify new important parameters.

Hansen S, Hahn T, Lehr C-M, Schaefer U F

15th Congress on Alternatives to Animal Testing, Linz, Austria, September 19-21<sup>th</sup> 2008

A numerical model for predicting drug concentration-depth profiles in human stratum corneum

Hahn T, Hansen S, Schaefer U F, Neumann D

Occupational and Environmental Exposure of Skin to Chemicals, Edinburgh, Scotland, June 14-17<sup>th</sup> 2009

In-silico models of skin penetration under finite dose conditions

Naegel A, Hahn T, Hansen S, Neumann D, Lehr C-M, Schaefer U F, Wittum G, Heisig M

Occupational and Environmental Exposure of Skin to Chemicals, Edinburgh, Scotland, June 14-17<sup>th</sup> 2009

Multiphoton microscopy for investigating the penetration of gold nanoparticles through human skin

Labouta H I, Hahn T, Muijs L, Schneider M

8<sup>th</sup> International Conference and Workshop on Biological Barriers, Saarbruecken, March 21<sup>th</sup> - April 1<sup>st</sup> 2010

The role of the lateral compartment in in-vitro finite dose skin penetration experiments

Selzer D, Hahn T, Neumann D, Lehr C-M, Schaefer U F

DPhG Jahrestagung, Braunschweig, October 4-7<sup>th</sup> 2010

## 14 Acknowledgement

Zunächst möchte ich mich bei Prof. Dr. Claus-Michael Lehr für die Möglichkeit bedanken, meine Arbeit an seinem Institut anzufertigen, sowie für das Anfertigen des Gutachtens. Besonders möchte ich Prof. Dr. Schäfer danken für die gute Betreuung und ständige Diskussionsbereitschaft während der gesamten Dauer der Promotion und das Erstellen des Gutachtens.

Zudem möchte ich Prof. Dr. Vogt für das Anfertigen des Gutachtens, sowie den weiteren Mitgliedern der Prüfungskommission Prof. Dr. Rolf W. Hartmann und Dr. Britta Diesel, danken.

Außerdem möchte ich mich beim gesamten Institut für die Unterstützung und schöne Zeit bedanken. Hierbei möchte ich zunächst Peter Meiers erwähnen, durch dessen tiefgehende HPLC-Kenntnisse so manche Probleme gelöst werden konnten. Außerdem Leon Muis für das Anfertigen von Cryo-Schnitten, sowie den weiteren Technikern Petra König, Heike Stumpf und Chris Schild für regelmäßige Hilfe bei der Beschaffung und Suche von Materialien. Des Weiteren möchte ich Simon Räsch nennen, der mir durch seine engagierte Mithilfe einiges an Arbeit abgenommen hat. Letztendlich wäre die Arbeit ohne Material nicht möglich gewesen, deshalb möchte ich mich auch bei Herrn Prof. Dr. Kostka für das Bereitstellen der Haut bedanken.

Im Bereich der Haut waren die Diskussionen im Haut-Team um Dominik, Steffi, Ana, Hagar und Dirk immer wieder hilfreich. Hierbei ist Steffi zu erwähnen, besonders für die Einführung in das Arbeiten mit Haut, sowie die Zusammenarbeit mit Dominik, welche mir Einblicke in die Sichtweise der Bioinformatik erlaubte.

Zudem wäre die Arbeit nicht möglich gewesen ohne die Kooperationspartner vom Goethe Institut for Scientific Computing in Frankfurt um Prof. Dr. Wittum. Hierbei möchte ich mich besonders bei Arne Nägel und Michael Heisig für die gute Zusammenarbeit bedanken.

Aber nicht nur für die wissenschaftliche Unterstützung möchte ich nennen, sondern auch die schöne Zeit außerhalb der Arbeit. Insbesondere das nette Büroteam sorgte durch gemeinsames Quatschen, Lachen und Naschen für einen angenehmen Arbeitsalltag, so dass man sich teilweise wie zu Hause fühlte. Und durch die Beachvolleyball-Truppe wurden so einige Sommerabende verschönert.

Keine Arbeit ist möglich ohne Freunde, die einen in der Freizeit wieder Kräfte für die Arbeit sammeln lassen. Hierbei möchte ich mich besonders bei Julia bedanken, die die Einleitung auf sprachliche Fehler durchgelesen hat.

Besonders bedanken möchte ich mich bei meinem Freund Philipp, der mich über all die Jahre und Entfernung stets voll unterstützt und ermutigt hat. Außerdem hat er die Arbeit Korrektur gelesen und hatte bei Computerproblemen meist eine Lösung parat.

Zu guter Letzt danke ich meiner Familie für die Unterstützung, die sie mir immer gegeben hat. Danke!